Spring 2016

Microwave material characterization of alkali-silica reaction (ASR) gel in cementitious materials

Ashkan Hashemi

Department: Electrical and Computer Engineering

MICROWAVE MATERIAL CHARACTERIZATION OF ALKALI-SILICA REACTION (ASR) GEL IN CEMENTITIOUS MATERIALS

by

ASHKAN HASHEMI

A DISSERTATION

Presented to the Faculty of the Graduate School of the

MISSOURI UNIVERSITY OF SCIENCE AND TECHNOLOGY

In Partial Fulfillment of the Requirements for the Degree

DOCTOR OF PHILOSOPHY IN ELECTRICAL ENGINEERING

2016

Approved by

Dr. Reza Zoughi, Co-Advisor
Dr. Kristen M. Donnell, Co-Advisor
Dr. Jun Fan
Dr. Kimberly E. Kurtis
Dr. R. Joe Stanley

PUBLICATION DISSERTATION OPTION

This dissertation consists of the following six papers, formatted in the style used by the Missouri University of Science and Technology, listed as follows:

Paper 1 (pages 14-44), A. Hashemi, M. Horst, K.E. Kurtis, K.M. Donnell, and R. Zoughi, "Comparison of alkali–silica reaction gel behavior in mortar at microwave frequencies," has been published in IEEE Transaction on Instrumentation and Measurement, vol. 64, no. 7, pp. 1907–1915, Jul. 2015.

Paper 2 (pages 45-60), A. Hashemi, K.M. Donnell, R. Zoughi, and K.E. Kurtis, "Effect of humidity on dielectric properties of mortars with alkali-silica reaction (ASR) gel," has been published in IEEE International Instrumentation and Measurement Technology, Peer-Reviewed Proceedings, pp. 1502–1506, May. 2015.

Paper 3 (pages 61-87), A. Hashemi, I. Mehdipour, K.M. Donnell, and R. Zoughi, K.H. Khayat, "Effect of alkali addition on microwave dielectric properties of mortars," under review in NDT & E International Journal, 2015.

Paper 4 (pages 88-108), A. Hashemi, M. Rashidi, K.E. Kurtis, K.M. Donnell, and R. Zoughi, "Curing conditions effects on long-term dielectric properties of mortar samples containing ASR gel," to be submitted to IEEE Transaction on Instrumentation and Measurement, I2MTC special issue, 2016.

Paper 5 (pages 109-125), A. Hashemi, M. Rashidi, K.E. Kurtis, K.M. Donnell, and R. Zoughi, "Microwave dielectric properties measurements of sodium and potassium water glasses," accepted for publication in Materials Letters Journal, 2015.

Paper 6 (pages 126-164), A. Hashemi, K.E. Kurtis, K.M. Donnell, and R. Zoughi, "Empirical multi-phase dielectric mixing model for mortars containing alkali-silica reaction (ASR) gel," to be submitted to IEEE Transaction on Instrumentation and Measurement, 2015.

ABSTRACT

Since alkali-silica reaction (ASR) was recognized as a durability challenge in cement-based materials over 70 years ago, numerous methods have been utilized to prevent, detect, and mitigate this issue. However, quantifying the amount of produced ASR byproducts (i.e., ASR gel) in-service is still of great interest in the infrastructure industry. The overarching objective of this dissertation is to bring a new understanding to the fundamentals of ASR formation from a microwave dielectric property characterization point-of-view, and more importantly, to investigate the potential for devising a microwave nondestructive testing approach for ASR gel detection and evaluation. To this end, a comprehensive dielectric mixing model was developed with the potential for predicting the effective dielectric constant of mortar samples with and without the presence of ASR gel. To provide pertinent inputs to the model, critical factors on the influence of ASR gel formation on dielectric and reflection properties of several mortar samples were investigated at R, S, and X-band. Effects of humidity, alkali content, and long-term curing conditions on ASR-prone mortars were also investigated. Additionally, dielectric properties of chemically different synthetic ASR gel were also determined. All of these, collectively, served as critical inputs to the mixing model.

The resulting developed dielectric mixing model has the potential to be further utilized to quantify the amount of produced ASR gel in cement-based materials. This methodology, once becomes more mature, will bring new insight to the ASR reaction, allowing for advancements in design, detection and mitigation of ASR, and eventually has the potential to become a method-of-choice for in-situ infrastructure health-monitoring of existing structures.

ACKNOWLEDGMENTS

First and foremost, I would like to thank my beloved wife, Dina Hazzar for her enthusiasm, dedication, and camaraderie during a decade of living together. She was the only one who cheered me up during rough times, and it would not be possible to be where I am today without her emotional support and encouragement.

I would like to express my utmost gratitude to both Dr. Reza Zoughi and Dr. Kristen M. Donnell for their earnest support, devotion, and inspirations. Their admirable attitude, superior reassurance, and immense knowledge helped me throughout my entire Ph.D. studies and writing of this dissertation. Although this dissertation is an individual work, I could have never accomplished this without their help. I am also grateful to thank my advisory committee members Dr. Jun Fan, and Dr. Joe R. Stanley for their guidance and assistance. My special thanks goes to Dr. Kimberly E. Kurtis for her invaluable help, insights, and for educating me on the chemistry associated with cement-based materials.

It is a great pleasure to thank all my fellows at Applied Microwave Nondestructive Testing Laboratory (*amntl*), especially I would like to thank Dr. Mohammad T. Ghasr for his mentorship during my research work. I am also thankful to Mr. Marc Knapp and Mr. Mehdi Rashidi, my colleagues at Georgia Institute of Technology, for their collaboration on civil engineering aspects of this research.

I would like to acknowledge the National Science Foundation for financial support of this research under award No. 1234151, and the Missouri University of Science and Technology for awarding me the Dissertation Completion Fellowship.

Last but not least, this dissertation is dedicated to the spirits of my late parents, the two inspiring angels in my life whose memory will live on forever.

TABLE OF CONTENTS

LIST OF ILLUSTRATIONS

LIST OF TABLES

1. INTRODUCTION

1.1. MICROWAVE MATERIALS CHARACTERIZATION

Microwave materials characterization techniques have a long history dating back to the early 1950s [1]. However, tremendous advances have been made in that field within the past two decades. Microwave materials characterization techniques can be categorized as one of the diverse applications of microwave nondestructive testing (NDT) techniques, which is quite well established in the field of nondestructive evaluation. Microwave frequency spectrum spans form about 300 MHz to 30 GHz, which corresponds to the wavelength range of 1 meter to 10 mm. Figure 1.1, shows the frequency and wavelength ranges associated with microwaves.

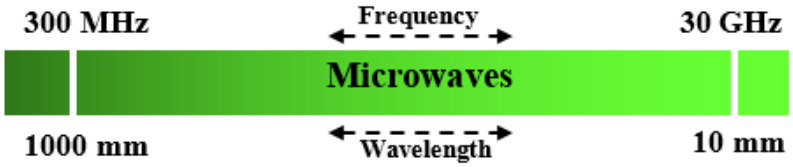

Figure 1.1. Microwave frequency range and associated wavelength.

Macroscopically, at microwave frequencies the electrical properties of materials can be related to those of its constituents and volume contents. Dielectric materials like concrete, since most of the charge carriers are bound, cannot contribute to electrical conduction. They allow microwave signals to penetrate into the medium and displace the bound charges; hence polarization. Ionic conduction, dipolar relaxation, atomic

polarization, and electronic polarization are the main mechanisms of that contribute to the polarization of a dielectric material [2]. In a linear isotropic medium the relationship between electric polarization vector ($\vec{P}_e$), electric displacement flux ($\vec{D}$), and dielectric constant (ε) are defined as denoted in the following equation [3].

$$\vec{P}_e = \varepsilon_0 \chi_e \vec{E} \tag{1}$$

$$\vec{D} = \varepsilon_0 \vec{E} + \vec{P}_e = \varepsilon_0 (1 + \chi_e) \vec{E} = \varepsilon \vec{E} \tag{2}$$

where ε_0, χ_e, and $\vec{E}$ represent the permittivity of free-space, electrical susceptibility and electric field, respectively. Complex dielectric constant (ε) is composed of two components and when referenced to free space, is denoted as:

$$\varepsilon_r = \varepsilon'_r - j\varepsilon''_r \tag{3}$$

where the real part (relative permittivity) represents the ability of a material to store microwave energy and the imaginary part (relative loss factor) represents the ability of a material to absorb microwave energy. Both permittivity and loss factor are frequency dependent and are unique to every single material independent of the measurement method. At low frequencies, ε is dominated by the influence of ion conductivity, while the variation of permittivity in the microwave range is mainly caused by dipolar relaxation. The absorption peaks in the infrared region and above is mainly due to atomic and electronic polarizations. Figure 1.2 shows a typical behavior of relative permittivity and loss factor as a function of frequency [4].

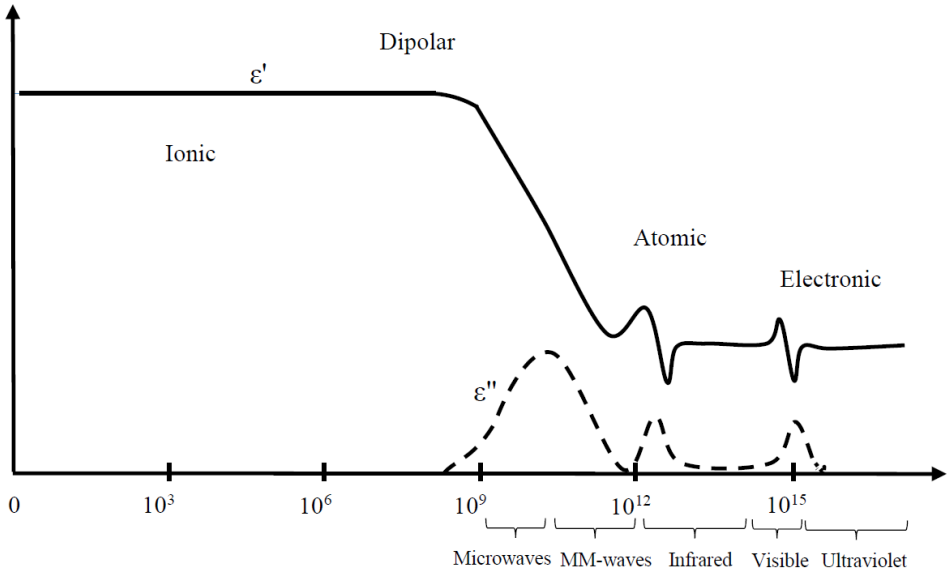

Figure 1.2. Frequency dependence of complex dielectric constant.

Significant research has been carried out within the past decades to apply microwave materials characterization techniques to variety of problems in materials research and engineering disciplines. Some of those efforts include dielectric property characterization, mixture constituent determination, porosity evaluation in polymers, moisture content measurements, cure monitoring of binders, rubber products, and cement-based materials [5]–[19]. Most recently, microwave materials characterization techniques have shown great potential in evaluation of other chemical reactions such as carbonation, and alkali-silica reaction (ASR) within cement-based materials [20]–[30]. This dissertation is mainly focused on evaluation of the alkali-silica reaction (ASR) formation in cementitious materials, using microwave materials characterization techniques.

1.2. ALKALI-SILICA REACTION BACKGROUND

Alkali-silica reaction (ASR) was first identified by Stanton in the late 1930s [31]. Since then, ASR has been recognized as one of the most common causes of cementious structures deterioration. It is defined as the reaction between the alkalis (sodium and potassium) in portland cement and certain siliceous rocks or minerals such as opaline, chert, strained quartz, and acidic volcanic glass, present in some aggregates [32]. The reaction commences in the pore solution of the cement-based structures in presence of sufficient amount of moisture.

Prior to ASR formation and in the presence of reactive aggregates, OH^- and the alkali Na^+ and K^+ react with reactive silica (SiO_2), as [33]:

$$Si\text{-}OH + OH^- + Na^+, K^+ \rightarrow Si\text{-}O\text{-}Na, K + H_2O \quad (4)$$

$$Si\text{-}O\text{-}Si + 2OH\text{-} + 2Na+, K+ \rightarrow 2(Si\text{-}O\text{-}Na, K) + H2O \quad (5)$$

The product of this reaction is known as ASR gel. The gel formed around and within the aggregate is hygroscopic and attracts water from surrounding cement paste. As a result, the gel starts to expand. Initially the gel expands and fills the pores, once the pressure due to expansion (caused by ASR formation) surpasses the tensile strength of the surrounding paste, internal micro cracking in the structure commences and this reaction cycle continues repeatedly until such time that leads to surface cracking and eventually structure deterioration.

Conforming to above discussion on reaction and expansion procedure, three fundamental requirements for ASR damage are vital; reactive silica, sufficient alkali, and sufficient moisture [34], as shown in Figure 1.3.

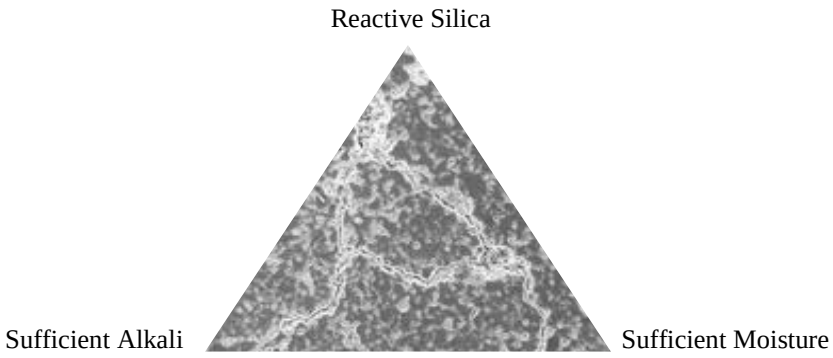

Figure 1.3. Three requirements for ASR[1].

Given that rocks are composed of minerals, reactive silica can be found in reactive minerals in different types of rocks. For instance, opal, tridymite, cristobalite, volcanic glass and strained quartz are of those minerals that can be found in various rocks such as shale, limestone, sandstone, chert, flint and so on. However, it should be noted that all sources of such rocks will not result in ASR damage and the reactivity of a certain rock only depends on the type and quantity of reactive minerals present in the rock. The other requirement (i.e., sufficient alkali) for ASR damage is mainly found in portland cement. However, other cementing materials (e.g., fly ash, slag and silica fume), chemical admixtures, wash water and external sources (e.g., sea water, deicing chemicals) may also provide additional amounts of alkali to the reaction. Moisture is the third requirement for ASR damage. It both sustains the reaction and provides for gel expansion.

It is known that below about 80% of relative humidity ASR production is not likely to occur anymore [35]. This highlights the significance of moisture content observation while studying ASR gel formation and characterization. Microwave materials

[1] Image courtesy of Amal Jayapalan from Georgia Institute of Technology.

characterization techniques are quite sensitive to the presence of water [36]. Particularly in concrete, ASR gel has the tendency to imbibe free water from its surroundings, where it subsequently binds with the gel causing its expansion. The gradual transformation of free to bound water manifests itself as change in the measured temporal dielectric properties of cement-based materials containing ASR gel. This behavior is due the fact that free water has significantly different dielectric properties than that of bound water. As a result, microwave dielectric property characterization is a great candidate to evaluate ASR formation, where the specimens containing ASR gel interact differently to the amount of available water, compared to the samples with no ASR gel.

1.3. DIELECTRIC MIXING MODEL BACKGROUND

Dielectric mixing models relate the macroscopic dielectric properties of a heterogeneous mixture to the volumetric content of the individual components and their dielectric properties [37]. In a dielectric mixing model development, it is desired to treat a mixture as a homogeneous medium and characterize it through an effective dielectric constant. The effective dielectric constant of the mixture (e.g., concrete, mortar) is then related to the volumetric content of its constituents, and the dielectric constants of the individual components (i.e., inclusions). Since several mixing models can be true for one mixture, any proposed dielectric mixing model needs to be validated through experimental data. In dielectric mixing modeling a background or host medium is determined with dielectric constant of ε_h, within which, inclusions with simple geometry are randomly distributed.

There exist various dielectric mixing models, each model characterizing a specific material with unique properties. For instance, multiple dielectric mixing models have been applied to soil [38]–[41], and granular materials [42]. Classical mixing models have also been utilized to characterize snow [43], sea ice [37] , and woody biomass [44].

In general, dielectric mixing models can be divided into multiple categories according to their derivations, applications, inclusion shapes, conditions, and assumptions. As such, mixing models can be derived either empirically or semi-empirically. Also they can be applied on either single phase (inclusion) or multiphase mixtures. Maxwell-Garnet rule, power law, Polder van Santen, Wiener, and Pearce are other examples of well-known classical dielectric mixing models that are discussed in literature [45]–[47].

1.4. RESEARCH OBJECTIVES

The overarching objective of this dissertation is to bring a new understanding to the fundamentals of alkali-silica reaction (ASR) formation, and develop a dielectric mixing model capable of determining the volumetric content of the inclusions of mortars containing ASR gel. To achieve this goal, two primary tasks were followed. First, the temporal complex dielectric constants of chemically different mortar samples were measured (measurement phase). Second, an empirical dielectric mixing model was developed based on the measurements in order to obtain volumetric information regarding the mortars' constituents (modeling phase).

1.4.1. Measurement Phase. Due to the sensitivity of microwave signals to the moisture content of dielectric materials (e.g., mortar, concrete), temporal microwave dielectric property measurements were conducted to track the water content of the mortar

samples as an indication of ASR gel formation. Since this dissertation is the first effort of its type as it relates to ASR evaluation with microwaves, multiple mortar samples (with different aggregate types and mix designs) were cast and their dielectric properties examined at three distinct frequency bands: R-band (1.7 - 2.6 GHz), S-band (2.6 - 3.95 GHz), and X-band (8.2 - 12.4 GHz). This significant amount of data provided a comprehensive database for further analysis of ASR temporal behavior, and served as a critical input to the modeling phase. Table 1.1 summarizes the various mortar batches that were produced and their temporal dielectric constants measured in order to analyze different influential factors on ASR formation.

Table 1.1. Temporal dielectric properties measurements.

Set #	Frequency Band	Mix Design				Purpose	Comment
		R*	NR**	NaOH	Agg. size		
1	S, X	●	●	●	Fine (F)	investigate effect of soaking	3 cycles, each 65 days
2	S, X	●	●	●	F	carbonation detection	after soaking
3	R	●	●	●	F	investigate effect of humidity	low humidity – 85 days
4	R	●	●	-	F		
5	R	●	●	●	F	compare with S and X-band measurements	hot and humid - 85 days
6	S	●	●	-	F	compare with samples having NaOH	85 days
7	X	●	●	-	F		85 days
8	S	●	-	●/-	F	investigate effect of NaOH in early cement hydration	reactive w/ and w/o NaOH
9	S	●	-	●	F	evaluate air content, hydration effects, etc. (1-year test)	air content
10	S	●	-	●	F		humid
11	S	●	-	●	F		dry
12	S	●	-	●	F		hybrid
13	x	●	-	●	F		Air content
14	x	●	-	●	F		humid
15	x	●	-	●	F		dry
16	x	●	-	●	F		hybrid
17	R, S, X	●	●	●	Coarse (C)	made for preliminary measurements of 8” blocks	Concrete (2 months)
18	R, S, X	●	●	●	C		
19	R, S, X	●	●	●	C,F	according to the matrix from G-tech, for long term measurements (1-year test)	8"x8"x8" blocks
20	R, S, X	●	●	●	C,F		
21	R, S, X	●	●	●	C,F		
22	R, S, X	●	●	●	C,F		
23	S	●	●	●	F	keep the samples at different humidity levels to see the effect of humidity on ASR production	65% - 85 days
24	S	●	●	●	F		85% - 85 days
25	R, S, X	●	●	●	F	frequency sensitivity to humidity	aged mortar (20%, 65%, 75%, 85% RH)
26	S	●	●	●	F	to evaluate effect of water and NaOH exposure	-
27	S,X	●	●	-	F	reactive and non-reactive aggregate measurement	-
28	J, X, Ku	N/A	N/A	N/A	N/A	ASR powder measurement	-
29	X	N/A	N/A	N/A	N/A	different synthetic gels created in GT	13 different types

R*: Reactive
NR**:Non-reactive

1.4.2. Modeling Phase. For the modeling phase of the investigation, a comprehensive dielectric mixing model is developed for mortar samples with and without ASR gel. The model is developed based on the temporal changes of both dielectric properties and volumetric content of the inclusions (i.e., water, air, ASR gel). The dielectric properties of the inclusions were either modeled (as a function of frequency, temperature, ionic conductivity) or measured directly.

In the proposed dielectric mixing model, mortar is considered as a simple, homogeneous, and isotropic material. The paste is considered as the host (background) material, while air content (indication of porosity), water (at different states), and ASR gel (either liquid or solid) are determined as the inclusions. Figure 1.4 shows the simplified mortars' materials matrix with respect to the predefined host and inclusions. The details of the modeling process are explained in the following papers.

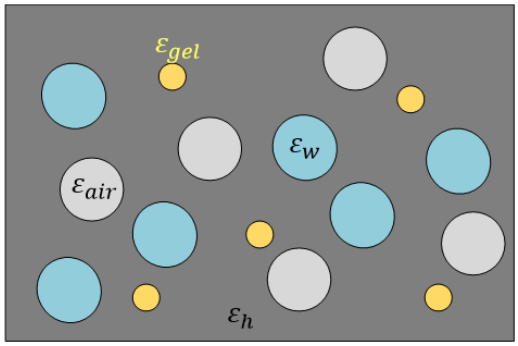

Figure 1.4. Simplified illustration of ASR-reactive sample with dielectric constant of host (ε_h), air (ε_{air}), water (ε_{water}), and ASR gel (ε_{gel}).

1.5. ORGANIZATION OF THE DISSERTATION

As mentioned earlier, this investigation is the first effort of its type as it relates to ASR evaluation with microwaves. Thus, various experiments, mix designs, modeling, and simulations have been conducted to examine different aspects of the complicated reaction of ASR. However, the most relevant and critical findings are outlined in this dissertation, and they appear in the following papers.

In paper I, dielectric constant measurements of mortar samples at R-band (1.7 - 2.6 GHz), S-band (2.6 - 3.95 GHz) and X-band (8.2 - 12.4 GHz) are presented. The main objective of this investigation was to evaluate the behavior of the mortar samples at different microwave frequency bands and find out which frequency band suits best for monitoring of ASR gel behavior. The paper presents the measured results for mortar samples made with reactive and non-reactive aggregates. The measurement results and subsequent analyses aid in a better understanding of the microwave signals interaction with ASR-affected cement-based materials.

Paper II investigates the effect of humidity as well as chemical composition on ASR gel production in mortars. In the paper three different experiments have been discussed and reported. In each experiment, two sets of mortar samples, each set consisting of 3 samples for averaging purposes, were cast using different types of crushed aggregates; reactive (i.e., with tendency to produce ASR gel) and non-reactive. The purpose of this experiment was to study the effect of humidity levels (above and below 80%) on ASR formation and subsequent dielectric properties.

In paper III, two sets of mortar samples at S-band (2.6 – 3.95 GHz) were cast and cured in hot and humid conditions, with one set including sodium hydroxide (i.e., ASR

accelerator) in the mix design and the other set without sodium hydroxide (NaOH). Both sets of samples contained reactive aggregates only. The main purpose of this study was to compare how NaOH accelerates ASR gel production. The influence of alkali addition on the heat of hydration, compressive strength, water absorption, and bulk resistivity of the mortars were also investigated. A correlation was observed between the measured dielectric loss factor, bulk resistivity, and compressive strength of the mortars. However, the trends in high-alkali mortars did not follow the same trend as in the low-alkali mortars. This fact may be an identifying parameter that can be further utilized to develop a versatile microwave nondestructive technique capable of evaluating alkalinity in cement-based materials.

In paper IV, six sets of reactive mortar samples were cast at S-band (2.6 – 3.95 GHz). The main purpose of this study was to keep the samples at different curing conditions and compare the behavior of their dielectric constants (and also possible ASR gel formation) during prescribed conditions. The three sets of samples were exposed to different humidity conditions for different amounts of time. The results showed slightly different permittivities for the differently cured samples, potentially indicating different amount of ASR gel production. This observation was corroborated through optical microscopy imaging, where different ASR indices were observed in the mortar samples. The outcome of this paper can be further utilized in future pertinent investigations to develop a robust nondestructive microwave technique in evaluation of ASR formation in cement-based structures.

The dielectric constant of ASR gel is a critical input into the dielectric mixing model of the ASR affected mortars. Paper V in this dissertation presents the results of

microwave dielectric property measurement of twelve laboratory-produced (synthetic) ASR gels at X-band (8.2-12.4 GHz). Results show an exponential decay of loss factor as a function of increasing silica-to-alkali content of gels, suggesting a correlation with increase in bound water in the samples and a decrease in the fluid ionic concentration. The results of this study, provide a critical input that is required for development of the dielectric mixing model.

Paper VI incorporates all of the findings of this research, and presents an empirical multi-phase dielectric mixing model capable of predicting the effective dielectric constants of the mortars with and without ASR gel. From a microwave point-of-view, the finding of this paper are important objective of the entire project through which critical information of ASR formation may be obtained. The model incorporates the complex microwave dielectric constant of the mortars' inclusions (as a function of frequency, temperature, ionic conductivity, etc.) as well as their volumetric contents to find out the effective dielectric constant of the mortars. The modeling results are then compared to the temporal dielectric measurement of the mortars, showing a very close correlation.

The overall findings of this research, reported through this dissertation, indicate a great potential for microwave NDT techniques to become a method-of-choice for ASR detection and evaluation, where other NDT techniques may be deficient.

PAPER

I. COMPARISON OF ALKALI–SILICA REACTION GEL BEHAVIOR IN MORTAR AT MICROWAVE FREQUENCIES

ABSTRACT

Alkali-silica reaction (ASR) is one common cause of concrete deterioration and has been a growing concern for decades. Water, in the presence of reactive aggregates used to make concrete, plays a major role in the formation, sustainment and promotion of this reaction. In this process, free water becomes bound within ASR gel, resulting in expansion and deterioration of concrete. Devising a test approach that is sensitive to the state of water (free or bound) has the potential to become a method-of-choice for ASR detection and evaluation, since such measures can be used to detect ASR and potentially quantify reaction progression. Microwave signals are sensitive to the presence of water, since the water relaxation frequency occurs in this frequency range. Recently microwave nondestructive evaluation techniques have shown great potential to evaluate and distinguish between ASR-affected mortar samples and those without ASR gel. Given the complex chemistry of ASR products, their behavior is expected to differ at different microwave frequency bands. To evaluate the sensitivity of different frequencies to the presence of ASR, dielectric constant measurements were conducted at R-band (1.7 - 2.6 GHz), S-band (2.6 - 3.95 GHz) and X-band (8.2 - 12.4 GHz). This paper presents the measured results for mortar samples made with reactive and non-reactive aggregates. The measurement results and subsequent analyses aid in a better understanding of the microwave signals interaction with ASR-affected cement-based materials. Moreover, the

results indicate that S-band appears to be the most appropriate frequency band for ASR evaluation in the microwave regime.

Index Terms: Alkali–silica reaction (ASR) gel, concrete, dielectric constant, microwave nondestructive testing.

1. INTRODUCTION

Alkali-silica reaction (ASR), either in concrete or mortar, takes place between reactive minerals present in some aggregate and alkali hydroxides, contributed most often by the cement or from external sources (e.g., deicing chemicals). The product of ASR is a gel which expands and, in the presence of sufficient moisture, leads to cracking. Understanding the mechanisms of ASR damage and methods to mitigate it has been the focus of research for many years. However, devising a robust method to determine the extent of damage to existing structures has yet to occur [1].

The current nondestructive evaluation (NDE) techniques for ASR assessment can be divided into four major categories, namely: visual inspection, expansion measurements, electromagnetic methods and seismic-wave methods. The first two methods are rather simple, but often inaccurate and inefficient while the last two are more scientific and well-established, but are also more sophisticated. Diffused ultrasonic techniques [2], linear and nonlinear acoustic methods [3-5], and seismic tomography [6-7] can be classified as seismic-wave methods, while ground penetrating radar (GPR), electrical resistivity, and capacitive methods belong to the electromagnetic techniques [8]. Each of these methods has its own benefits and limitations and none by itself is fully effective and robust.

Microwave nondestructive testing and evaluation (NDT&E) techniques have shown tremendous potential for evaluation of a wide range of material properties associated with a diverse array of cement-based materials such as:

- evaluation of water-to-cement ratio (w/c) and compressive strength of hardened cement paste [9-12],

- evaluation of fresh concrete; porosity and sand-to-cement (s/c) ratio in mortar [13],
- evaluation of coarse aggregate-to-cement (a/c) ratio in concrete [14],
- cure-state and material properties of concrete [12, 15-16],
- grout detection in masonry bricks [17],
- detection of delamination between hardened cement paste and fiber-reinforced polymer (FRP) composites[18-19],
- investigating effects of chloride and cyclical exposure to it in mortar [20-22],
- microwave imaging [23], and
- most recently, the potential for carbonation detection using microwave dielectric measurements [24].

In recent years, microwave materials characterization techniques have also been used to detect ASR gel production and study its behavior in mortar with different types of fine aggregates [25-27]. The encouraging results [25] led to further investigation involving new samples suitable for complex dielectric property measurements (intrinsic to material characteristics) at S- (2.6-3.95 GHz) and X-band (8.2-12.4 GHz) [26]. Furthermore, with respect to ASR gel, research by Kirkpatrick et. al. [28] suggests that water molecules are held between nano-particles within the gel and are thought to behave as bound water. Given that ASR gel formation involves transformation of free to bound water, and the fact that microwave signals are more sensitive to bound water at lower frequencies, and the ionic nature of the pore solution affecting dielectric loss factor, measurements at R-band (1.7-2.6 GHz) were conducted. Therefore, the goal was to see whether measurements at R-band

exhibited any unique characteristics that would be indicative of the aforementioned transformation. In addition and importantly, the pore solution chemistry of these samples was also considered in the overall analyses of these results.

2. ASR BACKGROUND

The chemical reaction between alkalis (sodium and potassium) present in portland cement (the most common type of cement used in concrete making) and certain siliceous minerals (e.g., opal, obsidian, cristobalite, tridymite, chalcedony, cherts) present in some aggregates is known as alkali-silica reaction (ASR).The product of this reaction is a gel whose expansion can limit service (e.g., impeding movement of spillway gates in dams) and also causes concrete to progressively crack and eventually deteriorate [29].

In concrete, aggregates are bound together by a nano- to micro-porous hydrated cement paste. Water held in the variously sized pores is known as the "pore solution". Alkali cations (Na+ and K+), along with lower concentrations of other cations, are balanced by hydroxyl ions (OH-) which altogether results in a relatively high pH level (12.4-13.9) [30]. In the presence of reactive aggregates, OH- and the alkali Na+ and K+ react with reactive silica (SiO2), as [31]:

$$\text{Si-OH} + \text{OH}^- + \text{Na}^+, \text{K}^+ \rightarrow \text{Si-O-Na, K} + \text{H}_2\text{O} \quad (1)$$

$$\text{Si-O-Si} + 2\text{OH-} + 2\text{Na+, K+} \rightarrow 2(\text{Si-O-Na, K}) + \text{H2O} \quad (2)$$

The ASR gel (Si-O-Na, K), formed around and within the aggregates, is hygroscopic and attracts water from the surrounding cement paste, leading to gel expansion. ASR damage, then, requires the presence of moisture; according to a related investigation in [32], damage is unlikely to occur below an internal relative humidity of ~80%, implying that structures that exposed to external sources of moisture are more vulnerable to ASR damage compared to those that remain in relatively dry conditions.

Once the pressure due to expansion exceeds the tensile capacity of the surrounding hardened paste, cracking will result. Crack growth and coalescence eventually increases the concrete permeability, increasing the rate of structural deterioration. Figure 1, depicts ASR formation, expansion and cracking pattern inside concrete structure.

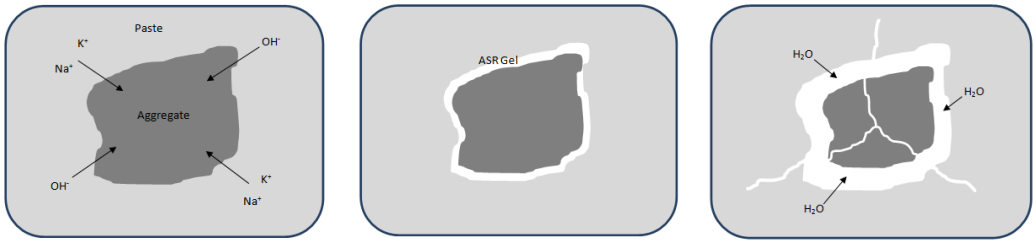

(a) (b) (c)

Figure 1. ASR formation in concrete: a) alkali ions attack reactive silica in aggregate, b) gel formation around aggregate, and c) gel expansion due to water absorption.

3. DIELECTRIC CONSTANT

Unlike metals, dielectric materials (e.g., concrete) consist of bound charges and cannot contribute to electrical conduction. Consequently, microwave signals which penetrate dielectric media displace these bound charges and result in material polarization. In a linear and isotropic medium (such as cementious materials) the relationship between electric polarization vector (P ⃗_e), electric displacement flux (D ⃗), and complex dielectric constant (ε) are defined as denoted in the following equation [33-34].

$$\vec{P}_e = \varepsilon_0 \chi_e \vec{E} \tag{3}$$

$$\vec{D} = \varepsilon_0 \vec{E} + \vec{P}_e = \varepsilon_0 (1 + \chi_e) \vec{E} = \varepsilon \vec{E} \tag{4}$$

where ε_0, χ_e, and $\vec{E}$ represent the permittivity of free-space, electrical susceptibility and electric field, respectively. Complex dielectric constant (ε) is composed of two components and when referenced to free space, is denoted as:

$$\varepsilon_r = \varepsilon'_r - j\varepsilon''_r \tag{5}$$

where the real part (relative permittivity) represents the ability of a material to store microwave energy and the imaginary part (relative loss factor) represents the ability of a material to absorb microwave energy. Both permittivity and loss factor are frequency dependent, intrinsic to a given material and independent of the method used to measure them. Dielectric constant (effective) of a mixture (e.g., concrete) is directly influenced by its respective constituent dielectric constants and their volumetric content (i.e., paste,

water-to-cement ratio, aggregate content, etc.) as well as any chemical reaction (i.e., cement hydration, ASR gel formation, etc.) that may be taking place [34]. Consequently, temporal dielectric property characterization of a material can provide significant information about its materials properties and any changes. Particularly in concrete, ASR gel has the tendency to imbibe free water from its surroundings, where it binds with the gel. The gradual transformation of free to bound water manifests itself as temporal change in the measured temporal dielectric constants of cement-based materials with ASR gel since free water has significantly different complex dielectric properties than that of bound water [35]. Thus, studying the temporal behavior of dielectric constants of mortar samples with and without ASR gel not only yields important information about the presence of ASR gel but also indicates the level of frequency sensitivity to the gel production. The latter may then be used for an optimal (future) NDE method for this purpose.

4. SAMPLE PREPARATION

4.1. MIX DESIGN

To evaluate and compare the presence of ASR gel in mortar, two sets of samples were produced using different types of crushed fine aggregate; namely, one which is known to be reactive and one non-reactive. Following the ASTM C1260 accelerated mortar bar test standard [36], the average 14-day expansions was measured to be 0.0787% and 0.383% for the non-reactive and reactive samples, respectively. Both mixtures had an aggregate-to-cement ratio (a/c) of 2.25 and a water-to-cement ratio (w/c) of 0.47, both by mass. To accelerate the reaction, sodium hydroxide (NaOH) was added to the mixing water of both mixtures for a total equivalent alkali content of 0.9% by mass of cement as per [39]. Table I summarizes the mix design for the samples.

Table 1. Mix design.

Mix Proportions	**Sample Type**	
	Reactive	***Non-Reactive***
Cement	Portland Type I/II	Portland Type I/II
Aggregate	Rhyolite	Limestone
w/c	0.47	0.47
a/c	2.25	2.25
Alkali Content	0.9%	0.9%

4.2. CURING CONDITION

Initially the samples were cast to fit tightly inside of rectangular waveguide sample holders at S-band (2.6 – 3.95 GHz) and X-band (8.2 – 12.4 GHz) [26]. Later, similar samples were cast for measurement at R-band (1.7 – 2.6 GHz). The temporal dielectric constants of these samples were then measured regularly using the well-known completely-filled waveguide technique [38]. Following are the corresponding waveguide dimensions in each frequency band, for the total of 18 samples (i.e., 3 sets, 3 reactive and 3 non-reactive samples per frequency band), six with a cross-section of 10.92 × 5.46 cm (R-band), six with a cross-section of 7.21 × 3.4 cm (S-band) and six with a cross-section of 2.28 × 1.01 cm (X-band). All samples were ~2-3 cm in length. Fig. 2 shows the actual samples for each frequency band. The samples were cast in molds, and were removed ~24 hours after mixing. In order to provide sufficient moisture to sustain ASR gel production, the samples were stored in a hot and humid chamber at a nominal temperature of 38ºC in a plastic container and placed above water which provided a constant relative humidity (RH) of 80% or more. Every 2-3 days, the samples were removed from the chamber for microwave measurements which took ~45 minutes per each frequency band. After 24-26 days, the samples were removed from the hot and humid container and placed in ambient conditions (23° C ± 2° C, 35% ± 5% RH). Microwave dielectric measurements continued in the same fashion for approximately another two months.

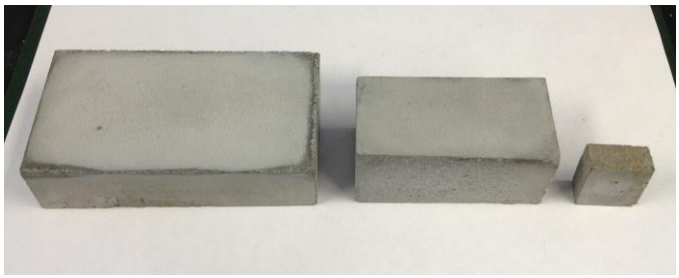

Figure 2. Representative samples for: a) R-band, b) S-band, and c) X-band.

5. MICROWAVE DIELECTRIC MEASUREMENTS

5.1. MEASUREMENT SETUP

The calibrated full two-port S-parameter measurements (i.e., S11, S21, S12 and S22) were conducted using an Agilent 8510C Vector Network Analyzer (VNA), shown in Fig. 3 with the R-band sample holder.

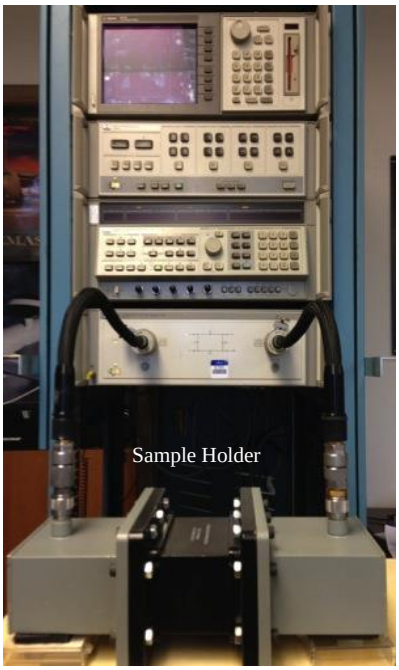

Figure 3. General measurement setup of VNA shown with R-band sample holder.

5.2. MEASUREMENT RESULTS

The dielectric property measurements at S-band and X-band have been already reported in [25]. However for comparison purposes, the corresponding figures were reproduced (by permission from the publisher) and provided here so that the results may

be readily compared with the newly investigated R-band samples. The measurement results can be divided into two separate periods; namely, when the samples were kept in a hot and humid condition (in an oven) and when they were drying in the ambient condition. Figures 4a-c, and Figs. 4d-f show the measured relative permittivity of the samples at 2 GHz (R-band), 3 GHz (S-band) and 10 GHz (X-band), and the loss factor at the same frequencies, respectively. It should be mentioned that the absence of data points in the X-band measurements (Figs. 4c, 4f) between Day 36 and the final day (Day 85) is simply due to the fact that no measurement was conducted during that period.

During the hot and humid period a slight increase can be observed in the (relative) permittivities at all three frequencies and for both sample types. However, it is clearly seen that the rate of increase in permittivity is higher for the non-reactive samples compared to the reactive samples during this period. This behavior may be explained by studying the dielectric constant of free water. To this end Fig. 5a shows the permittivity of pure and sea water (i.e., saline with a salinity of 32.54 g/Kg) at 20˚C and 38˚C as a function of frequency, based on the Debye model [39]. As it can be seen, free water has a high (relative) permittivity at frequencies ranging from 1 GHz to ~10 GHz, and thereafter it decreases. Given the relatively low permittivity of the other constituents of mortar, it is clear that the permittivity of free water dominates the overall permittivity of mortar at the measured frequencies. This means that the effective permittivity of the samples is highly affected by the permittivity of the available free water in them. Thus, any increase in the permittivities of the samples during hot and humid conditions is thought to be directly related to the presence of free water in the samples. During this time, the permittivity could be increased by transport of free water from the humid environment into the reactive and non-reactive

samples or decreased by the translation of formerly free water into bound water, as the cement hydration reactions – and potentially ASR – progress. It can be presumed that the effects of moisture transport and cement hydration are reasonably similar for the two sets of samples, and that variations between the two are likely related to differences in the aggregate reactivity.

Since in the reactive samples the additional free water becomes increasingly bound with the ASR gel, the relative permittivity of reactive samples indicate reduced temporal variation compared to the non-reactive samples, indicating a more of a temporal change. In other words, the smaller change in permittivity for the reactive samples indicates (at least partially) the transformation of free water into bound water through ASR gel formation. On the other hand, the larger change in the permittivity, in the non-reactive samples, is an indication of continual uptake of free water, since we expect less free water to be transformed into bound water in the absence of ASR gel.

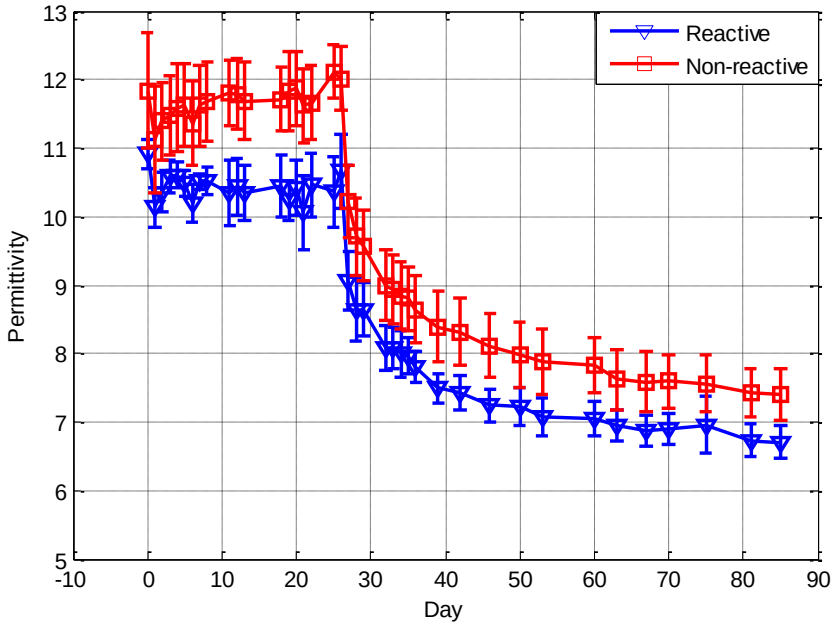

(a)

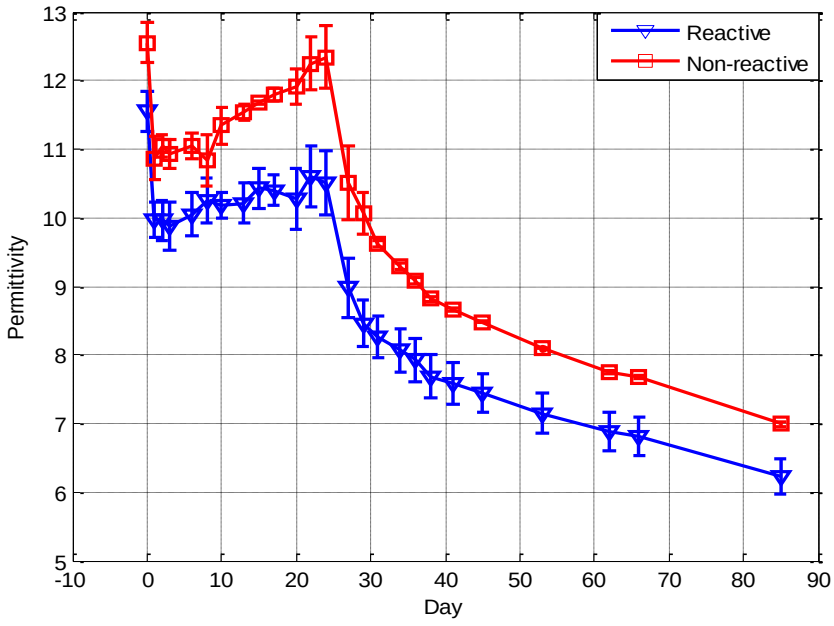

(b)

Figure 4. Measured relative permittivity at: a) 2 GHz (R-band), b) 3 GHz (S-band) and c) 10 GHz (X-band); and relative loss factor at: d) 2 GHz (R-band), e) 3 GHz (S-band) and f) 10 GHz (X-band). Figures at 3 GHz and 10 GHz are reproduced from [25], Materials Letters, by permission, © 2012 Elsevier.

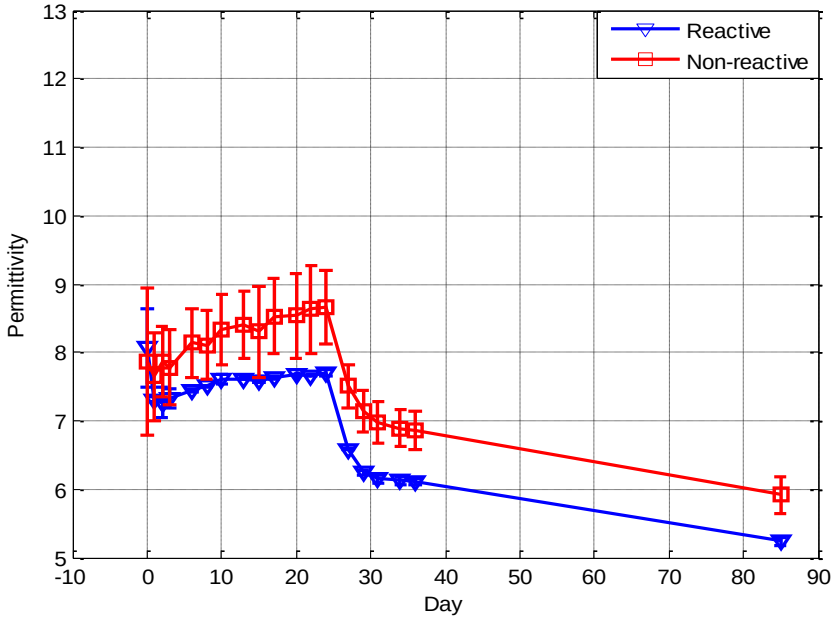

(c)

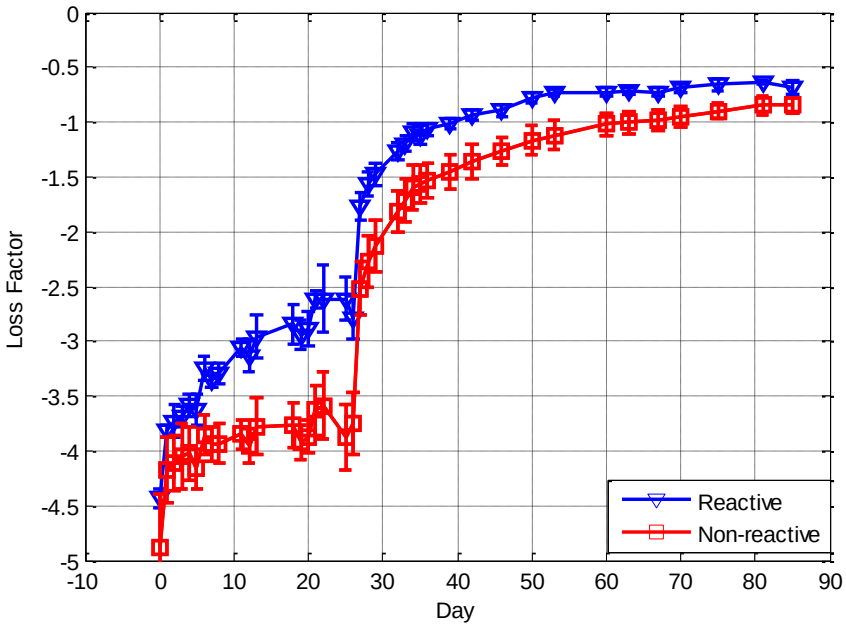

(d)

Figure 4. Measured relative permittivity at: a) 2 GHz (R-band), b) 3 GHz (S-band) and c) 10 GHz (X-band); and relative loss factor at: d) 2 GHz (R-band), e) 3 GHz (S-band) and f) 10 GHz (X-band). Figures at 3 GHz and 10 GHz are reproduced from [25], Materials Letters, by permission, © 2012 Elsevier (cont.).

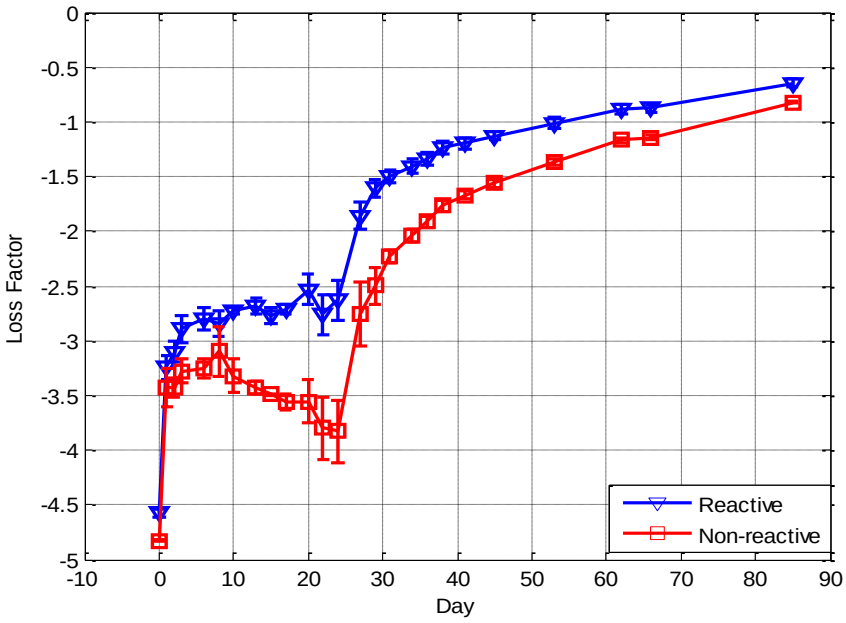

(e)

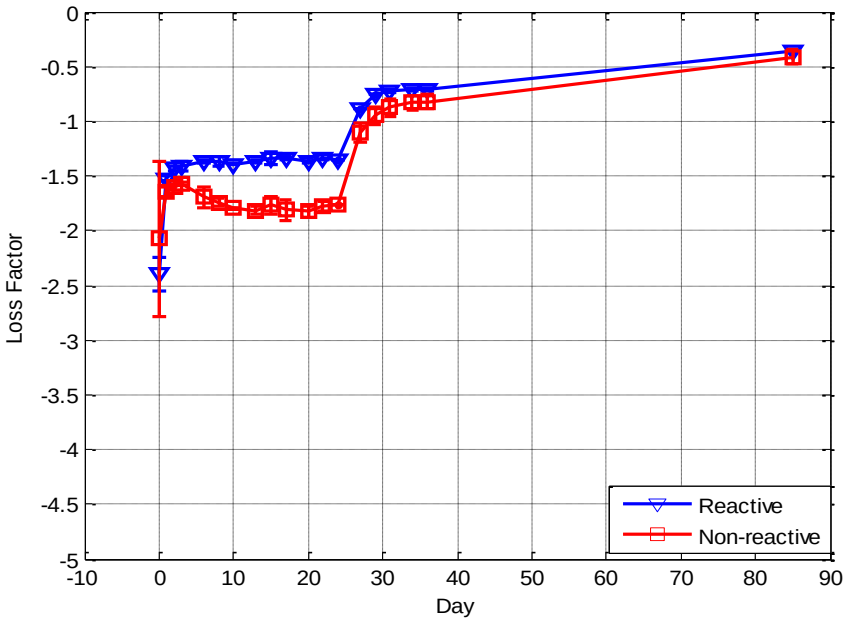

(f)

Figure 4. Measured relative permittivity at: a) 2 GHz (R-band), b) 3 GHz (S-band) and c) 10 GHz (X-band); and relative loss factor at: d) 2 GHz (R-band), e) 3 GHz (S-band) and f) 10 GHz (X-band). Figures at 3 GHz and 10 GHz are reproduced from [25], Materials Letters, by permission, © 2012 Elsevier (cont.).

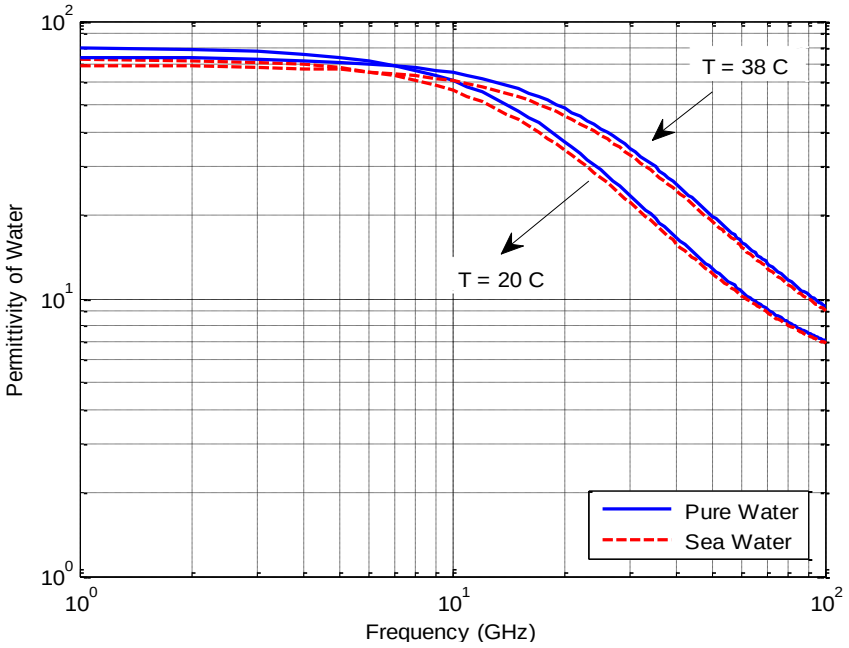

(a)

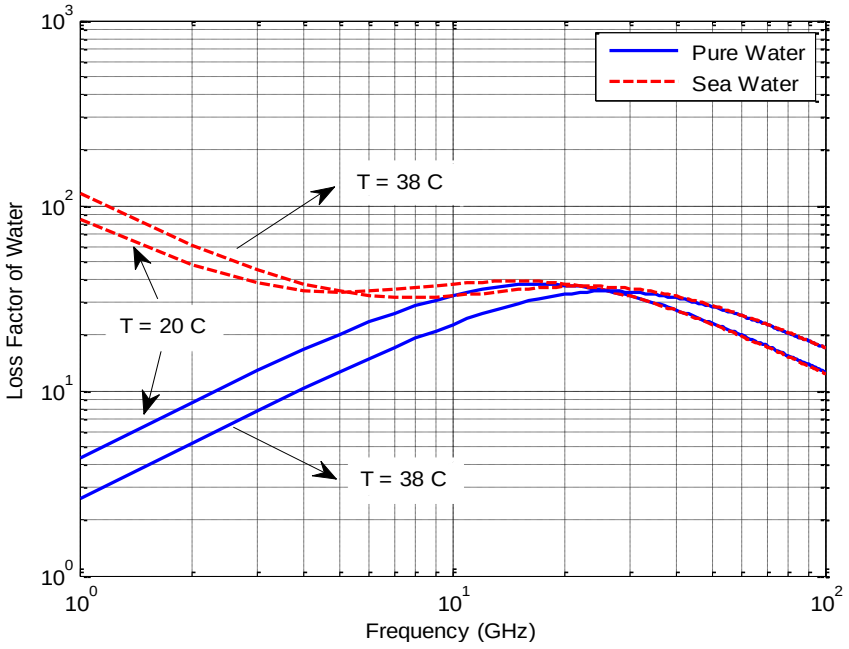

(b)

Figure 5. Dielectric constants of pure and saline water as a function of frequency, a) permittivity, and b) loss factor [39].

The behavior of loss factor is different at different frequency bands. Comparing R- and S-band results for the non-reactive samples during the hot and humid period the S-band results (Fig. 4e) show the loss factor increased (loss factor is a negative value in the figures), indicating greater availability of free water. On the other hand, the loss factor of the samples at R-band (Fig. 4d), continually decreased during this period. This may then be attributed to the higher sensitivity of S-band to free water and less sensitivity of R-band frequencies to presence of free water.

Looking at the loss factor of the reactive samples at S-band during the hot and humid condition when ASR gel formation is expected, a portion of the available free water becomes bound in the gel. This leaves less available free water in these samples compared to the non-reactive samples. Thus, observations of less change in the loss factor of the reactive sample compared to the non-reactive sample are consistent with the stated hypothesis in the previous paragraph (i.e., more sensitivity of S-band to free water). On the other hand, at R-band the change in loss factor during the same period is markedly more than those at S- and X-band. This points to the ability to monitor transformation of free water to bound water at R-band for these specific ASR-prone samples.

The changes in temporal permittivity and loss factor of the samples while they were kept in the oven (hot and humid condition), and during the drying period are illustrated in Fig. 6a and 6b, respectively (dots represent actual measurement and the lines are curve fit through the measured points using the same quadratic equation). During the drying period, the additional free water, which was readily available to the samples in the humid conditions, is continually lost to evaporation. This is also evident by the temporal decrease in both permittivity and loss factor of the samples for all the three frequency bands.

According to Fig. 6, S-band results show the most change followed by R-band and X-band, respectively. These changes are the consequence of either the presence of ASR gel (in reactive samples) or lack thereof (in non-reactive samples) during drying period. This behavior implies that S-band may be more sensitive to humidity/moisture level in the sample pores compared to the two other frequency bands. Moreover, the overall higher rate of change in S-band measurements during the hot and humid period also supports the expectation that S-band is more sensitive to changes in the relative humidity in the samples (i.e., presence of free water).

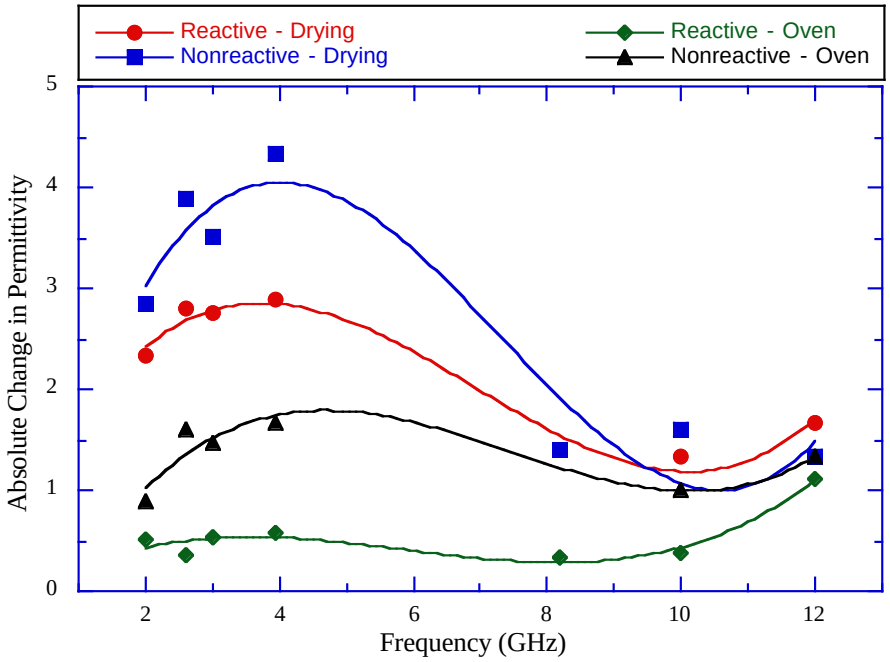

(a)

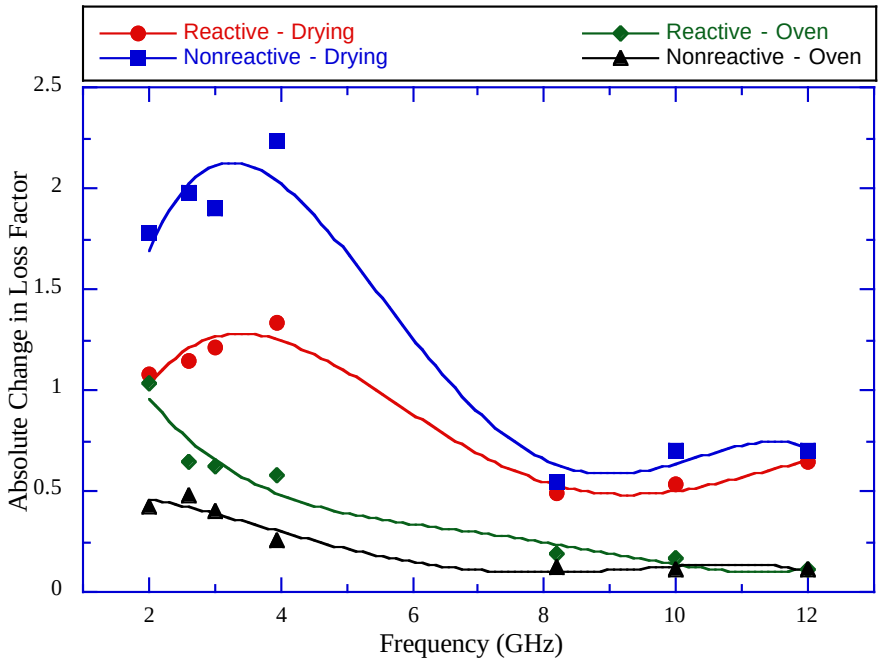

(b)

Figure 6. Total temporal change of dielectric constants during humid and drying periods, a) permittivity, b) loss factor.

6. DISCUSSION OF RESULTS

Generally, there is no robust method by which the dielectric properties of a moist composite material in which water plays a significant chemical role can be directly and accurately related to its total water content. There exist dielectric mixing rules capable of determining the dielectric and volumetric content of unknown constituents in a mixture material [34]. However, as the mixture becomes more chemically complex, then it becomes increasingly difficult to accurately estimate the dielectric properties of its constituents, so that they may be correlated to their respective volumetric contents. Consequently, the optimal choice of frequency becomes an important consideration. In this investigation and as it pertains to water, frequency plays a major role as a function of temperature, solution concentration, and the state of water (free, bound, liquid, solid and vapor) [35]-[39]. Relaxation frequency of (free) water occurs at microwave frequencies resulting in strong absorption of microwave signals. At microwave frequencies, there are two mechanisms that contribute to the effective loss factor, namely, polarization effect and conductive losses [35, 39]. The former is influenced by different types of polarization taking place in the material (i.e., atomic, electronic, or dipolar) that contribute to the total polarization, in addition to the frequency range of the applied field. For example, at microwave frequencies, dipolar polarization is dominant at lower frequencies while electronic and atomic polarizations are dominant at higher frequencies. The latter is related to the ionic concentration of solutions (i.e., conductivity) which is inversely dependent on frequency [35]. Consequently, at higher frequencies, the contribution of ionic concentration to loss factor becomes negligible while at lower frequencies the contribution of the second term cannot be ignored. Thus, as it relates to the measurements described in this investigation,

it may be stated that the loss factor is less dependent on the ionic concentration in the pore solution at 10 GHz compared to lower frequencies (i.e., S-, R-band). This may explain the nearly constant values of loss factor at X-band compared to the same at R- and S-band during the hot and humid period.

As mentioned earlier, the pore solution in the mortar samples used here (as in most cementitious materials) contains ions such as: OH-, K+, Na+, and minor amounts of others such as Ca2+ and SO42-. The hydroxyl (OH-) concentration in the pore solution is quite important for the likelihood of ASR in mortar containing potentially reactive aggregates [40]. Consequently, the presence of ionic solution in the pores results in a particular polarization mechanism known as the Maxwell-Wagner effect which stems from the charge buildup at the interface between different constituents in a heterogeneous mixture material [41]. Figure 7, shows the contribution of the Maxwell-Wagner effect to the loss factor in moist materials as a function of frequency. According to the figure, the Maxwell-Wagner effect takes place between 1 KHz to 100 MHz, peaking at around 100 KHz, with little to no effect at microwave frequencies. At lower microwave frequencies, this effect is more pronounced compared to higher microwave frequencies. ASR gel forms initially at the surface of reactive mineral phases, through interaction with the surrounding pore solution. Over time, as the gel product imbibes water, it expands and seeps into the generated cracks in the aggregate and paste. Thus, it is proposed that ASR gel formation and its propagation throughout the cement-based composite could be better tracked at lower microwave frequencies, where the effective contribution of Maxwell-Wagner polarization and dipolar polarization of water bound to the matrix of the material is stated according to (6).

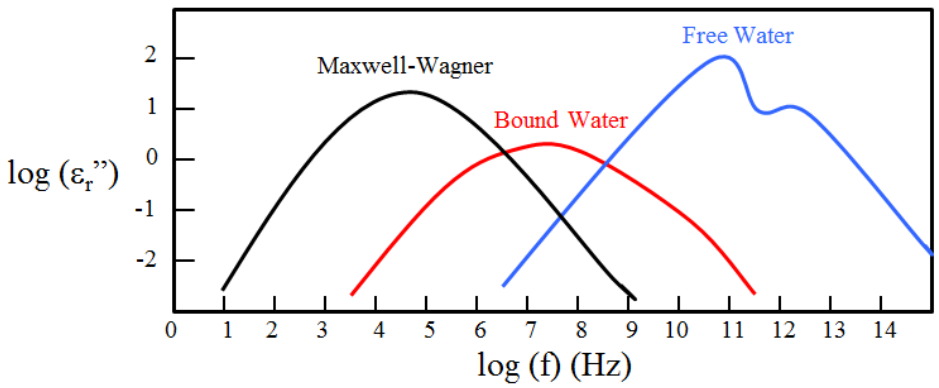

Figure 7. Contribution of various mechanisms to the loss factor of moist materials [35].

The ionic concentration of the pore solution is another important factor, which must be considered when interpreting data to distinguish between free and bound water in these mortar samples. For example, the loss factor of salt water is much higher at lower frequencies compared to higher frequencies. The same is not true about permittivity. As mentioned earlier, the ionic concentration in the pore solution has little effect beyond the relaxation frequency (~10 GHz) [42]. Looking from a different perspective and referring to [39] (see Fig. 5b), there is a marked difference between the loss factor of salt water and pure water up to ~7 GHz, while the permittivities follow almost the same values through the entire microwave frequency region (Fig. 5a). This implies that lower frequencies appear to be more sensitive (in terms of difference in loss factor) to the pore solution chemistry. To further explore whether the measured loss factor values and trends confirm the pore solution chemistry (i.e., ionic content) as a function of frequency, the average values of loss factor measurements at different frequency bands during curing and drying are shown in Table II. According to the table, during the hot and humid conditions, the loss factor decreases as a function of increasing frequency in both reactive and non-reactive samples.

Likewise, during the drying period and as a function of increasing frequency, the loss factor decreases. However, the measured values for R- and S-band are too close to be distinguished. The permittivities behaved the same as did the loss factors. The reason that the values at R- and S-band are so close to each other can be attributed to the proximity of those bands at microwave frequencies (R-band: 1.7 – 2.6 GHz, S-band: 2.6 – 3.95 GHz). Thus, the loss factor measurements appear to confirm the trend for saline water [39]. However, direct measurements of pore solution composition (not readily possible) are needed to fully validate this.

Table 2. Average dielectric constants during curing and drying period.

Frequency	**Environ-ment**	**Reactive**		**Non-Reactive**	
		ε'_r	ε''_r	ε'_r	ε''_r
R-band	Hot and humid	10.37	-3.12	11.58	-3.88
S-band		10.32	-2.94	11.54	-3.56
X-band		7.56	-1.46	8.21	-1.76
R-band	While drying	7.49	-1.00	8.35	-1.45
S-band		7.62	-1.22	8.75	-1.74
X-band		6.07	-0.7	6.88	-0.83

7. CONCLUSIONS

Based on the results of this investigation, for this particular ASR-affected set of samples and corresponding measurements, S-band showed more sensitivity to the presence of free water, while R-band showed more sensitivity to the presence of bound water. However, it also must be mentioned that conducting measurements at R-band frequencies, which is not much lower than S-band frequencies, may not reveal a significant difference. Furthermore, the measured results showed a different behavior of dielectric constant of the same samples (i.e., same mix design) cured in the same conditions as a function of frequency. In particular, different trends were observed in the loss factor. This clearly indicates that in order to better understand and evaluate the frequency behavior of the samples, the contribution of various mechanisms of the materials must be considered. It was also realized that for this specific of sample set and given the sensitivity of microwave frequencies to ionic solution present in their pore solutions, lower microwave frequencies might be more suitable and sensitive for ASR evaluation compared to higher frequencies. These results are encouraging and can be built upon with further investigations involving a more expanded set of parameters such as temperature, humidity, salinity, porosity, mix design, etc. These results, and those of future studies, will be critical for developing a dielectric mixing model capable of accounting for the influence of bound water vs. free water. Given that such a dielectric mixing model will be frequency dependent, its value will be maximized at frequencies where the effect of bound water is better detected.

REFERENCES

[1] E. Giannini et al., "Non-destructive evaluation of in-service concrete structures affected by alkali-silica reaction (ASR) or delayed ettringite formation (DEF)," Center Transp. Res., Univ. Texas Austin, Austin, TX, USA, Tech. Rep. FHWA/TX-13/0-6491-1, Apr. 2013.

[2] J. Becker, L. J. Jacobs, and J. Qu, "Characterization of cement-based materials using diffuse ultrasound," J. Eng. Mech., vol. 129, no. 12, pp. 1478–1484, 2003.

[3] K. J. Lesnicki, J.-Y. Kim, K. E. Kurtis, and L. J. Jacobs, "Accelerated determination of ASR susceptibility during concrete prism testing through nonlinear resonance acoustic spectroscopy," Georgia Institute of Technology, Atlanta, GA, USA, Tech. Rep. FHWA-HRT-13-085, 2013.

[4] K. J. Le´snicki, J.-Y. Kim, K. E. Kurtis, and L. J. Jacobs, "Characterization of ASR damage in concrete using nonlinear impact resonance acoustic spectroscopy technique," NDT&E Int., vol. 44, no. 8, pp. 721–727, Dec. 2011.

[5] J. Chen, A. R. Jayapalan, K. E. Kurtis, J. Y. Kim, and L. J. Jacobs, "Ultra-accelerated assessment of alkalireactivity of aggregates by nonlinear acoustic techniques," Ph.D. dissertation, School Civil Environ. Eng., Georgia Inst. Technol., Atlanta, GA, USA, Aug. 2010.

[6] A. Gibson and J. S. Popovics, "Lamb wave basis for impact-echo method analysis," J. Eng. Mech., vol. 131, no. 4, pp. 438–443, 2005.

[7] F. Saint-Pierre, "Monitoring of ASR evolution with ultrasonic method and seismic tomography (in French)," Ph.D. dissertation, Dept. Civil Eng., Univ. de Sherbrooke, Sherbrooke, QC, Canada, 2006.

[8] O. Metalssi, B. Godart, and F. Toutlemonde, "Effectiveness of nondestructive methods for the evaluation of structures affected by internal swelling reactions: A review of electric, seismic and acoustic methods based on laboratory and site experiences," Experim. Techn., pp. 1–12, Jan. 2013, doi: 10.1111/ext.1, 2010.

[9] R. Zoughi, S. D. Gray, and P. S. Nowak, "Microwave nondestructive estimation of cement paste compressive strength," ACI Mater. J., vol. 92, no. 1, pp. 64–70, Jan./Feb. 1995.

[10] W. Shalaby and R. Zoughi, "Analysis of monopole sensors for cement paste compressive strength estimation," Res. Nondestruct. Eval., vol. 7, nos. 2–3, pp. 101–105, 1995.

[11] K. Mubarak, K. J. Bois, and R. Zoughi, “A simple, robust, and on-site microwave technique for determining water-to-cement ratio (w/c) of fresh Portland cement-based materials,” IEEE Trans. Instrum. Meas., vol. 50, no. 5, pp. 1255–1263, Oct. 2001.

[12] K. J. Bois, A. D. Benally, P. S. Nowak, and R. Zoughi, “Cure-state monitoring and water-to-cement ratio determination of fresh Portland cement-based materials using near-field microwave techniques,” IEEE Trans. Instrum. Meas., vol. 47, no. 3, pp. 628–637, Jun. 1998.

[13] K. J. Bois, A. Benally, P. S. Nowak, and R. Zoughi, “Microwave nondestructive determination of sand-to-cement ratio in mortar,” Res. Nondestruct. Eval., vol. 9, no. 4, pp. 227–238, 1997.

[14] K. J. Bois, A. D. Benally, and R. Zoughi, “Microwave near-field reflection property analysis of concrete for material content determination,” IEEE Trans. Instrum. Meas., vol. 49, no. 1, pp. 49–55, Feb. 2000.

[15] K. J. Bois and R. Zoughi, “A decision process implementation for microwave near-field characterization of concrete constituent makeup,” Subsurf. Sens. Technol. Appl., vol. 2, no. 4, pp. 363–376, Oct. 2001.

[16] S. N. Kharkovsky, M. F. Akay, U. C. Hasar, and C. D. Atis, “Measurement and monitoring of microwave reflection and transmission properties of cement-based specimens,” in Proc. IEEE Instrum. Meas. Technol. Conf., Budapest, Hungary, pp. 513–518, May 2001.

[17] K. Bois, H. Campbell, A. Benally, P. S. Nowak, and R. Zoughi, “Microwave noninvasive detection of grout in masonry,” Masonry J., vol. 16, no. 1, pp. 49–54, Jun. 1998.

[18] S. Kharkovsky, A. C. Ryley, V. Stephen, and R. Zoughi, “Dual-polarized near-field microwave reflectometer for noninvasive inspection of carbon fiber reinforced polymer-strengthened structures,” IEEE Trans. Instrum. Meas., vol. 57, no. 1, pp. 168–175, Jan. 2008.

[19] J. Li and C. Liu, “Noncontact detection of air voids under glass epoxy jackets using a microwave system,” Subsurf. Sens. Technol. Appl., vol. 2, no. 4, pp. 411–423, Oct. 2001.

[20] K. J. Bois, S. D. Benally, and R. Zoughi, “Near-field microwave non-invasive determination of NaCl in mortar,” IEE Proc.-Sci., Meas. Technol., vol. 148, no. 4, pp. 178–182, Jul. 2001.

[21] S. Peer, J. T. Case, E. Gallaher, K. E. Kurtis, and R. Zoughi, "Microwave reflection and dielectric properties of mortar subjected to compression force and cyclically exposed to water and sodium chloride solution," IEEE Trans. Instrum. Meas., vol. 52, no. 1, pp. 111–118, Feb. 2003.

[22] S. Peer, K. E. Kurtis, and R. Zoughi, "An electromagnetic model for evaluating temporal water content distribution and movement in cyclically soaked mortar," IEEE Trans. Instrum. Meas., vol. 53, no. 2, pp. 406–415, Apr. 2004.

[23] M. T. Ghasr, Y. LePape, D. B. Scott, and R. Zoughi, "Holographical microwave imaging of corroded steel bars in concrete," ACI Mater. J., vol. 111, nos. 1–6, 2014.

[24] A. Hashemi, K. M. Donnell, K. E. Kurtis, M. C. L. Knapp, and R. Zoughi, "Microwave detection of carbonation in mortar using dielectric property characterization," in Proc. IEEE Int. Instrum. Meas. Technol. Conf. (I2MTC), Montevideo, Uruguay, pp. 216–220, May 2014.

[25] K. M. Donnell, S. Hatfield, R. Zoughi, and K. E. Kurtis, "Wideband microwave characterization of alkali-silica reaction (ASR) gel in cementbased materials," Mater. Lett., vol. 90, pp. 159–161, Jan. 2013.

[26] K. M. Donnell, R. Zoughi, and K. E. Kurtis, "Demonstration of microwave method for detection of alkali–silica reaction (ASR) gel in cement-based materials," Cement Concrete Res., vol. 44, pp. 1–7, Feb. 2013.

[27] A. Hashemi, S. Hatfield, K. M. Donnell, K. E. Kurtis, and R. Zoughi, "Microwave NDE method for health-monitoring of concrete structures containing alkali-silica reaction (ASR) gel," in Proc. 40th Annu. Rev. Prog. Quant Nondestruct. Eval. Conf., Amer. Inst. Phys., vol. 33A, pp. 787–792, 2014.

[28] R. J. Kirkpatrick, A. G. Kalinichev, X. Hou, and L. Struble, "Experimental and molecular dynamics modeling studies of interlayer swelling: Water incorporation in kanemite and ASR gel," Mater. Struct., vol. 38, no. 4, pp. 449–458, May 2005.

[29] ACI Concrete Terminology, ACI Standard CT-13, Jan. 2013.

[30] A. M. Neville, Properties of Concrete, 5th ed. Upper Saddle River, NJ, USA: Prentice-Hall, 2012.

[31] L. S. Dent-Glasser and N. Kataoka, "The chemistry of 'alkaliaggregate' reaction," Cement Concrete Res., vol. 11, no. 1, pp. 1–9, 1981.

[32] A. Pedneault, "Development of testing and analytical procedures for the evaluation of the residual potential of reaction, expansion and deterioration of concrete affected by ASR," M.S. thesis, School Civil Eng., Laval Univ., Québec City, QC, Canada, 1996.

[33] D. M. Pozar, Microwave Engineering. New York, NY, USA: Wiley, 2009.

[34] Sihvola, Electromagnetic Mixing Formulas and Applications. London, U.K.: IEEE Press, 1999.

[35] J. B. Hasted, Aqueous Dielectrics, vol. 17. London, U.K.: Chapman & Hall, 1973.

[36] Potential Alkali Reactivity of Aggregates (Mortar-Bar Method), ASTM C Standard 1260-07, 2007. [Online]. Available: http://dx.doi.org/10.1520/C1260-07.www.astm.org.

[37] Determination of Length Change of Concrete Due to Alkali-Silica Reaction (Concrete Prism Test), ASTM C Standard 1293-08b, 2008. [Online]. Available: http://dx.doi.org/10.1520/C1293-08B. www.astm.org.

[38] K. J. Bois, L. F. Handjojo, A. D. Benally, K. Mubarak, and R. Zoughi, "Dielectric plug-loaded two-port transmission line measurement technique for dielectric property characterization of granular and liquid materials," IEEE Trans. Instrum. Meas., vol. 48, no. 6, pp. 1141–1148, Dec. 1999.

[39] F. T. Ulaby, R. K. Moore, and A. K. Fung, Microwave Remote Sensing: Active and Passive, Volume II: Radar Remote Sensing and Surface Scattering and Emission Theory. Dedham, MA, USA: Artech House, 1986, pp. 1797–1848.

[40] W. Chen, Z. H. Shui, and H. J. H. Brouwers, "A computed-based model for the alkali concentrations in pore solution of hydrating Portland cement paste," in Excellence in Concrete Construction Through Innovation, M. C. Limbachiya and H. Y. Kew, Eds. London, U.K.: Taylor & Francis, 2009.

[41] J. Mijovi´c, J. Kenny, A. Maffezzoli, A. Trivisano, F. Bellucci, and L. Nicolais, "The principles of dielectric measurements for in situ monitoring of composite processing," Compos. Sci. Technol., vol. 49, no. 3, pp. 277–290, 1993.

[42] S. Laurens, J. P. Balayssac, J. Rhazi, G. Klysz, and G. Arliguie, "Nondestructive evaluation of concrete moisture by GPR: Experimental study and direct modeling," Mater. Struct., vol. 38, no. 9, pp. 827–832, 2005.

II. EFFECT OF HUMIDITY ON DIELECTRIC PROPERTIES OF MORTARS WITH ALKALI-SILICA REACTION (ASR) GEL

ABSTRACT

Microwave materials characterization techniques have been extensively and successfully used for evaluating important properties of a wide range of cement-based materials and structures. Recent investigations using these techniques for studying properties of mortar with alkali-silica reaction (ASR) gel have also been very promising. In this research, microwave dielectric properties of multiple mortar samples with different compositions and when subjected to different humidity levels are investigated. This paper presents the results of these experiments and the subsequent analysis pertinent to humidity-related issues in the mortar samples.

Index Terms: alkali-silica reaction (ASR); microwave nondestructive techniques; dielectric constant measurements; humidity.

1. INTRODUCTION

Alkali-silica reaction (ASR) is one of the most common causes of deterioration in concrete structures. This is the chemical reaction between alkalis in the pore solution of portland cement-based materials and amorphous, strained or cryptocrystalline reactive siliceous minerals (e.g., opal, obsidian, cristobalite, tridymite, chalcedony, and chert) that may be present in aggregates. The product of this reaction is ASR gel, which, in the presence of sufficient moisture in concrete pore solution, expands and causes internal microcracking in the structure [1]. This is a complex process and early information about ASR gel formation and expansion would be very useful for predicting and preventing future damage.

Microwave signals can readily penetrate inside of dielectric materials and interact with their inner structures. The interaction of microwave signals with physical and chemical properties of materials makes them an effective candidate to evaluate changes related to these properties. To this end, microwave materials characterization techniques have been successfully employed for studying various critical properties of cement-based materials [2-7]. Moreover, using these techniques easily facilitates a temporal study of material properties related to curing, cyclical chloride permeation, ASR gel formation, etc.

Microwave signals are also sensitive to the presence and state of water in materials. Given that the presence of moisture (in the form of humidity in the pores) is essential for ASR gel production and expansion, microwave techniques are expected to be useful in providing information about this mechanism [8]-[10]. In this paper, the results of an investigation into the influence of humidity on ASR gel production are presented and discussed in detail in the following sections.

2. BACKGROUND

Prior to ASR gel formation and in the presence of reactive aggregates, hydroxyl ions OH- and the alkalis Na+ and K+ react with reactive silica (SiO2), as [9]:

$$\text{Si-OH} + \text{OH}^- + \text{Na}^+, \text{K}^+ \rightarrow \text{Si-O-Na, K} + \text{H}_2\text{O} \quad (1)$$

$$\text{Si-O-Si} + 2\text{OH-} + 2\text{Na+, K+} \rightarrow 2(\text{Si-O-Na, K}) + \text{H2O} \quad (2)$$

The ASR gel (Si-O-Na, K) formed is hygroscopic and imbibes water from the surrounding cement paste, leading to gel expansion, progressive cracking, and eventually causes loss of serviceability and in some cases failure of the structure. Thus, the presence of moisture (i.e., internal relative humidity) is a critical requirement for ASR gel formation. It is reported in [10] that structural damage due to ASR is unlikely to occur below an internal relative humidity (RH) of ~80%. In other words, sufficient moisture must be present for ASR gel formation. In this work, the potential for microwave dielectric property characterization to confirm this expectation (i.e., no ASR gel production below 80% RH) was investigated. When fully developed, this type of materials characterization can be potentially used as a means to detect and monitor ASR gel production.

Dielectric constant at microwave frequencies is a complex intrinsic parameter which is a macroscopic measure of the interaction of dielectric materials with microwave signals. Once referenced to the dielectric constant of the free-space and as indicated in (3), the real part of the relative complex dielectric constant indicates the ability of the material to store microwave energy and the imaginary part represents the ability of the material to absorb microwave energy. The former is called relative permittivity and the latter is relative loss factor.

$$\varepsilon_r = \varepsilon'_r - j\varepsilon''_r \quad (3)$$

Being an intrinsic material property, dielectric constant is independent of the method used to measure it. Recently, a series of investigations have been conducted on different aspects of mortars with ASR gel and their interaction with microwave signals [11-13]. In this investigation, a similar approach is used to study the influence of humidity on ASR gel production through measuring the complex dielectric constant of several mortar samples exposed to different humidity levels

3. EXPERIMENTS

3.1 SAMPLE PREPARATION AND COMPOSITION

To examine and compare the effect of humidity as well as chemical composition on ASR gel production in mortar, three different experiments were conducted. In each experiment, two sets of mortar samples (each set having 3 similar samples for averaging purposes) were cast using different types of crushed fine aggregate; namely, reactive (i.e., with tendency to produce ASR gel) and non-reactive. Table 1 summarizes the mix design for the samples.

Table 1. Mix design.

Mix Proportions	**Sample Type**	
	Reactive	**Non-Reactive**
Cement	Portland Type I/II	Portland Type I/II
Aggregate	Rhyolite	Limestone
water-to-cement ratio (w/c)	0.47	0.47
aggregate-to-cement ratio (a/c)	2.25	2.25

In the first experiment (batch #1), all samples (reactive and non-reactive) were kept in a humidity chamber at a constant temperature of 38ºC and ~85% relative humidity (RH) for 26 days. Sodium hydroxide (NaOH) was added to the mixing water of this batch to "boost" the total equivalent alkali content to 0.9% by mass of cement as per [14]. The addition of NaOH accelerates ASR gel formation. In the second experiment (batch #2), the samples were kept at the same temperature but at a lower RH of ~65% during the first 26

days, and NaOH was not added to the mixing water of these samples. In the third experiment (batch #3), the samples were kept in the same conditions as those for batch #2 was (temperature of 38ºC and a ~65% RH), except that NaOH was added (0.9% by mass of cement as per [14]) to the mixing water to accelerate ASR (if any). All the three batches were removed from their respective hot and humid environment after 26 days, and then were kept at ambient conditions for almost 2 months. Table 2 shows the experiments and their respective humidity levels.

Table 2. Batch composition.

Experiment	**Temperature and Humidity During Hot and Humid Period**	**Sample Type**	**Mixing Water**
Batch #1	T: 38ºC, RH: ~85%	Reactive and Non-reactive	With NaOH
Batch #2	T: 38ºC, RH: ~65%	Reactive and Non-reactive	Without NaOH
Batch #3	T: 38ºC, RH: ~65%	Reactive and Non-reactive	With NaOH

3.2. MEASUREMENT PROCEDURE

The dielectric properties of the samples were measured using the well-known completely-filled waveguide technique at R-band (1.7 – 2.6 GHz), as shown in Fig. 1, using an Agilent Vector Network Analyzer (VNA) [15]. The samples were made to fit tightly inside of the rectangular waveguide sample holders (cross-section of 10.92 cm × 5.46 cm).

All samples were cast in molds at ambient conditions (23° C ± 2° C, 35% ± 5% RH) and were removed between ~24 to ~48 hours after mixing, then immediately placed in the chamber. As mentioned earlier, all (reactive and non-reactive) samples were stored in a hot and humid chamber at a nominal temperature of 38ºC, but the humidity was ~85% for batch #1 and ~65% (where ASR gel production would be expected to be limited) for batches #2 and #3.

During the hot and humid period, dielectric constants measurements were conducted on a regular basis (every 2-3 days). After 26 days being in the humid chamber, the samples were removed from the hot and humid environment and placed in ambient conditions (23° C ± 2° C, 35% ± 5% RH). Regular microwave dielectric constant measurements continued in the same fashion (while the samples were kept in the ambient conditions) for approximately another two months.

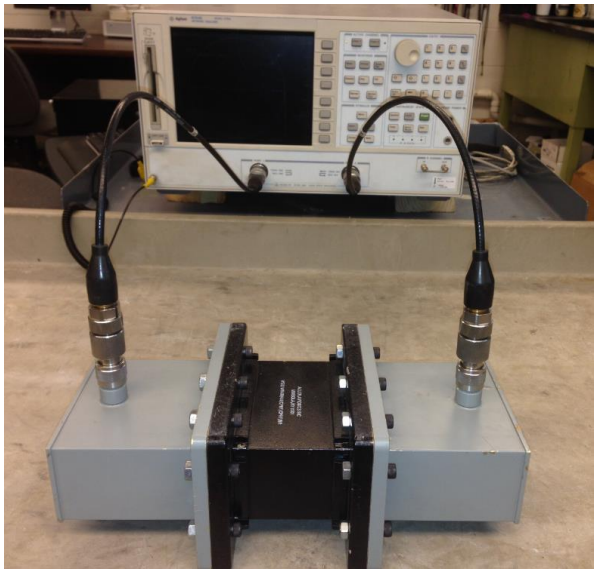

Figure 1. VNA measurement setup with R-band sample holder.

4. RESULTS

The measured temporal dielectric constants of the three batches are shown in Fig. 2a-c. The samples in batch #1 were “alkali- boosted” and kept at 85% RH. As it can be seen in Fig. 2a-1, the permittivity of the non-reactive samples increased slightly, while the permittivity of the reactive samples remained almost unchanged during the first 26 days (i.e., hot and humid period). Assuming ASR production in reactive samples, less free water (i.e., more bound water) would be available in the reactive samples (compared to the non-reactive case), and the pores would be partially filled with ASR gel. As such, no additional free water/moisture can be added to the samples; hence the permittivity would remain relatively constant during this hot and humid period. On the other hand, for the non-reactive samples during the hot and humid conditions, since ASR gel is not generated in these samples, the pores will remain available for the transport of additional free water/moisture into these samples, resulting in a slight increase in permittivity values. Related to this, during the hot and humid period, the loss factor (Fig. 2a-2), decreased (loss factor is a negative number) more significantly for the reactive samples as compared to the non-reactive samples. This behavior is consistent with the transformation of free to bound water (i.e., less lossy free water) in the reactive samples. The reason that the difference between the non-reactive and reactive samples is more pronounced in the loss factor (compared to permittivity) is due to the fact that loss factor values are more different (at R-band) for different pore solution compositions (free water vs. bound water or ASR gel) as compared to permittivity [16]. Overall, the dielectric constants measurements for batch #1, where ASR production was expected, turned out to be consistent with behavioral expectations of ASR-affected samples.

For the samples in batch #2, the humidity level was kept at 65% and NaOH was not added to their mix. As such, for this set of samples, no ASR gel is expected to be produced [10]. As indicated in Fig. 2b-1, the permittivities of the samples followed the same trend for both reactive and non-reactive samples. Unlike batch #1, these samples manifested the same rate of change (in permittivity) during the time in the humidity chamber and the drying period. This behavior implies a similar response of both types of samples (i.e., reactive and non-reactive) in the presence of water (i.e., wetting during the hot and humid period) and during evaporation (i.e., moisture loss during the drying period). This consistency in behavior suggests that ASR did not occur in samples containing reactive aggregates, due to the limited availability of moisture. The same trend can be seen in Fig. 2b-2, where changes in loss factor also showed the same rate of change.

By comparing the difference between the behavior of the dielectric constants of samples in batch #1 and batch #2, the influence of moisture on ASR gel production can be assessed. Because ASR was produced in the reactive samples of batch #1 and not in batch #2, potentially, the differences between these two sets can be quantified through pertinent dielectric mixing modeling. This may reveal invaluable information regarding samples with and without ASR gel.

The samples in batch #3 had the exact same mix design as in batch #2, except that NaOH was added to their mix. This alkali boosting facilitated evaluating the effect of cement hydration reactions, but ASR production was still expected to be limited by the lower humidity. As indicated in Fig. 2c-1, the permittivities showed the same rate of change during the hot and humid and drying periods. Also, in Fig. 2c-2, it can be seen that the loss factor values had the same rate of change for reactive samples compared to the non-reactive

ones. This similar rate of change again implies that same amount of free water was lost (either due to transformation of free to bound water or evaporation) in the reactive and non-reactive samples during the two periods. As a result, and by comparing batch #3 and batch #1, it can be deduced that no ASR was produced in the former.

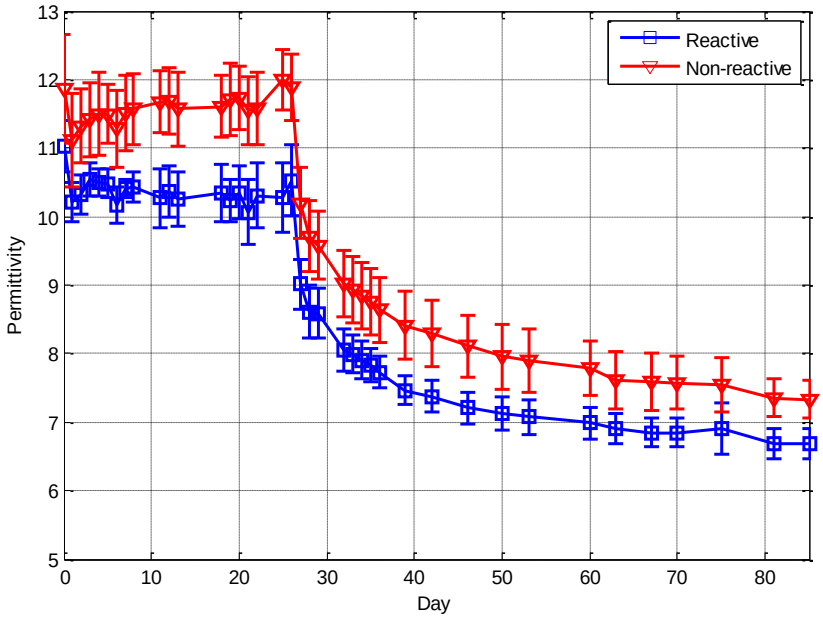

a-1

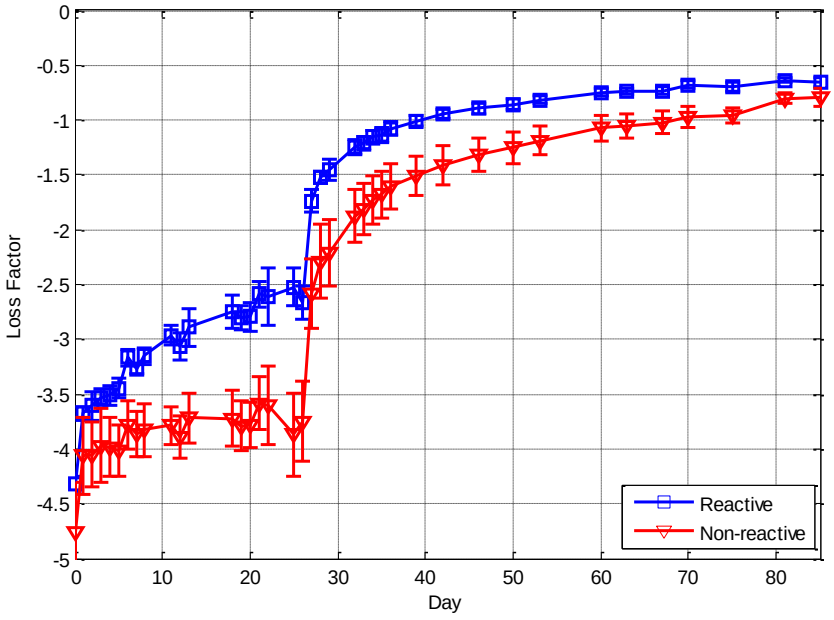

a-2

Figure 2. Dielectric constant measurements, a1-2) Batch #1, b1-2) Batch #2, c1-2) Batch #3.

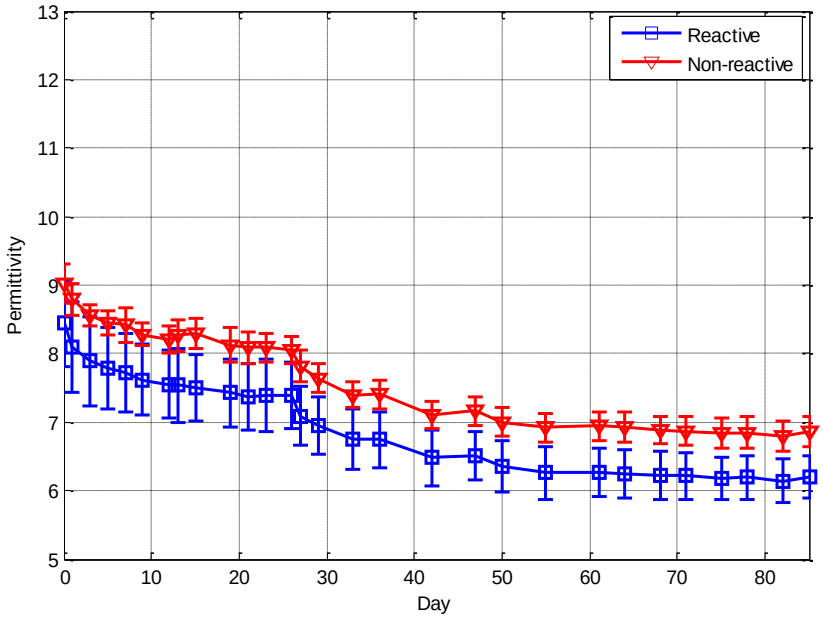

b-1

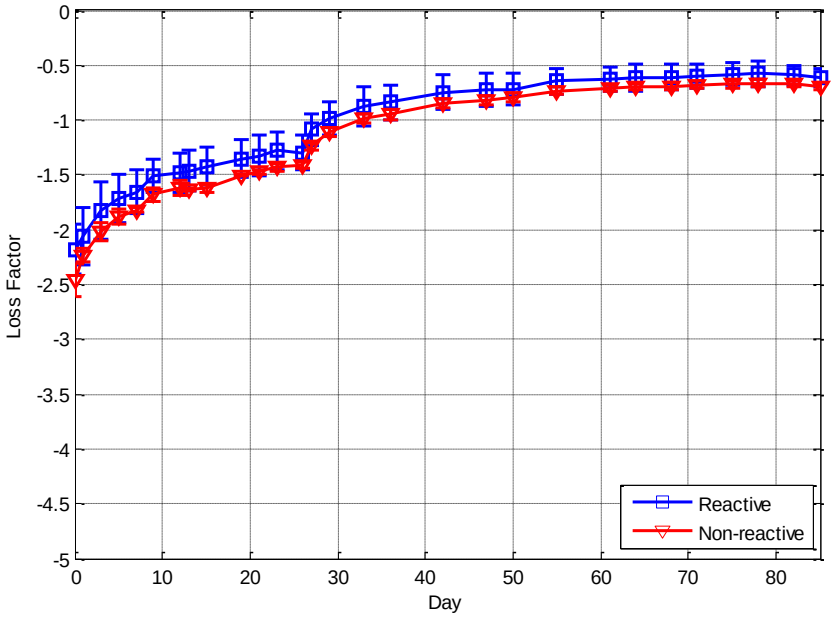

b-2

Figure 2. Dielectric constant measurements, a1-2) Batch #1, b1-2) Batch #2, c1-2) Batch #3 (cont.).

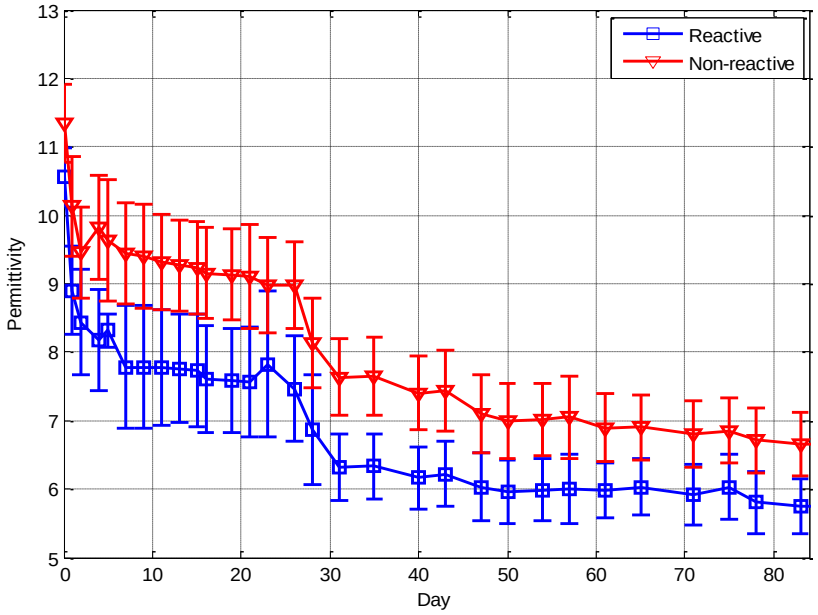

c-1

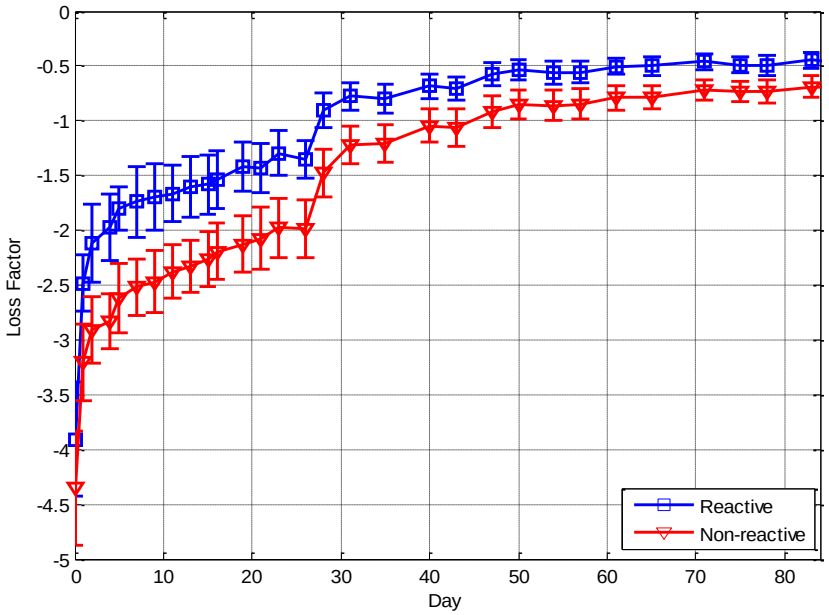

c-2

Figure 2. Dielectric constant measurements, a1-2) Batch #1, b1-2) Batch #2, c1-2) Batch #3 (cont.).

5. CONCLUSION

In this research, three different mortar batches were cast in order to investigate the interaction of microwave signals with chemically different samples at different humidity levels. First, two different batches of mortar samples (with reactive and with non-reactive aggregate) were cast, and kept at temperature of 38ºC in a relatively low and relatively high humidity condition at 65% RH and 85% RH, respectively. Temporal dielectric constant measurements were performed, and according to the results, it appeared that ASR production did not occur for samples that were kept at the relative humidity of ~65%, as expected. In the next step, another set of samples was cast in order to examine the effect of alkali boosting during storage at lower humidity levels. The pertinent results indicate that the addition of NaOH to the mix design did not produce ASR gel. Overall, the findings of this investigation are promising and corroborate the expectation in [10]. However, these samples need to be destructively tested for the presence of ASR gel, to confirm the microwave measurements results. In addition, further investigation will follow that may include more samples with different make-ups, kept at controlled humidity levels. This additional experiments, will aid to better understand the relationship between ASR production and humidity through microwave measurements and the subsequent practical ramifications.

REFERENCES

[1] ACI CT-13, ACI concrete terminology, An ACI standard, American Concrete Institute Pubs., USA, January 2013.

[2] R. Zoughi, S. Gray, and P. S. Nowak, "Microwave nondestructive estimation of cement paste compressive strength", ACI Mater. J., vol. 92, no. 1, pp. 64–70, Jan.-Feb. 1995.

[3] K. Mubarak, K. J. Bois, and R. Zoughi, "A simple, robust and on-site microwave technique for determining water-to-cement (w/c) ratio of fresh portland cement-based materials", IEEE Trans. Instrum. Meas., vol. 50, pp. 1255–1263, Oct. 2001.

[4] K. Bois, A. Benally, P. S. Nowak, and R. Zoughi, "Microwave nondestructive determination of sand to cement (s/c) ratio in mortar", Res. Nondestructive Eval., vol. 9, no. 4, pp. 227–238, 1997.

[5] K. Bois, A. Benally, and R. Zoughi, "Microwave near-field reflection property analysis of concrete for material content determination", IEEE Trans. Instrum. Meas., vol. 49, pp. 49–55, Feb. 2000.

[6] S. Kharkovsky, M. Akay, U. Hasar, and C. Atis, "Measurement and monitoring of microwave reflection and transmission properties of cement-based specimens", in Proc. IEEE Instrum. Meas. Technol. Conf, Budapest, Hungary, pp. 513–518, May 2001.

[7] A. Hashemi, K.M. Donnell, K.E. Kurtis, M. Knapp, and R. Zoughi, "Microwave Detection of Carbonation in Mortar Using Dielectric Property Characterization", Proceedings of the IEEE International Instrumentation and Measurement Technology Conference (I2MTC), pp. 216-220, Montevideo, Uruguay, May 12-15, 2014.

[8] A. Hashemi, M. Horst, K. E. Kurtis, K. M. Donnell, and R. Zoughi, "Comparison of Alkali–Silica Reaction Gel Behavior in Mortar at Microwave Frequencies," IEEE Trans. Instrum. Meas., vol. 64, no. 7, pp. 1907–1915, Jul. 2015.

[9] D. Glasser, L. S., and Kataoka, "The chemistry of alkali-aggregate reactions", in proce. 5th international conference on alkali-aggregate reaction. Cape Town, South Africa, S253/23.

[10] A. Pedneault, "Development of testing and analytical procedures for the evaluation of the residual potential of reaction, expansion, and deterioration of concrete affected by ASR", M.Sc Memoir, Laval university. Quebec city, Canada, 133p.

[11] K. M. Donnell, S. Hatfield, R. Zoughi, K.E. Kurtis, “Wideband microwave characterization of alkali-silica reaction (ASR) gel in cement-based materials”, Materials Letters, vol. 90, January 2013.

[12] K. M. Donnell, R. Zoughi, and K. E. Kurtis. “Demonstration of microwave method for detection of alkali–silica reaction (ASR) gel in cement-based materials”, Cement and Concrete Research 44, pp 1-7, 2013.

[13] A. Hashemi, S. Hatfield, K.M. Donnell, K.E. Kurtis and R. Zoughi, “Microwave NDE for Health Monitoring of Concrete Structures Containing Alkali-Silica (ASR) Gel”, Proceedings of the 40th Annual Review of Progress in Quantitative Nondestructive Evaluation Conference, American Institute of Physics, Conference proceedings 1581, vol. 33A, pp. 787-792, 2014.

[14] ASTM C 1293 “Determination of length change of concrete due to alkali-silica reaction (concrete prism test)”, American Society for Testing and Materials, West Conshohocken, PA.

[15] K.J. Bois, Handjojo, L.F.; Benally, A.D.; Mubarak, K.; Zoughi, R., “Dielectric plug-loaded two-port transmission line measurement technique for dielectric property characterization of granular and liquid materials”, IEEE Transactions on Instrumentation and Measurement, vol. 48, no. 6, pp. 1141-1148, December 1999.

[16] Ulaby, F. T., R. K. Moore, and A. K. Fung. "Microwave Remote Sensing: Active and Passive, vol. III, Volume Scattering and Emission Theory, Advanced Systems and Applications." Inc., Dedham, Massachusetts, pp. 1797-1848, 1986.

III. EFFECT OF ALKALI ADDITION ON MICROWAVE DIELECTRIC PROPERTIES OF MORTARS

ABSTRACT

This paper investigates the effect of alkali addition on dielectric properties of mortar using microwave dielectric property characterization of two different sets of mortars made with relatively low and high-alkali contents. Microwave measurements were conducted at S-band (2.6–3.95 GHz). High-alkali mortars were prepared with sodium hydroxide (NaOH) addition of 0.9% to the mixing water. The influence of alkali addition on the heat of hydration, compressive strength, water absorption, and bulk resistivity of the mortars were also investigated. The microwave measurement results indicated sensitivity to detecting the different alkali contents while corroborating a higher ionic concentration for the mortars with high-alkali content relative to those made with low-alkali content. A correlation was observed between the measured dielectric loss factor, bulk resistivity, and compressive strength of the mortars. However, the trends in high-alkali mortars did not follow the same trend as in the low-alkali mortars. This fact may be an identifying parameter that can be further utilized to develop a versatile microwave nondestructive technique capable of evaluating alkalinity in cement-based materials.

Index Terms: Alkalis, cement-based materials, compressive strength, dielectric properties, microwave nondestructive testing.

1. INTRODUCTION

The amount of alkalis in cement-based materials should be sufficiently low to ensure desired performance and serviceability. For instance, the expansive and undesired reaction between alkalis, present in cement powder, and certain aggregates is known as alkali-silica reaction (ASR). This reaction results in excessive expansion, internal microcracks, and eventual deterioration of concrete structures [1]. Juenger and Jennings [2] examined the effect of sodium hydroxide (NaOH) addition on cement hydration and porosity of cement paste, where the addition of 1M NaOH solution significantly accelerated the initial hydration, while resulted in reduced hydration and strength at later ages. Accelerated hydration rate caused by NaOH results in the formation of coarser or more heterogeneous microstructures, which may lead to a reduction in strength. Smaoui *et al.* [3] investigated the effect of alkali addition on microstructure and mechanical properties of concrete made with water-to-cement ratio (*w/c*) of 0.41 and cement content of 420 kg/m^3. The authors reported that an increase in total equivalent alkali content $(Na_2O)_{eq}$ from 0.6% to 1.25%, by mass of cement, resulted in 5% to 20% reduction in compressive, splitting tensile, and flexural strengths.

In addition, the results from SEM observations showed that high-alkali cement paste developed a microstructure with higher porosity compared to the low-alkali paste, thus leading to lower mechanical properties. In another effort, Bu and Weiss [4] examined the influence of alkali addition on the transport properties of cement-based materials. The results showed that a higher concentration of alkali decreased the electrical resistivity of the pore solution. In most of these common approaches, the evaluation of alkali effects was

solely investigated based on the mechanical and durability properties of mortars, while their complex dielectric properties were never characterized and studied in this context.

As mentioned earlier, concrete in the presence of siliceous minerals found in certain aggregates, with sufficient concentrations of alkali, and moisture can undergo deleterious expansion and cracking due to ASR formation. Current laboratory test methods for assessment of the potential for producing damaging ASR expansion have been criticized for numerous reasons, including poor correlation to field results. The concrete prism test, ASTM C1293, is considered among the most reliable laboratory test methods for the assessment of potential for ASR formation [5]. However, this test requires adding sodium hydroxide (NaOH) to the mixing water in order to increase the $(Na_2O)_{eq}$ to a certain value to accelerate ASR formation. Consequently, using cement powder in combination with the addition of NaOH in the mixing water alters the pore solution concentration of the specimen. To this end, microwave materials characterization techniques, involving the study of complex dielectric properties of these materials, may be used to evaluate the effects of alkali addition on cement-based materials.

Microwave material characterization methods as well as microwave nondestructive testing (NDT) techniques have been extensively used to evaluate and characterize materials properties of a diverse array of cement-based materials. Content determination of constitutive materials, such as *w/c*, sand-to-cement ratio (*s/c*), and coarse aggregate-to-cement ratio (*ca/c*) [6], chloride permeation [7], carbonation evaluation [8], and most recently evaluation of ASR gel formation [9-12] have been investigated using microwave techniques. In most of the aforementioned investigations, the main contributing factor is an intrinsic parameter representing the interaction of microwave signals with materials

media, known as the complex dielectric constant (ε). Dielectric constant is referred to as *relative* dielectric constant (ε_r) once it is referenced to the dielectric constant of the free-space. The relative dielectric constant can be further defined by its real and imaginary parts, as expressed in Eq. (1),

$$\varepsilon_r = \varepsilon'_r - j\varepsilon''_r \quad (1)$$

where ε_r' indicates the ability of the material to store microwave energy (relative permittivity), and the ε_r'' represents the ability of the material to absorb microwave energy (relative loss factor). For a material such as mortar, this parameter is a function of the volumetric content of all constituents making up the material and their respective dielectric properties. In addition, any existing chemical reactions also affect this parameter. Hence, through the study of temporal variations in this parameter, one can gain significant amount of information about the chemical and physical changes occurring on within it (for example transformation of free water to bound water in ASR gel formation).

Thus, pertinent to this investigation, and given the uniqueness of the dielectric constant of a material, temporal microwave dielectric property measurements has the potential to provide information that can be further utilized to evaluate the effect of increasing alkali content in cement-based materials. To this end, microwave dielectric property measurements were conducted on two different sets of mortars prepared with and without addition of NaOH, at S-band (2.6 – 3.95 GHz). The effect of alkali (NaOH) addition on heat of hydration, compressive strength, water absorption, and bulk resistivity of the mortars were also evaluated (henceforth, these parameters will be referred to as

engineering properties throughout the text for brevity). This was done to investigate any potential correlation between the microwave measurements and the engineering properties of these mortars.

2. EXPERIMENTAL APPROACH

The experimental approach presented in this investigation consisted of two phases. The first phase involved quantifying the effect of alkali (NaOH) addition on engineering properties of mortars. The second phase aimed to evaluate the effect of alkali addition on the complex dielectric properties of the mortars.

2.1. MATERIALS, MIXTURE PROPORTIONS, AND CURING CONDITIONS

Type I/II ordinary Portland cement (OPC) and a reactive aggregate with maximum aggregate size of 6 mm were used for all mixtures. Tables 1 and 2 summarize the chemical and physical characteristics of the cement and mix design of the mortars, respectively. For the high-alkali mortars, 0.9% NaOH, by mass of cement, was added to the mixing water, and no NaOH was added to the mixing water of the low-alkali mortars. Therefore, the total $(Na_2O)_{eq}$ for the relatively low and high-alkali mortars were 0.45% and 1.15%, respectively.

Table 1. Physical and chemical characteristics of cement.

Properties	
SiO_2, %	19.8
Al_2O_3, %	4.5
Fe_2O_3, %	3.2
CaO, %	64.2
MgO, %	2.7
SO_3	3.4
Na_2O eq., %	0.45
Blaine surface area, m^2/kg	420
Specific gravity	3.14
LOI, %	1.5

Table 2. Mixture proportions of investigated mortars.

Mix design	**Mixture type**	
	High-Alkali	***Low-Alkali***
Cement	Portland Type I/II	Portland Type I/II
w/c	0.47	0.47
aggregate-to-cement ratio (a/c)	2.25	2.25
NaOH,%	0.9	-
Na2Oeq.,%	1.15	0.45

All mortars were cast in one layer, and consolidated on a vibration table for 30 seconds. They were kept at ambient conditions ($23^{\circ C} \pm 2$ and 35% ± 5% relative humidity (RH)) for approximately 24 hours after casting and while in their molds. Subsequently, they were demolded and kept in a hot and humid condition (in an environmental chamber) at $38^{\circ C} \pm 2$ and 90% ± 5% RH, mimicking similar conditions for the prism test used for ASR evaluation [13]. Both engineering and microwave dielectric property measurements were performed during the first 28 days of curing while the samples were kept in the environmental chamber.

2.2. TEST METHODS

2.2.1. Engineering Properties Measurements. In order to study the influence of alkali addition on the rate of reaction, heat of hydration was measured using isothermal calorimetry in accordance with ASTM C1679. According to the standard, the measured heat generated by the hydration process corresponds to the rate of reaction. The test method consisted of transferring approximately 100 g of mortar mixture to a container immediately after mixing. The container was then placed into a chamber and maintained at 23°C for approximately 72 hours. The ambient temperature around the sample was kept constant. The test setup for the calorimetry measurements is shown in Fig. 1a. A thermal hydration curve is provided (in the results section) based on the heat flow generated by the early hydration reaction of the material.

The effect of alkali addition on the compressive strength development of the mortars was also investigated. The compressive strength of these mortars was measured using 50 mm cube specimens in accordance to ASTM C109. The compressive strength measurements were conducted at ages 3, 7, and 28 days.

Water absorption was evaluated in accordance with ASTM C642 using 50 mm-cube specimens. This test method determines the water absorption of mortars after immersion in water, and the results can be related to the porosity of the mortars. In this test, samples were dried in an oven at a temperature of 110°C ± 5 until the difference between any two consecutive mass values was less than 0.5% of the obtained lowest value. The specimens were immersed in water with a temperature of ~21°C for 48 hours to determine their saturated surface dried mass. The water absorption rate for each mortar was

calculated as the percentage of the difference between the saturated surface-dried and oven-dried masses divided by the oven-dried mass of specimen.

The bulk resistivity test was conducted on a 100 mm × 100 mm cylindrical sample using the uniaxial bulk resistance testing, operating at 12 volts [14]. Figure 1.b shows the schematic of bulk resistivity measurement setup. The bulk resistivity was calculated as follows:

$$\rho = \frac{AR}{L} \tag{2}$$

where ρ is the resistivity (kΩ.cm) and *R*, *A*, and *L* refer to the measured resistance, cross section area and length of the sample, respectively.

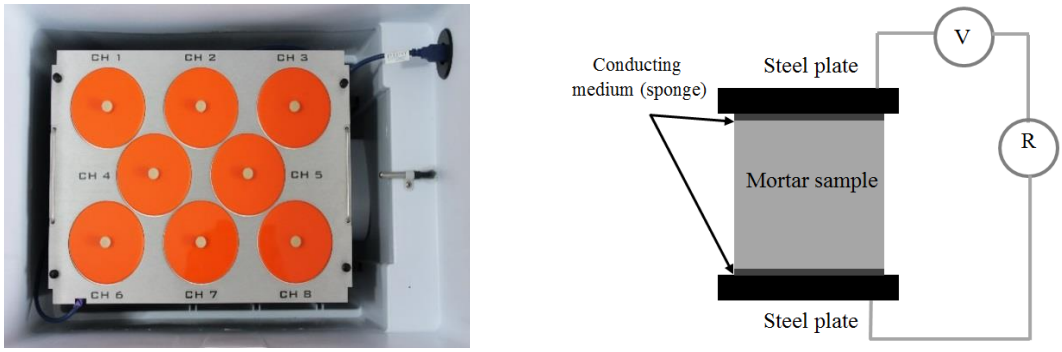

(a) (b)

Figure 1. Measurement setup for: a) isothermal calorimetry, and b) bulk resistivity.

2.2.2 Microwave Dielectric Property Measurements. The completely-filled waveguide measurement technique was employed to measure the dielectric properties of mortar samples [15]. The measurements were conducted on samples measuring 72.1 mm × 34 mm corresponding to the S-band (2.6 – 3.95 GHz) rectangular waveguide cross-section dimensions. The length of the mortars was chosen to be ~30-40 mm (microwave measurements are independent of sample length).

Scattering parameters (i.e., S_{11}, S_{21}, S_{12}, and S_{22}) of the samples were measured at S-band (2.6 – 3.95 GHz) using a calibrated vector network analyzer (VNA), as shown in Fig. 2. S_{11} (or S_{22}) is the complex ratio of the total reflected to the incident signal at ports 1 and 2 of the VNA, respectively. Similarly, S_{21} (or S_{12}) is the complex ratio of the total transmitted to the incident signal measured at each port. Figure 3 illustrates the measurement schematic showing the signal interaction with the sample. Subsequently, relative dielectric constants of the samples were calculated according to the detailed procedure outlined in [15]. For every measurement the samples were taken out of the chamber (hot and humid environment), then put inside of the waveguide sample-holder, to measure the scattering parameters. They were subsequently placed back in the chamber.

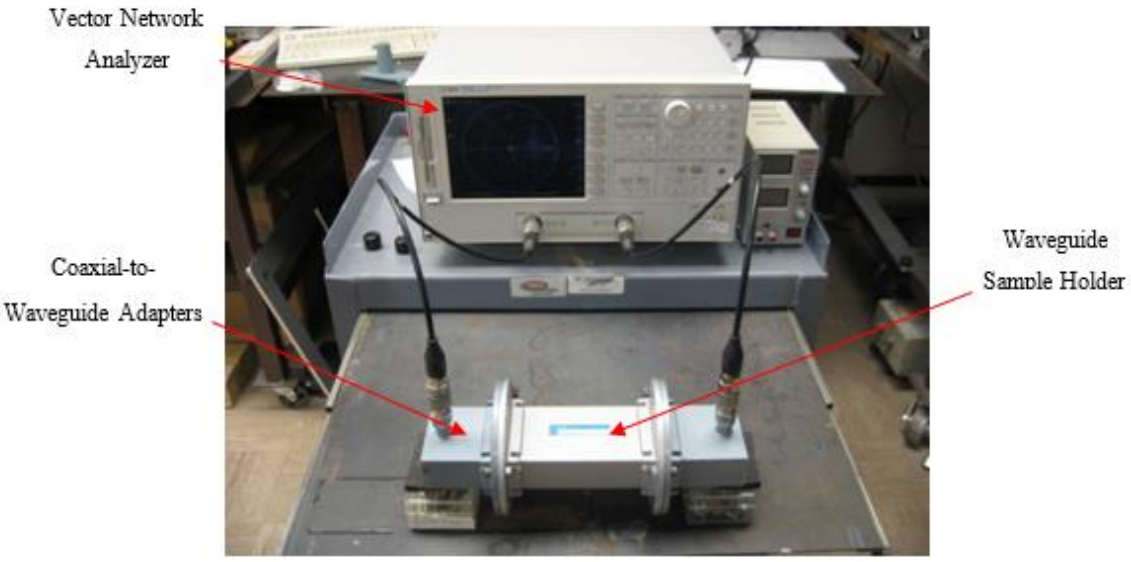

Figure 2. Microwave measurement setup.

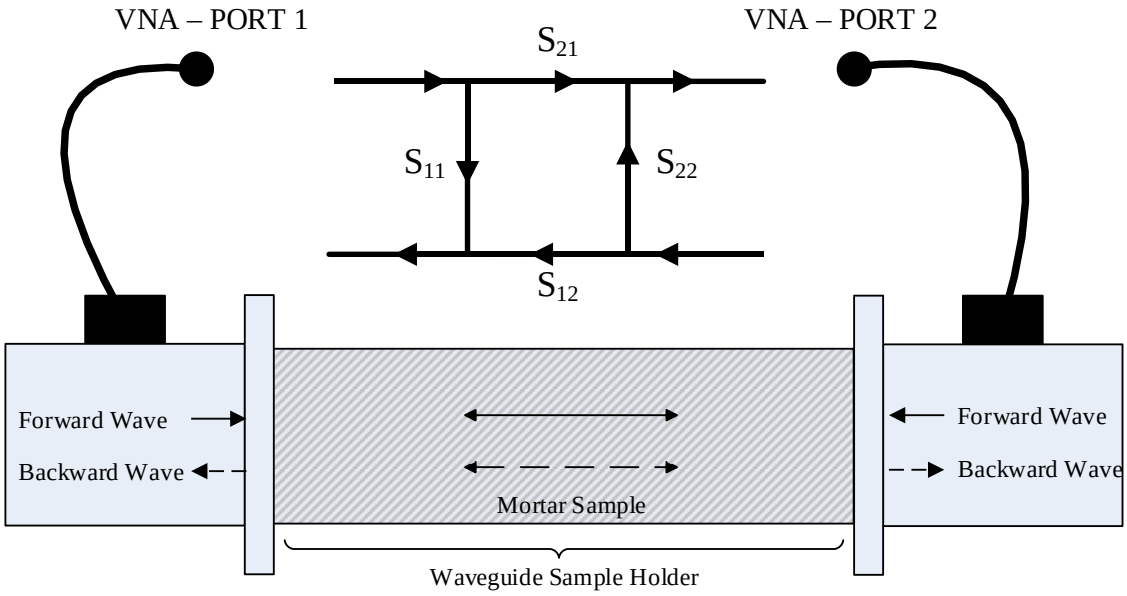

Figure 3. Measurement schematic illustrating interaction of microwave signals with sample.

3. RESULTS

3.1. ENGINEERING PROPERTIES

The results of cumulative heat evolution of the mortars evaluated over 72 hours are illustrated in Fig. 4. The high-alkali mortar showed greater heat of hydration compared to the low-alkali mortar. After 40 hours, the difference in heat of hydration between high and low-alkali mortars slightly decreased. The increase in heat of hydration caused by the addition of NaOH is in agreement with the results of other studies [2-3, 16-17], where it was noted that the addition of NaOH accelerates hydration of C_3S and C_3A. It is also reported in [2] that the addition of NaOH to the mixing water increases the initial hydration of Portland cement and retards it after the first day.

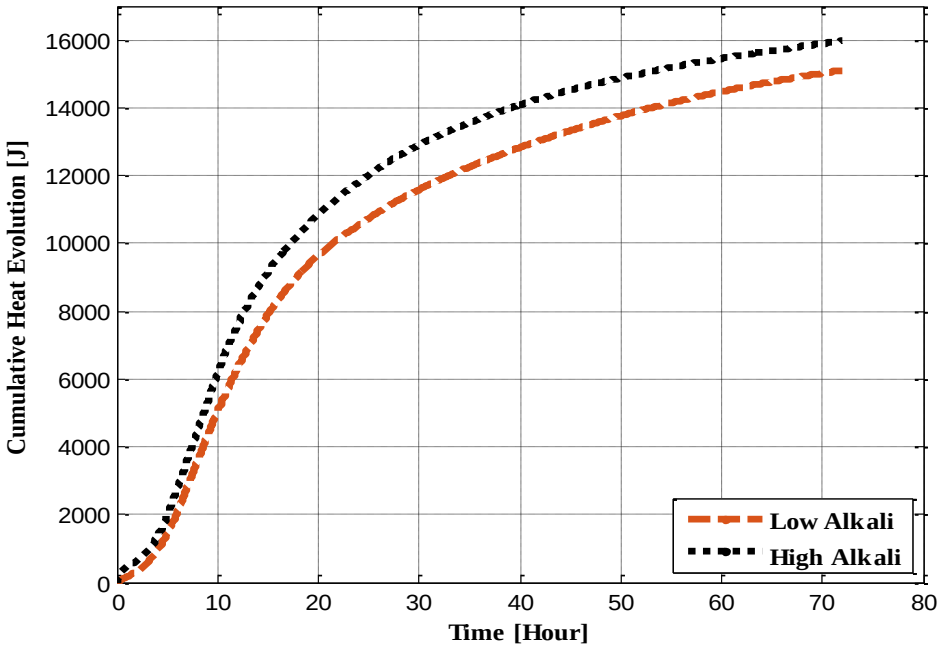

Figure 4. Effect of alkali addition on cumulative heat evolution of mortars.

Figure 5 presents the compressive strength development of the mortars. The low-alkali mortar developed 13% to 19% higher compressive strength compared to those made with additional NaOH. The difference in compressive strength is more pronounced at later ages (after 7 days). This may be partially due to the relatively more porous structure (less dense microstructure) of the high-alkali mortar. The higher porosity associated with the high-alkali mortar was confirmed through water absorption testing. The water absorption results showed that the high-alkali mortar had 20.5% higher water absorption compared to the low-alkali mortar. This finding is consistent with results reported in [2-3] where it was mentioned that alkali addition in cement paste affects the microstructure. Greater non-uniformity in microstructure of high-alkali paste can lead to localized stresses and greater porosity, which can reduce mechanical properties.

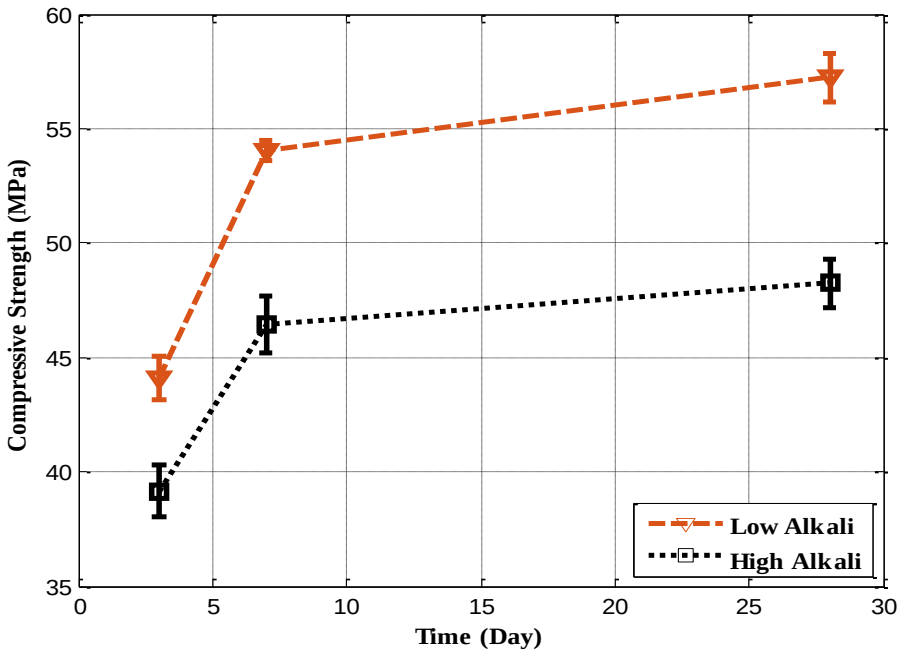

Figure 5. Effect of alkali addition on compressive strength development of mortars.

Figure 6 shows the measured bulk resistivity of mortars as a function of curing time. At first day of age, mortar made with NaOH addition exhibited 24% higher bulk resistivity, while this trend was reversed at later age (i.e., after five days). The higher bulk resistivity of high-alkali mortar observed for the first day may be due to the higher degree of hydration compared to the low-alkali mortar, indicating a denser microstructure at early age. However, the reduction in bulk resistivity for high-alkali mortar at later ages (after 5 days of age) can be attributed to the higher porosity of the microstructure. The relatively more porous nature of high-alkali mortar was validated earlier through the compressive strength and water absorption test results.

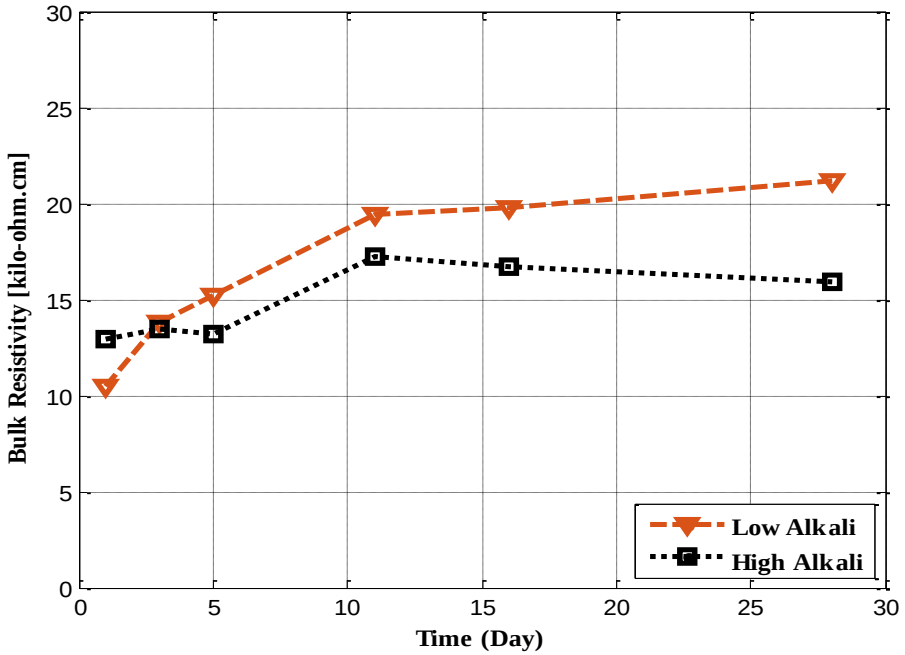

Figure 6. Effect of alkali addition on bulk resistivity of mortars.

3.2. MICROWAVE DIELECTRIC PROPERTY RESULTS

Thus far, the engineering properties of the mortars were quantified for two reasons: first, to ensure they follow the expected trends, and second, to utilize those results to evaluate any potential correlation between engineering and dielectric properties of the mortars.

Figure 7 shows the measured relative permittivity and loss factor of the mortars during the first 28 days (curing period). The results reported here represent the average values for three mortar samples for each mortar mix. As can be seen in Fig. 7.a, after the first few days, where the mortars showed similar behavior in their permittivities, this value was consistently measured to be different for the two mixes where the permittivity of the high-alkali mortars showed to be higher compared to the low-alkali mortars.

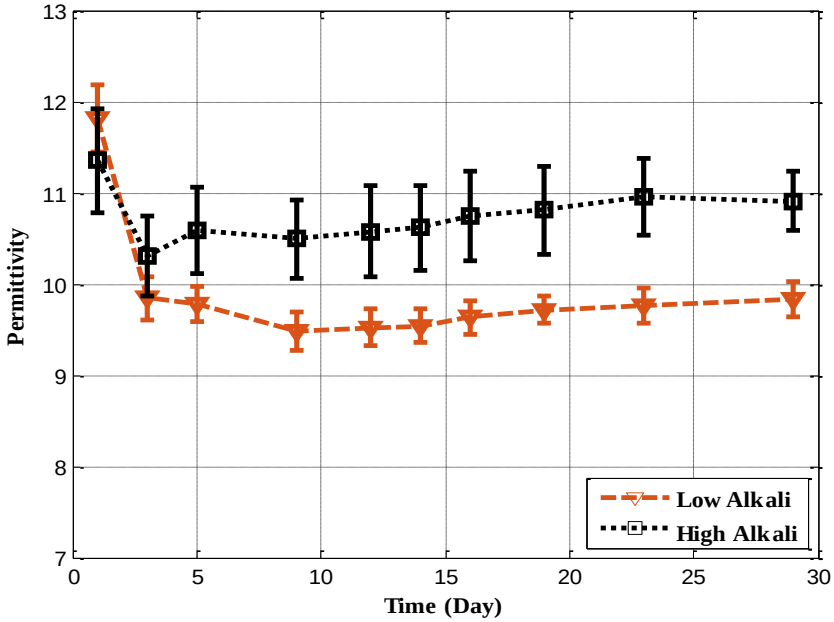

(a)

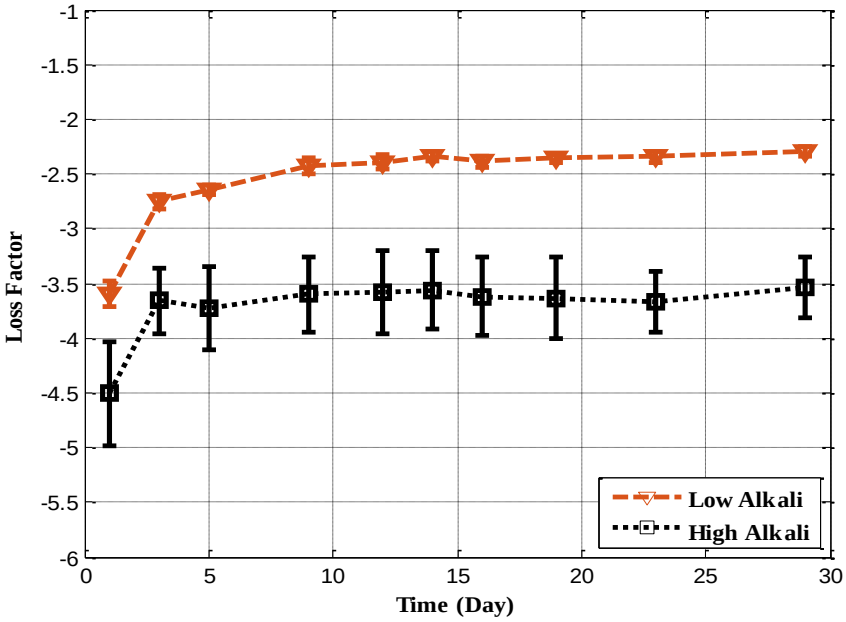

(b)

Figure 7. Dielectric constant measurements of mortars (a) permittivity, and (b) loss factor.

Unlike permittivity measurements which had similar values initially, loss factor started with a significant difference between the high and the low-alkali mortars. As can be seen in Fig. 7.b, mortars with high-alkali content have higher loss factor compared to the low-alkali mortars during the measurement period of 28 days. This behavior (i.e., high loss factor) is an indication of higher ionic concentration in the pore solution of the high-alkali mortars. The difference in microwave dielectric properties of the mortars, can be further explained by considering the Debye model for the dielectric constant of pure versus ionic water [18]. Expressions related to permittivity and loss factor of pure water (based on the Debye model) are shown in Eqns. (3) and (4), respectively. Equations (5) and (6) formulate permittivity and loss factor of ionic water (saline water) based on the same model.

$$\varepsilon'_{pw} = \varepsilon_{pw\infty} + \frac{\varepsilon_{pw0} - \varepsilon_{pw\infty}}{1+(2\pi f \tau_{pw})^2} \tag{3}$$

$$\varepsilon''_{pw} = \frac{2\pi f \tau_{pw}(\varepsilon_{pw0} - \varepsilon_{pw\infty})}{1+(2\pi f \tau_{pw})^2} \tag{4}$$

$$\varepsilon'_{iw} = \varepsilon_{iw\infty} + \frac{\varepsilon_{iw0} - \varepsilon_{iw\infty}}{1+(2\pi f \tau_{iw})^2} \tag{5}$$

$$\varepsilon''_{iw} = \frac{2\pi f \tau_{iw}(\varepsilon_{iw0} - \varepsilon_{iw\infty})}{1+(2\pi f \tau_{iw})^2} + \frac{\sigma_{iw}}{2\pi\varepsilon_0 f} \tag{6}$$

where,

$\varepsilon_{p/iw0}$ = static dielectric constant of water (pure/ionic), dimensionless

$\varepsilon_{p/iw\infty}$ = high frequency limit of $\varepsilon_{p/I}$, dimensionless

ε_0 = 8.854×10^{-12} F/m

$\tau_{p/iw}$ = relaxation time of water, S

f = frequency, Hz

$\sigma_{p/iw}$ = ionic conductivity, S/m

As it can be inferred from the equations, and the results shown for pure water and saline water in [11-18], the permittivities at S-band (i.e., 2.6 – 3.95 GHz) are quite similar as they are shown in Fig. 7.a. Hence, similar values of permittivity at the beginning of the measurements period are corroborated. According to the results shown in Fig. 7.a, after the first few days, once the dominant effect of overwhelming amount of available free water (either pure or ionic) begins to diminish (due to the hydration process), the measurements reflect more of the intrinsic properties of the entire material's matrix. Afterwards, the permittivities of both low and high-alkali mortars show a slight increasing trend while the values diverge from each other. However, the permittivities are substantially different during the hydration process

On the other hand, by comparing (4) and (6), it can be seen that there exists an additional term for loss factor of ionic water (compared to pure water). This additional term accounts for the ionic conductivity of the solution which in this case is directly influenced by the amount of alkali within the pore solution of the mortars. Thus, the ionic conductivity of the mortars contributes significantly to the loss factor measurements. As such, this explains the reason for the distinct values of loss factor measurements in low and high-alkali mortars at first few days. As a result, according to the Debye model and the measurements results, higher measured values of loss factor for the mortar with high-alkali content may be attributed to the fact that pore solution of those mortars have more ionic concentration compared to the mortars with low-alkali content.

Another point that must be addressed with respect to the microwave measurements, is the higher variations in the measured dielectric properties of high-alkali mortars compared to the low-alkali mortars (i.e., larger standard deviation). As mentioned earlier, the addition of NaOH to the mortar affects the mortar's porosity. This change in porosity of the high-alkali mortars may have been occurred non-uniformly within the three samples. Consequently, this difference in porosity of the three "similar" samples manifested itself as a higher standard deviation in the high-alkali mortars. However, it should be emphasized that the standard deviation of both mortar mixtures are within the expected range of this measurement technique (±5% and ±10% for permittivity and loss factor, respectively). More importantly, according to the measurement results, the two mortar mixtures are unequivocally distinguishable from each other through their different dielectric properties.

4. DISCUSSION

As it was shown, engineering properties results confirmed the expected behavior for both low and high-alkali mortars. Furthermore, we intended to investigate any potential correlation between the dielectric and engineering properties of these mortars. However, the only parameters that could be appropriately correlated to the dielectric properties appeared to be the bulk resistivity and compressive strength of the mortars, as discussed here.

Figure 8.a depicts the correlation between the measured loss factor and bulk resistivity of the high and low-alkali mortars. The results show that as the loss factor decreases, there is an increase in bulk resistivity of the mortars, however with different rates for each mortars. The overall trend is meaningful, since the lower loss factor is an indication of lower amount of absorbed water (from the humid environment) and, at the same time, an indication of transformation of higher amount of free water into bound water.

Figure 8.b shows the correlation between the loss factor and compressive strength. Similar to bulk resistivity, the compressive strength also increased as a function of decreasing loss factor. However, the rate of change is different in the high-alkali and low-alkali mortars.

In order to evaluate this correlation from a civil engineering point-of-view, the amount of absorbed water by the mortars was examined. In addition to ASTM C642 that was mentioned earlier, the mass of samples were measured on a daily basis and immediately after removal from the hot and humid chamber. Figure 9 shows the normalized mass change in the two sets of mortars, showing the increase in mass is more pronounced in high-alkali mortar compared to the low-alkali. This suggests an increased

water absorption (more porosity) in the former mortar compared to the latter. Moreover, the water absorption results, bulk resistivity and compressive measurements confirmed that low-alkali mortar developed lower porosity (or higher compressive strength) compared to the high-alkali mortar. Therefore, the corresponding loss factor of high-alkali mortar should be higher compared to the low-alkali mortar.

Referring back to Fig. 8, the low-alkali mortars showed a monotonic correlation between loss factor, compressive strength, and bulk resistivity. However, for the high-alkali mortar, these correlations turned out to be different and the increase in bulk resistivity and compressive strength did not continue monotonically. This difference in behavior of the mortars appears to be directly related to the effect of alkali addition on the material properties, and may be quantified appropriately to extract a unique parameter than can be further utilized to detect the alkalinity level of mortars with different alkali contents.

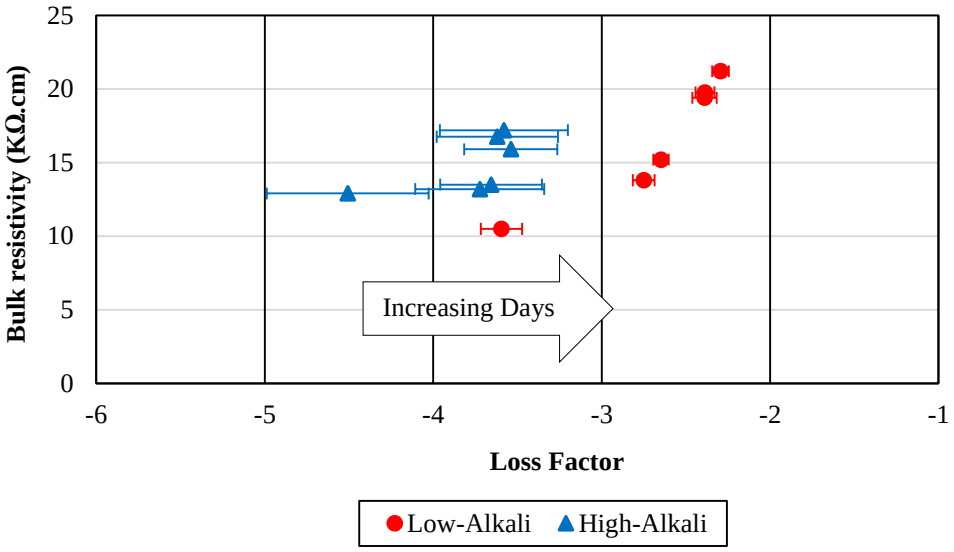

(a)

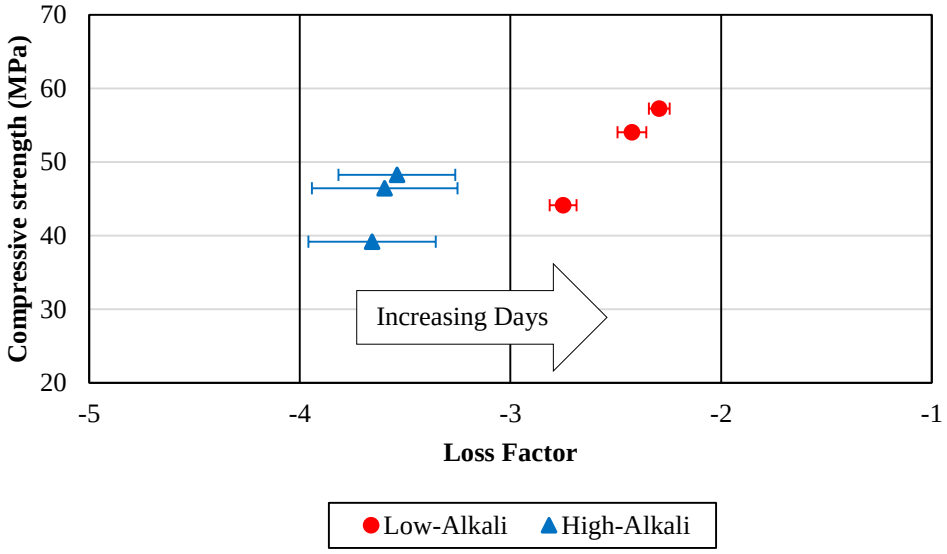

(b)

Figure 8. Correlation between loss factor and: a) bulk resistivity, and b) compressive strength.

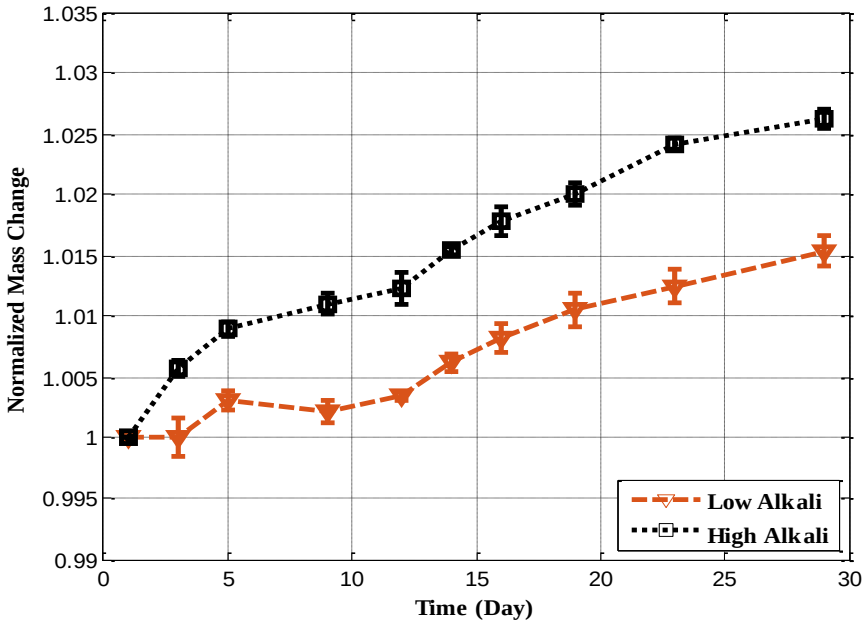

Figure 9. Variation in mass of the mortars over time.

This investigation aimed to evaluate the potential of microwave dielectric property measurements for evaluating of alkalinity in mortars. However, in order to be able to draw a solid conclusion and formulate any relationship between these parameters, larger samples sets of mortar mixtures cast with different alkalinity levels must be examined. However, the results outlined here show potential for viability of such investigation in the future.

5. CONCLUSION

In this investigation the effect of alkali addition on engineering properties of mortars were evaluated. The feasibility of using microwave dielectric properties to differentiate mortars with and without NaOH addition was also investigated. Through microwave dielectric measurements, it was demonstrated that the changes in material properties of mortars with low and high-alkali contents render substantially different values for each. It was shown that high-alkali mortars manifested a higher complex dielectric constant compared to the low-alkali mortars. This is an indication of a higher ionic concentration in the high-alkali mortars. Additionally, a monotonic correlation was observed between the measured loss factor, bulk resistivity, and compressive strength of the low-alkali mortar. However, the high-alkali mortar did not follow the same trends as in low-alkali mortar. This difference in trends may be an identifying parameter that may be further utilized to develop a versatile microwave nondestructive evaluation technique capable of detecting the level of alkalinity in cement-based materials.

6. ACKNOWLEDGMENTS

This work was partially supported by the National Science Foundation (NSF) as a collaborative grant under award 1234151. Any opinions, findings, and conclusions or recommendations expressed in this material are those of the authors and do not necessarily reflect the views of the NSF.

REFERENCES

[1] ACI CT-13, ACI concrete terminology, An ACI standard, American Concrete Institute Pubs., USA, January 2013.

[2] Juenger MCG, Jennings HM. Effects of highly alkalinity on cement pastes. Mater J 2001; 98:251–5. doi:10,14359/10280.

[3] Smaoui N, Bérubé M a., Fournier B, Bissonnette B, Durand B. Effects of alkali addition on the mechanical properties and durability of concrete. Cem Concr Res 2005; 35:203–12. doi:10.1016/j.cemconres.2004.05.007.

[4] Bu Y, Weiss J. The influence of alkali content on the electrical resistivity and transport properties of cementitious materials. Cem Concr Compos 2014; 51:49–58. doi:10.1016/j.cemconcomp.2014.02.008.

[5] AASHTO. 2011. PP65-11. Standard practice for determining the reactivity of concrete aggregates and selecting appropriate measures for preventing deleterious expansion in new concrete construction. 2011; Washington, D.C.

[6] Bois KJ, Benally AD, Zoughi R. Microwave near-field reflection property analysis of concrete for material content determination. IEEE Trans Instrum Meas 2000; 49:49–55. doi:10.1109/19.836308.

[7] Peer S, Case JT, Gallaher E, Kurtis KE, Zoughi R. Microwave reflection and dielectric properties of mortar subjected to compression force and cyclically exposed to water and sodium chloride solution. IEEE Trans Instrum Meas 2003; 52:111–8. doi:10.1109/TIM.2003.809099.

[8] Hashemi A, Donnell KM, Zoughi R, Knapp MCL, Kurtis KE. Microwave detection of carbonation in mortar using dielectric property characterization. 2014 IEEE Int. Instrum. Meas. Technol. Conf. Proc., IEEE; 2014, p. 216–20. doi:10.1109/I2MTC.2014.6860739.

[9] Donnell KM, Hatfield S, Zoughi R, Kurtis KE. Wideband microwave characterization of alkali-silica reaction (ASR) gel in cement-based materials. Mater Lett 2013; 90:159–61. doi:10.1016/j.matlet.2012.09.017.

[10] Hashemi A, Donnell KM, Zoughi R, Kurtis KE. Effect of humidity on dielectric properties of mortars with alkali-silica reaction (ASR) gel. 2014 IEEE Int. Instrum. Meas. Technol. Conf. Proc., IEEE; 2015, p. 1502-1506.

[11] Hashemi A, Horst M, Kurtis KE, Donnell KM, Zoughi R. Comparison of Alkali–Silica Reaction Gel Behavior in Mortar at Microwave Frequencies. IEEE Trans Instrum Meas 2015; 64:1907–15. doi:10.1109/TIM.2014.2367771.

[12] Hashemi A., Hatfield S, Donnell KM, Zoughi R, Kurtis KE. Microwave NDE method for health-monitoring of concrete structures containing alkali-silica reaction (ASR) gel. AIP Conf Proc 2014; 1581 33:787–92. doi:10.1063/1.4864901.

[13] ASTM C 1293-08b, Determination of Length Change of Concrete due to Alkali–silica Reaction (concrete prismtest), ASTM International,West Conshohocken, PA, 2008., http://dx.doi.org/10.1520/C1293-08B, www.astm.org.

[14] Gu P, Xie P, Beaudoin JJ, Brousseau R. AC impedance spectroscopy (II): microstructural characterization of hydrating cement–silica fume systems. Cement Concr Res 1992; 23(1):157–68.

[15] Bois KJ, Handjojo LF, Benally AD, Mubarak K, Zoughi R. Dielectric plug-loaded two-port transmission line measurement technique for dielectric property characterization of granular and liquid materials. IEEE Trans Instrum Meas 1999;48:1141–8. doi:10.1109/19.816128.

[16] Multon S, Cyr M, Sellier A, Diederich P, Petit L. Effects of aggregate size and alkali content on ASR expansion. Cem Concr Res 2010; 40:508–16. doi:10.1016/j.cemconres.2009.08.002.

[17] Bentz DP. Influence of alkalis on porosity percolation in hydrating cement pastes. Cem Concr Compos 2006; 28:427–31. doi:10.1016/j.cemconcomp.2006.01.003.

[18] Ulaby FT, Moore RK, Fung AK. Microwave remote sensing: active and passive, vol. iii, volume scattering and emission theory, advanced systems and applications." Inc., Dedham, Massachusetts (1986): 1797-1848.

IV. CURING CONDITIONS EFFECTS ON THE LONG-TERM DIELECTRIC PROPERTIES OF MORTAR SAMPLES CONTAINING ASR GEL

ABSTRACT

Alkali-silica reaction (ASR) is a chemical reaction between alkalis present in portland cement and amorphous or otherwise disordered siliceous minerals in particular aggregates. Through this reaction, reactive silica binds with hydroxyl and alkali ions and forms a gel, known as ASR gel which may be detected in mortar samples using microwave materials characterization techniques. While there are only few studies on the characterization of ASR-affected mortar samples using microwave techniques, the comprehensive understanding of variables that affect the extent of ASR in mortar and their effect on microwave signals, in particular the effect of curing condition, requires more studies. Therefore, parameters related to curing conditions must be considered when using microwave signals for ASR detection and evaluation. In this paper, the effect of curing condition on the ASR gel formation and microwave dielectric properties of mortar samples is investigated.

To this end, extended measurements of the complex dielectric constants of three different sets of mortar samples are presented at S-band (2.6 – 3.95 GHz). Samples were cast with reactive aggregates, and cured at different conditions. Results shows slightly different permittivities for the differently cured samples, potentially indicating different amount of ASR gel. This observation was corroborated through UV fluorescence microscopy, where different amounts of ASR gel were observed in the samples. Moreover, results indicate that ASR gel evolution may be better tracked through loss factor

measurements, while pre-existing-gel may be better detected through permittivity measurements.

Index Terms: microwave material characterization, alkali-silica reaction, optical microscopy, cement-based materials, dielectric constant.

1. INTRODUCTION

Alkali-silica reaction (ASR) is a chemical reaction between alkalis present in portland cement and amorphous or otherwise disordered siliceous minerals in particular aggregates (i.e., ASR-reactive aggregates). In this reaction, reactive silica binds with hydroxyl and alkali ions and forms an alkali-silica gel, known as ASR gel [1]. ASR gel may imbibe water (moisture) from its surroundings and expand. If the tensile stress caused by the expansion of gel exceeds that the tensile capacity of aggregate/paste, it creates microcracking within aggregate/paste. As long as sufficient moisture (typically internal RH > 80%) is available, the reaction progresses and may result in the higher extent of microcracking and deterioration of concrete structures. There are three main requirements for ASR gel formation, namely: sufficient alkali, amorphous silica, and moisture. To bring a better understanding to ASR gel formation from the standpoint of dielectric property measurements, one must monitor the influence of curing condition as it affects the availability of moisture in cement-based materials.

Microwave materials characterization techniques have shown the capability of evaluating a number of critical properties associated with cement-based materials, such as: material content [2], chloride permeation [3], [4], carbonation [5], and most recently ASR gel formation [6]–[10]. Microwave signals are sensitive to the presence of moisture within dielectric materials. In general, the interaction of microwave signals with dielectric materials is described by a parameter known as the complex dielectric constant, which is intrinsic to the material, and is independent of the method with which it is measured. This complex parameter is referred to as relative dielectric constant (εr) once it is referenced to the dielectric constant of the free-space. As indicated in (1), the complex-valued relative

dielectric constant can be further defined by its real and imaginary parts, where the former (relative permittivity) indicates the ability of the material to store microwave energy and the latter (relative loss factor) indicates the ability of the material to absorb microwave energy:

$$\varepsilon_r = \varepsilon'_r - j\varepsilon''_r \quad (1)$$

The complex dielectric constant of mortar is affected by curing condition. In fact the duration and type of curing of mortar samples affects cement hydration—a chemical reaction between water and cement particles in which part of free water transforms to the chemically bound water of reaction products—and the dielectric constants of hydration products.. Given that mortar cures over time, monitoring of its temporal complex dielectric constant can provide information about its curing process as well as ASR formation in the presence of ASR-reactive aggregates.

This paper presents long-term measurements of relative dielectric constants of three different sets of mortar samples at S-band (2.6 – 3.95 GHz), cast with ASR-reactive aggregates, and cured at different conditions. Mortar samples were exposed to both humid and dry conditions for two reasons. First, to determine the potential relationship between different curing conditions and the dielectric constant of samples at the end of curing period. Second, to investigate the difference in the ultimate dielectric constants of mortar samples corresponding to the amount of produced ASR gel.

The first objective is achieved by monitoring the long-term dielectric constant of the samples, cured at different environmental conditions. The second objective is

accomplished by examining the correlation between the amount of ASR gel formation, quantified by the analysis of UV fluorescence microscopy images of samples, and their dielectric measurements.

2. SAMPLE PREPARATION AND CURING CONDITIONS

Three sets of mortars, each set having two similar samples were cast with an aggregate-to-cement (a/c) ratio of 2.25 and water-to-cement (w/c) ratio of 0.47. Furthermore, the reactivity of the aggregate type was examined following the ASTM-C1260 standard also known as Accelerated Mortar Bar Test (AMBT).The standard classifies the aggregate type as potentially reactive since the average fourteen-day expansion of mortar bars cast with this aggregate type was 0.383%, which exceeds the fourteen-day expansion limit of ASTM C 1260 standard. In addition, To accelerate ASR gel formation, sodium hydroxide (NaOH) was added to the mixing water to achieve 1.25% soda equivalent by mass. Each sample was cast in a Plexiglas mold with a cross section of 7.21 cm × 3.4 cm, corresponding to the S-band rectangular waveguide cross-section dimensions. The length of samples were ~2-3 cm (the dielectric constant measurements are independent of sample length). Every sample within each set was exposed to different temperature and relative humidity (RH) levels for different time periods. Hot and humid conditions was realized by keeping samples above water in a sealed container in an environmental chamber, which was set to 39ºC ± 1ºC and 91% ± 5% RH similar to the conditions for the ASTM C 1293 [11]. Moreover, the temperature and relative humidity of ambient condition was 24ºC ± 1ºC and 35% ± 10% RH, respectively.

Samples in batch #1 were cured in the chamber for 28 days, and remained in there for an additional 152 days. After 180 days, sample 1 was removed from the chamber and put in ambient conditions, while sample 2 remained in the chamber. On day 320, sample 2 was also removed from the chamber and put in ambient conditions until the end of the experiment.

Samples in batch #2 were cured for the initial 28 days in the chamber. Afterwards, sample 3 was removed from the chamber and kept in ambient conditions for the rest of the experiment. Sample 4 was also removed from the chamber after the first 28 days. However, it was returned into the chamber on day 180, for 140 days. Afterwards it was put back in ambient conditions.

Contrary to the batch#1 and batch#2 samples, batch #3 were kept in the ambient conditions during their first 28 days of curing. However, after the first 28 days, sample 6 was put in the chamber for 140 days, and then returned back to ambient conditions. Sample 5 was out of the chamber for the entire period of the measurements. Table I, summarizes the curing condition of the samples within each set.

Table 1. Curing conditions of the samples

Mortars		Day 1-28	Day 28-180	Day 180-320	Day 320-430
Batch #1	**Sample 1**	Chamber	Chamber	Ambient	Ambient
	Sample 2	Chamber	Chamber	Chamber	Ambient
Batch #2	**Sample 3**	Chamber	Ambient	Ambient	Ambient
	Sample 4	Chamber	Ambient	Chamber	Ambient
Batch #3	**Sample 5**	Ambient	Ambient	Ambient	Ambient
	Sample 6	Ambient	Ambient	Chamber	Ambient

3. DIELCTRIC PROPERTY MEASUREMENT RESULTS

The relative permittivity and loss factor of each sample were measured on a weekly basis using the completely-filled waveguide technique as outlined in [12]. Fig. 1 shows the measurement setup.

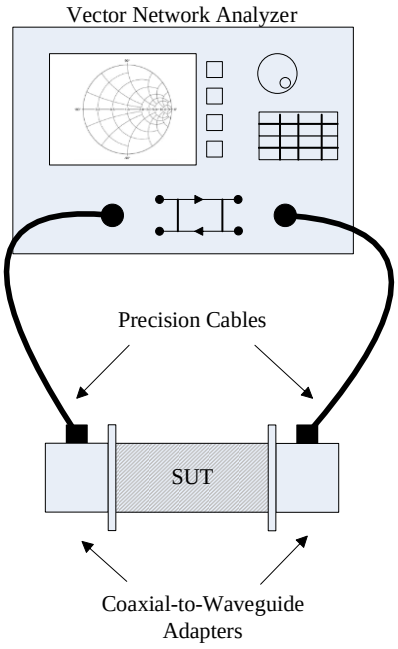

Figure 1. Measurement setup.

The measured relative permittivity and loss factor of samples are shown in Figs. 2a and 2b, respectively. During the time that samples were kept in the chamber a higher (relative) permittivity and loss factor (loss factor is a negative-valued number) were measured for the samples, and during the exposure to ambient conditions those values started to decrease. These trends were expected, since during humid conditions samples

were introduced to additional water, which increased their dielectric constant. In contrast, during the drying period, evaporation of water decreased in the dielectric constant of samples.

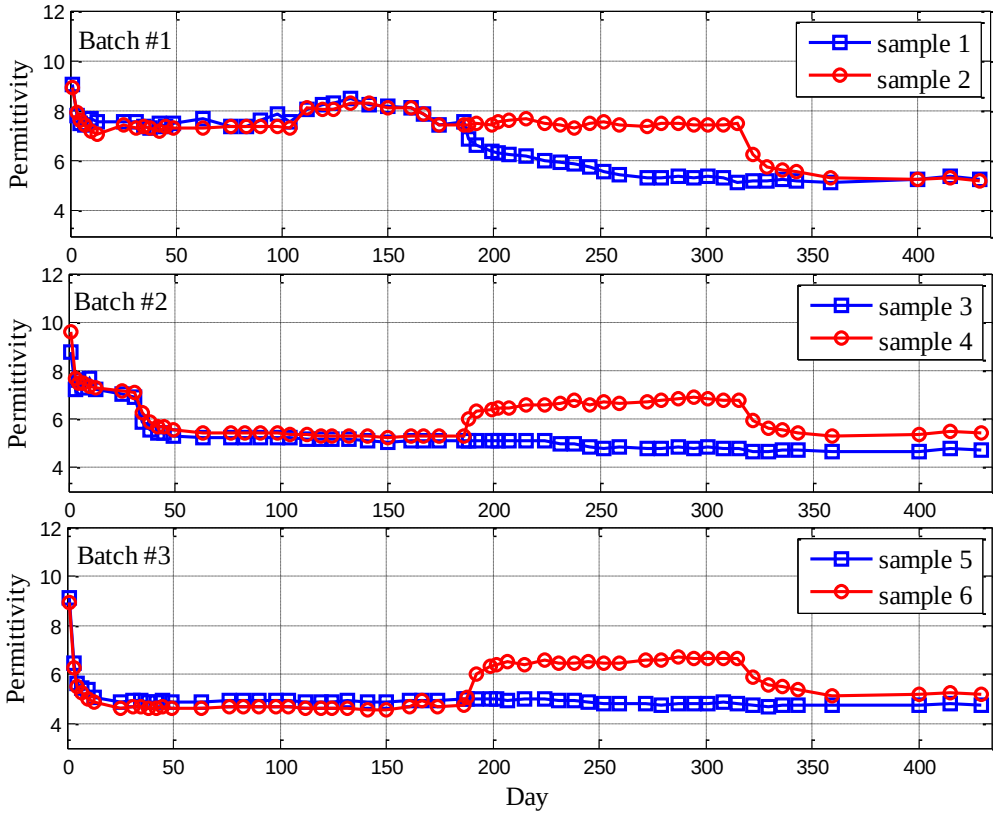

(a)

Figure 2. Dielectric constant measurements, a) permittivity, b) loss factor.

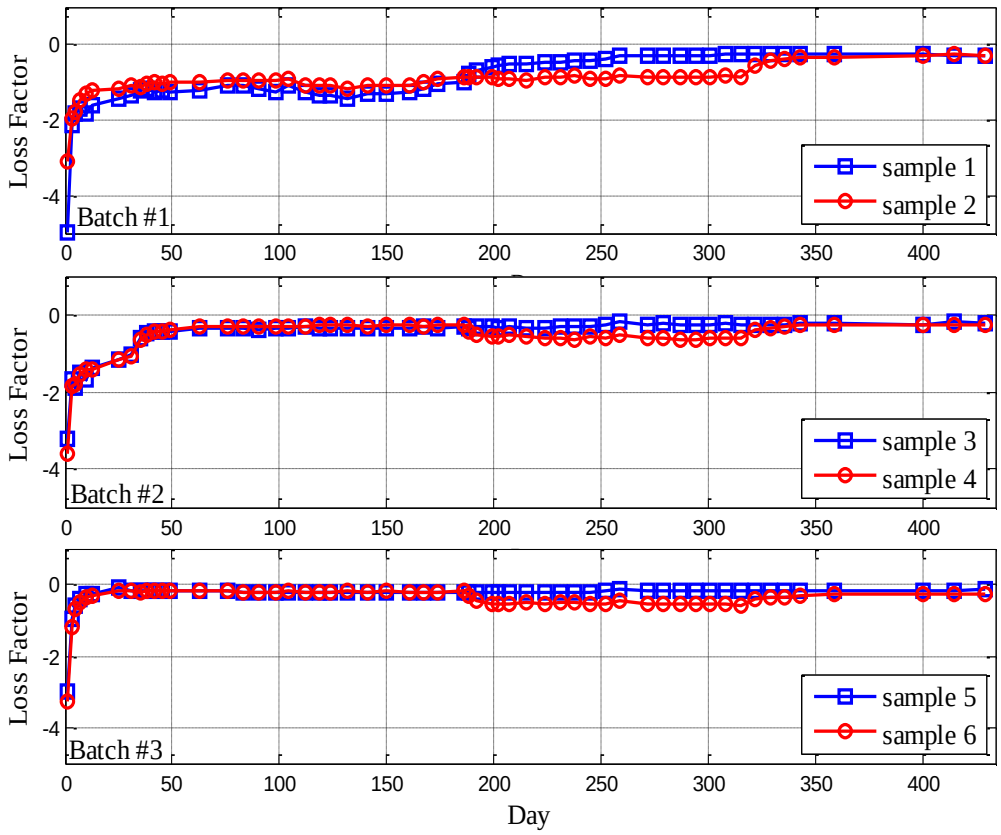

(b)

Figure 2. Dielectric constant measurements, a) permittivity, b) loss factor (cont.).

Comparing the results for the last day measurements of the six mortar samples, the ultimate (last day) permittivities are somewhat different among the samples. To investigate whether this difference in permittivity values is due to ASR gel or the remaining moisture, corresponding loss factors results are examined. According to Fig. 2b, the (last day) loss factor measurements are almost identical. Since loss factor (compared to permittivity) is more sensitive to the moisture content of the mortars susceptible to ASR [10], similar values of loss factor (at last day) implies the equivalent amount of moisture (even though very little) in mortar samples. This is meaningful since the majority of the remaining free

water in samples had sufficient amount of time (~110 days before the last day measurement) to evaporate. Therefore, slight differences in permittivity measurements may be attributed directly to the difference in the materials matrix (or ASR gel formation) rather than the remainder of water in samples. Consequently, to verify that whether the differences in permittivities are indication of ASR gel, microstructural characterization was performed using UV fluorescence microscopy, which was followed by image analysis to quantify the amount of ASR gel in mortar samples.

4. MICROSTRUCTURAL CHARACTERIZATION

Microstructural characterization of ASR affected samples was performed following the ASTM C856 standard [13], which is adopted based on the work of Natesaiyer and Hover [14]. In this process, samples of freshly cut concrete/mortar are stained with 5% uranyl acetate aqueous solution. During the staining period, uranyl ions replace the adsorbed sodium, potassium and calcium ions [14]. Furthermore, since uranyl fluorescences greenish-yellow under the short-wave UV light (254 nm wave length) [13, 14], obtaining images under that light indicates locations of having high concentration of alkali ions or calcium, such as in ASR gel. Furthermore, uranyl ions do not adsorb to the hydration product [14]. However, there are some limitations associated with this method. For instance, some aggregate types may naturally florescent under the short wave UV light (Fig. 3.) To avoid this problem, the surface of concrete/mortar sample should be prescreened for the natural fluorescence of those aggregates [13]. Furthermore, carbonation and and pozzolanic reactions in concrete/mortar may contribute to the fluorescence [13]. Another issue that may contribute to the fluorescence of uranyl acetate during the optical microscopy is the precipitation of uranyl acetate due to the drying of sample. While uranyl acetate solution does not fluoresce, its salt fluoresces dull green [14]. However, this color is distinct from the bright greenish-yellow due to the ASR gel formation. The background dull green fluorescence in the 4-a, e, f images are attributed to fluorescence of uranyl acetate salt rather than ASR gel. Overall, although this staining method has limitations, it is easy to apply, and the amount of ASR gel in the samples can be readily evaluated.

The procedure of staining using uranyl acetate and UV fluorescence microscopy of sample sections were as follows: One section per each sample was cut using slow speed

ethanol-cooled saw. After cutting, surfaces were wiped to remove debris. Furthermore, to minimize gel removal, sections were not polished. The staining procedure was performed immediately after cutting. In this procedure, the surface of sections was first damped with de-ionized water. Afterwards, 5% uranyl acetate solution was applied to the surface of sections for one minute. Then sections were hold vertically and washed three times with de-ionized water to remove excessive uranyl acetate. Imaging was performed instantly after staining under the shortwave UV light at 25x magnification. The imaging process was performed systematically from the center to the edges of each section. On average, nine images per sample type per section were acquired. The experimental setup of imaging replicates the one used in [15].

The representative images of six mortar samples are shown in Fig. 4a-f, where the bright green color in those is the indication of ASR gel. To approximately quantify the amount of ASR gel in each sample, binary images of the UV fluorescence microscopy images were produced, and the ratio of the ASR pixels to the whole image pixels is defined as the ASR index, which is reported in Table II.

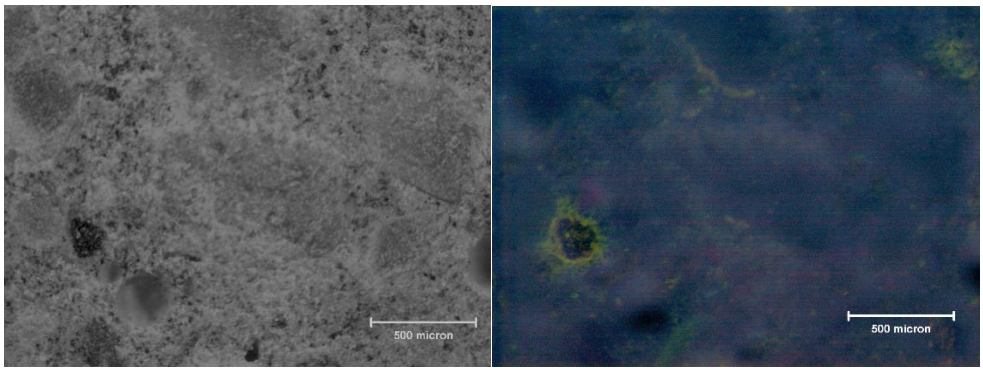

Figure 3. Optical microscopy image of a sample section exposed to white light (left), natural fluorescence of aggregates—yellow and green colors—under short wave UV light (right).

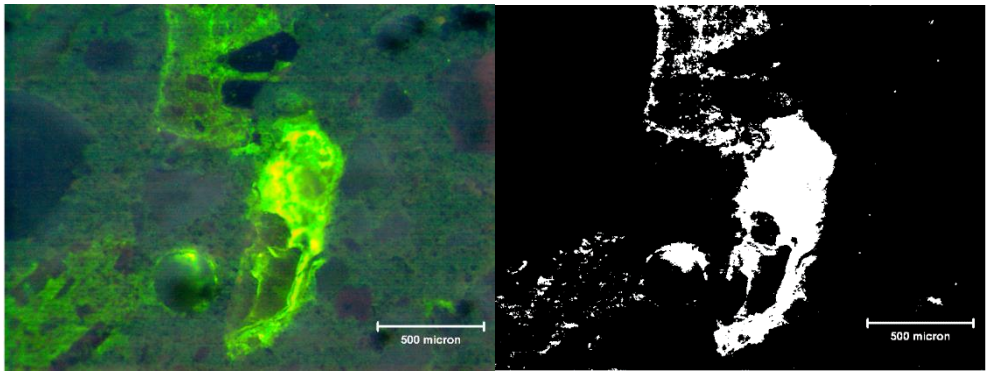

a) Sample 1

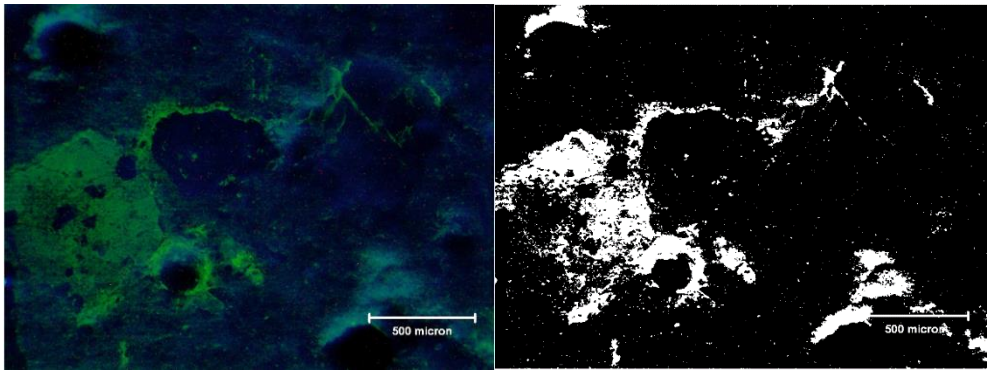

b) Sample 2

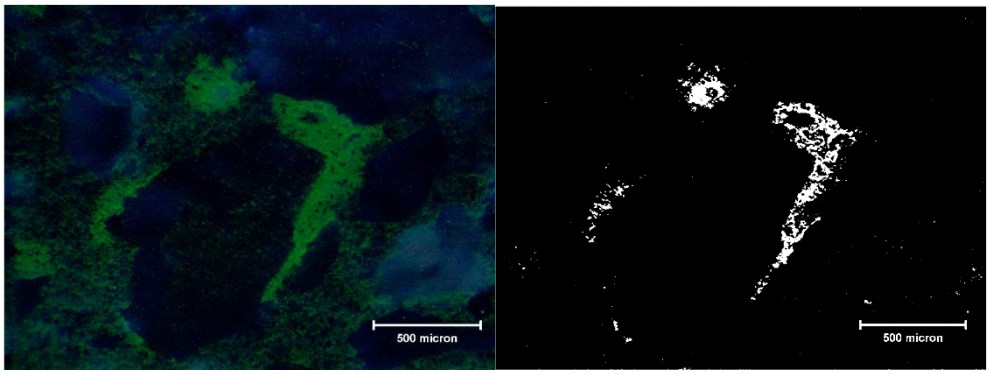

c) Sample 3

Figure 4. Optical microscopy images of the mortar samples (left), and their corresponding binary images (right) to quantify ASR index.

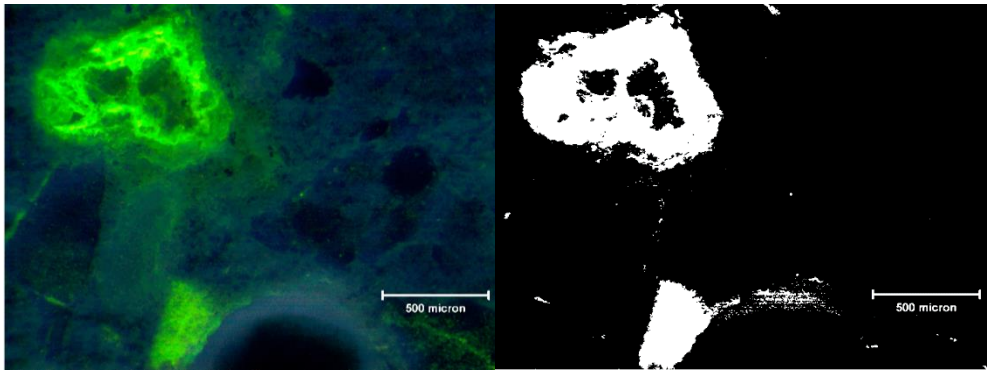

d) Sample 4

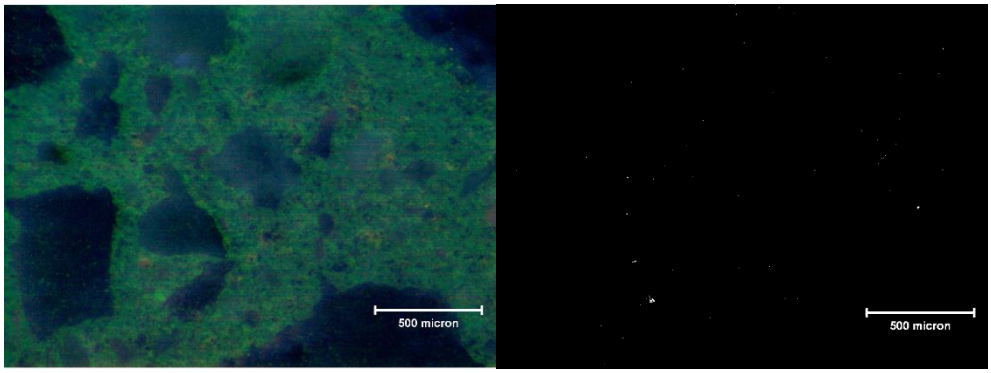

e) Sample 5

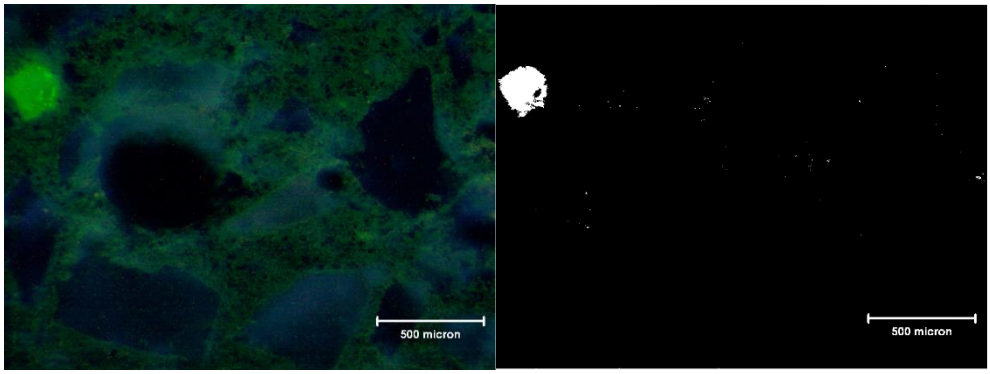

f) Sample 6

Figure 4. Optical microscopy images of the mortar samples (left), and their corresponding binary images (right) to quantify ASR index (cont.).

Table 2. ASR index of the mortar samples

Sample	Curing conditions (days)	ASR index	Last day permittivity
1	CH*(180)+A**(250)	0.108	5.28
2	CH(320)+A(110)	0.114	5.19
3	CH(28)+A(402)	0.023	4.72
4	CH(28)+A(152)+CH(140)+A(110)	0.131	5.40
5	A(430)	0.003	4.77
6	A(180)+CH(140)+A(110)	0.011	5.20

*CH: Chamber, **A: Ambient

According to the curing conditions of samples in batch #1, since the exposure time to hot and humid conditions is longer for sample 2 than sample 1, more ASR gel formation in the former than the latter is expected. However, samples have similar permittivities, which suggests the same amount of ASR gel formation. In addition, as shown in Table 2, the UV fluorescence microscopy images of samples 1 and 2 show similar ASR index, indicating the same amount of ASR gel formation. This corroborates that permittivity measurements are correlated to ASR formation.

In batch #2, since sample 4 is further exposed to humid conditions after 180 days of curing period, more ASR gel formation in that sample than sample 3 is expected. Moreover, according to Fig. 2a for batch #2, the permittivity measurements also show a discrepancy between the permittivity of the two samples, suggesting different material properties. Furthermore, as shown in Fig. 4, the UV fluorescence microscopy images of those samples also show different amounts of ASR gel formation (different ASR index)

within the samples. Hence, UV fluorescence microscopy corroborates that the difference in permittivities is an indication of ASR gel. In addition, it is unlikely that the difference in the permittivities of sample 4 is due to remainder of moisture for two reasons: first, sample 4 was at ambient condition before the final-day measurement for ~110 days, which should be sufficient for the sample to lose its excessive moisture and reach the same level of internal moisture as in sample 3. Second, and more importantly, the loss factor measurements of batch #2, in Fig. 2b, show similar values for both sample 3 and 4, indicating the same amount of moisture content in those samples. Hence, the difference in the permittivity of sample 3 and 4 may be attributed to ASR gel formation, rather than moisture content.

In batch #3, since samples 5 and 6 were cured at low humidity environment (i.e., ambient conditions), no ASR gel formation is expected. However, Sample 6 was exposed to humid conditions after 180 days to investigate the effect of ASR gel formation on the complex dielectric constant of mortar at later ages. Discussing results for these two samples, permittivity measurements in Fig. 2a show slightly different values for samples 5 and 6. Similarly, the UV fluorescence microscopy images of those sample in Fig. 4 and the corresponding ASR index reported in Table 2, also show a slight difference in the amount of produced ASR gel. Similar to batch #2, optical microscopy images corroborate that the difference in permittivity of the samples is due to the formation of ASR gel. The same reason (similar loss factor) as in batch #1, #2, holds true for this set of samples, supporting that the difference in permittivity measurements are indication of different amount of produced ASR gel rather than different moisture content of the samples.

5. CONCLUSION

Three sets of mortar samples were cast with ASR-reactive aggregate type, exposed to different curing conditions, and their long-term dielectric constants were measured temporally. Through dielectric constant measurements, although mortar samples showed similar loss factor at the end of the experiment, their permittivities were slightly different. Similar values of measured loss factor suggested that the difference in permittivities could be mainly related to the amount of produced ASR gel, and not the moisture remainder. To verify this, UV fluorescence microscopy images of samples stained with uranyl acetate were obtained. Images showed different amount of ASR gel formation, which was quantified using image analysis and expressed as ASR index for different samples, corroborating the hypothesis that the difference in the permittivities are directly related to ASR gel formation.

This investigation also provides an insight to determine a figure of merit in future investigation on ASR formation. Recently, it was shown that ASR formation can be better tracked through loss factor measurements during the early stages of cement curing process [10]. However, in this investigation, it was shown that the amount of produced ASR gel in long-term (once the overwhelming effect of the internal moisture diminishes) can be better determined through permittivity measurements. In other words, ASR gel evolution may be better tracked through loss factor measurements, while readily-available-ASR-gel may be better detected through permittivity measurements.

Through this investigation the capability of microwave materials characterization techniques was further explored to find out a more precise figure of merit in ASR evaluation. These findings and the previous efforts in ASR characterization, collectively, can be further utilized in future pertinent investigations to develop a robust nondestructive microwave technique in evaluation of ASR formation in cement-based structures.

REFERENCES

[1] "ACI Concrete Terminology, ACI Standard CT-13, Jan." 2013.

[2] K. J. Bois, A. D. Benally, and R. Zoughi, "Microwave near-field reflection property analysis of concrete for material content determination," IEEE Trans. Instrum. Meas., vol. 49, no. 1, pp. 49–55, 2000.

[3] S. Peer, K. E. Kurtis, and R. Zoughi, "Evaluation of microwave reflection properties of cyclically soaked mortar based on a semiempirical electromagnetic model," IEEE Trans. Instrum. Meas., vol. 54, no. 5, pp. 2049–2060, 2005.

[4] K. Munoz, R. Zoughi, and A. Microwave, "Influence of Cyclical Soaking in Chloride Bath and Drying of Mortar on Its Microwave Dielectric Properties : the Forward Model," in AIP conference proceedings, vol 22, pp. 470-477, 2003.

[5] A. Hashemi, M. C. L. Knapp, K. M. Donnell, K. E. Kurtis, and R. Zoughi, "Microwave detection of carbonation in mortar using dielectric property characterization," 2014 IEEE Int. Instrum. Meas. Technol. Conf. Proc., pp. 216–220, May 2014.

[6] A. Hashemi, K. M. Donnell, R. Zoughi, and K. E. Kurtis, "Effect of humidity on dielectric properties of mortars with alkali-silica reaction (ASR) gel," in 2015 IEEE International Instrumentation and Measurement Technology Conference (I2MTC) Proceedings, pp. 1502–1506, July 2015.

[7] A. Hashemi, S. Hatfield, K. M. Donnell, R. Zoughi, and K. E. Kurtis, "Microwave NDE method for health-monitoring of concrete structures containing alkali-silica reaction (ASR) gel," in AIP Conference Proceedings,, vol. 1581, no. 33, pp. 787–792, 2014.

[8] K. M. Donnell, S. Hatfield, R. Zoughi, and K. E. Kurtis, "Wideband microwave characterization of alkali-silica reaction (ASR) gel in cement-based materials," Mater. Lett. vol. 90, pp. 159–161, 2013.

[9] K. M. Donnell, R. Zoughi, and K. E. Kurtis, "Demonstration of microwave method for detection of alkali-silica reaction (ASR) gel in cement-based materials," Cem. Concr. Res., vol. 44, pp. 1–7, 2013.

[10] A. Hashemi, M. Horst, K. E. Kurtis, K. M. Donnell, and R. Zoughi, "Comparison of Alkali–Silica Reaction Gel Behavior in Mortar at Microwave Frequencies," IEEE Trans. Instrum. Meas., vol. 64, no. 7, pp. 1907–1915, Jul. 2015.

[11] ASTM C 1293-08b, "Determination of length change of concrete due to alkali–silica reaction (concrete prism test)," ASTM Int., 2008.

[12] K. J. K. Bois, L. F. L. Handjojo, A. D. Benally, K. Mubarak, and R. Zoughi, “Dielectric plug-loaded two-port transmission line measurement technique for dielectric property characterization of granular and liquid materials,” IEEE Trans. Instrum. Meas., vol. 48, no. 6, pp. 1141–1148, 1999.

[13] ASTM C856-14, “Standard practice for petrographic examination of hardened concrete,” ASTM Int, 2014.

[14] K. Natesaiyer, and K. C. Hover. "Insitu identification of ASR products in concrete,” Cem. Concr. Res., vol. 18, no. 3, pp. 455-463, 1988.

[15] K. J. Leśnicki, J.-Y. Kim, K. E. Kurtis, and L. J. Jacobs, “Assessment of alkali–silica reaction damage through quantification of concrete nonlinearity,”.Mater. struct,, vol. 46, no. 3, pp. 497-509, 2013.

V. MICROWAVE DIELECTRIC PROPERTIES MEASUREMENTS OF SODIUM AND POTASSIUM WATER GLASSES

ABSTRACT

Dielectric properties of alkali silicates (Na,K)2(SiO2)nO) or ‘water glasses’ are a critical input into the electromagnetic modeling of these materials, which have a broad range of applications. Recent increased interest in understanding geopolymerization of aluminosilicates with water glasses and the potential to improve understanding of the role of moisture in damage due to alkali-silica reaction (ASR) in concrete (where water glass is a suitable analogue for ASR gel) motivates this research. This investigation presents the results of microwave dielectric property measurement of twelve laboratory-produced (synthetic) water glass samples at X-band (8.2-12.4 GHz). Results show an exponential decay of loss factor as a function of increasing silica-to-alkali ratio, suggesting a correlation with increase in bound water in the samples and a decrease in the fluid ionic concentration. The results provide an insight into the temporal changes of the dielectric properties of ASR-affected materials, as well as geopolymers.

Index Terms: Alkali-silica reaction (ASR) gel, microwave materials characterization, dielectric properties, geopolymers, cement-based materials, dielectric mixing model.

1. BACKGROUND

Alkali silicates (i.e., (Na,K)2(SiO2)nO) or ‘water glasses’ are used in a variety of industries, spanning water treatment to the automotive sector, with a range of applications including in refractories, fireproofing, and as coatings and adhesives. Increasingly, water glasses are used along with alkali hydroxides to combine with finely divided, largely amorphous aluminosilicates to form ‘geopolymers’, which are finding growing use as an alternative to traditional portland cement-based concrete. In addition, water glasses are similar compositionally to alkali-silica reaction gels that may form in concrete whose aggregate is affected by the deleterious alkali-silica reaction (ASR) [1]. There is interest examining the binding of moisture in water glasses as pathways to (1) better understanding geopolymerization between aluminosilicates and water glasses toward optimizing these materials and (2) better understanding the mechanisms of ASR gel expansion toward improving resistance of concrete to damage by this reaction.

Microwave materials characterization techniques have great potential for evaluating moisture state and water migration in a broad range of materials. For example, in cement-based materials, microwave methods have been used to assess water-to-cement ratio [2], and permeation of chloride-containing water [3]. Most recently, microwaves have been demonstrated for monitoring of temporal ASR gel formation in mortars and concrete [4–7]. The early detection of ASR-affected concrete structures and determination of the root cause of damage, is an important practical concern for systematic management of infrastructure. This approach can also be extended to emerging classes of infrastructure materials, such as geopolymers, where the transition of moisture from the free to bound

state during initial polymerization or due to environmental interactions in service are of interest.

Complex dielectric constant, ε_r, as shown in (1), is an intrinsic property and independent of the measurement method, describing the interaction of microwave signals with material media. The real part (relative permittivity) indicates the ability of the material to store microwave energy and the imaginary part (relative loss factor) represents the ability of the material to absorb microwave energy.

$$\varepsilon_r = \varepsilon'_r - j\varepsilon''_r \quad (1)$$

Critical information about the material composition and the nature of water binding within the material structure may be obtained by measuring microwave reflection properties of a structure using a predictive model for the effective dielectric properties of a mixture (i.e., concrete or geopolymer). The model requires both the effect of chemical interactions (i.e., geopolymerization, cement hydration, and ASR gel production, all of which involve transformation between free and bound water), which can be applied empirically [3], and information on the volumetric and dielectric properties of mixture constituents [8]. Here, dielectric properties of twelve water glass samples of varying composition were measured at X-band (8.2-12.4 GHz). Compositionally, these samples represent both geopolymer precursors (e.g., alkali activator solutions [9,10]) and laboratory-produced (synthetic) ASR gels as per [11]. Thus, information on the dielectric properties of water glass is necessary to, for example, first identify ASR in concrete and also importantly to evaluate the extent of ASR damage, via measures of gel volume and,

potentially, composition. For geopolymers, this dielectric information can be used to assess the extent of geopolymerization, providing important insight on microstructure and strength development, as well as potential extension for in situ monitoring of performance. Objectives of this investigation were as follows:

1. to investigate possible relationship between the dielectric properties and chemical composition (silica-to-alkali ratio (S/A)) of several water glass samples, and
2. to measure the dielectric properties of these materials for incorporating in dielectric mixing models.

2. WATER GLASS SAMPLES

Water glass was prepared in the laboratory by the addition of amorphous fumed silicon (IV) oxide (300–350 m2/g surface area, Alfa Aesar) with concentrated solutions of sodium hydroxide (1.85M NaOH) or potassium hydroxide (1.82M KOH), prepared with deionized water and ACS-grade reagents. Both sodium-based (Na-based) and potassium-based (K-based) water glasses were prepared at silica-to-alkali ratios (SiO2/Na2O or SiO2/K2O as S/A) by mass of zero, one, two, three, four, and five. Overall, six Na-based and six K-based samples were prepared in sealed polypropylene containers, which were agitated for ten minutes after the addition of the silica. This approach follows that of Zhang et al. [11]. The concentration of alkali solutions were slightly different to maintain a constant water-to-alkali ratio (W/A) by mass of 58. The W/A was selected based on the observed rheology of the most viscous samples, those prepared with sodium at S/A=5.0.

3. DIELECTRIC PROPERTY MEASUREMENT APPROACH

Dielectric properties of the water glass were measured using the open-ended waveguide technique [12,13]. An X-band open-ended rectangular waveguide probe along with a calibrated 8510C vector network analyzer (VNA) was utilized to measure the reflection coefficient over the frequency band, and subsequently the dielectric properties were calculated. The aperture of the waveguide was covered by a transparent cellophane (and was calibrated for) to accommodate fluid samples, as shown in Fig. 1. As a result of the high permittivity and loss factor of the samples, extents around the waveguide probe aperture are electrically large and to verify this, distilled water was first measured as a reference and the measurements results closely matched those reported in [14].

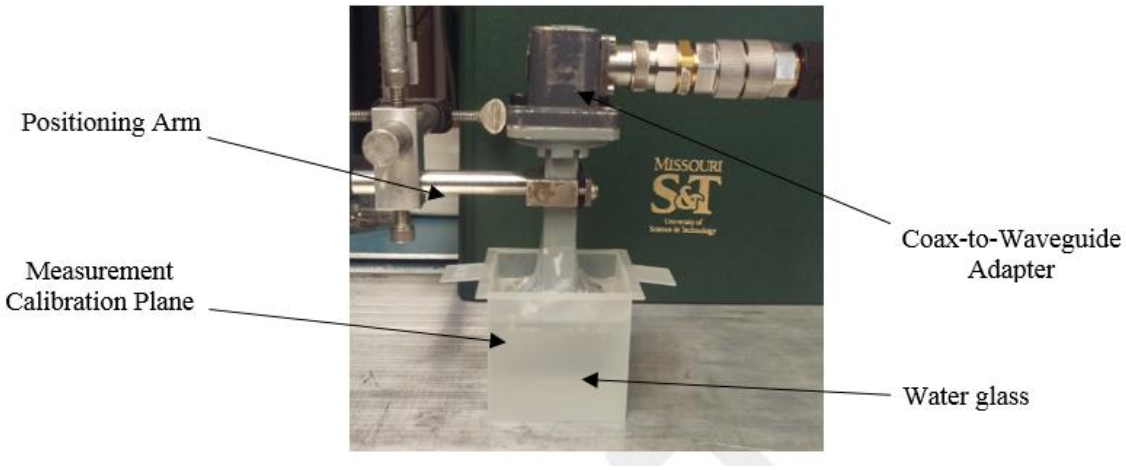

Figure 1. Open-ended waveguide measurement setup.

4. DIELECTRIC PROPERTY MEASUREMENT RESULTS

Figure. 2a shows relative permittivity and loss factor values for the twelve water glass samples, varying in alkali type and S/A. The Na-based sample at the S/A of zero shows higher permittivity but a comparable loss factor to the K-based sample. This suggests that the alkali cation type – Na vs. K – plays a role in the observed dielectric behavior. However, in the presence of silica, the permittivity of K-based samples is higher than for the Na-based samples at all S/A observed (i.e., 1-5). The greatest difference in relative permittivity is observed at S/A of five, where the Na-based sample is 32% lower than the K-based sample. It is proposed that these observations can be associated with the differences in the effective hydrated ion radius of the two alkalis examined, with sodium having a greater hydrated ion radius than potassium. Since the bare ionic radius of sodium is smaller than potassium, it has a larger surface charge density and subsequently the sodium ion attracts more water molecules than the potassium ion [15]. As a result, since samples were produced at the same water content, a greater fraction of water in the Na-based samples is more tightly bound, which results in the lower dielectric properties measured. While permittivity values decrease slightly as a function of increasing S/A, loss factor values decrease significantly. Furthermore, although in this study Na- and K-based samples were measured separately, pore solution of concrete often contains both ions which contribute to ASR gel formation and a mixture of sodium and potassium could be used in a geopolymer precursor. To consider this case, trends are illustrated when averaging the permittivity and loss factor values of K- and Na-based samples at the same S/A. Fig. 2b shows a logarithmic fit of average values as a function of S/A. As a result, one may estimate S/A from measured loss factor (LF) using:

$$S/A = exp\left(\frac{LF+50.47}{21.14}\right) \quad (2)$$

Decrease in relative permittivity and loss factors can be associated with increase in bound water and decrease in the ionic concentration, as S/A increases and water and ionic species become bound into an alkali-silicate gel. While bound water has lower relative permittivity and loss factor than free water, it is proposed that the decrease in ionic concentration significantly affects the loss factor while it has a minor effect on the relative permittivity at the X-band frequency [14]. As a result, the reduction of loss factor values is more significant than those of relative permittivity values. The process of binding water and decrease in the ionic concentration can be explained by the formation of gel, which incorporates water, alkalis, and hydroxides from the solution into its structure [16], [17]. This observation can be used to enhance understanding of the reaction rate during geopolymerization with precursors of varying composition and concentration and for understanding the relationship between ASR gel composition, its capacity to bind moisture, and potential for expansion. Demonstration of the utility of microwave measurements for assessment of water glasses is an important initial step in bringing new understanding to these two reactions, but also (given the broad use of water glasses) in other realms as well.

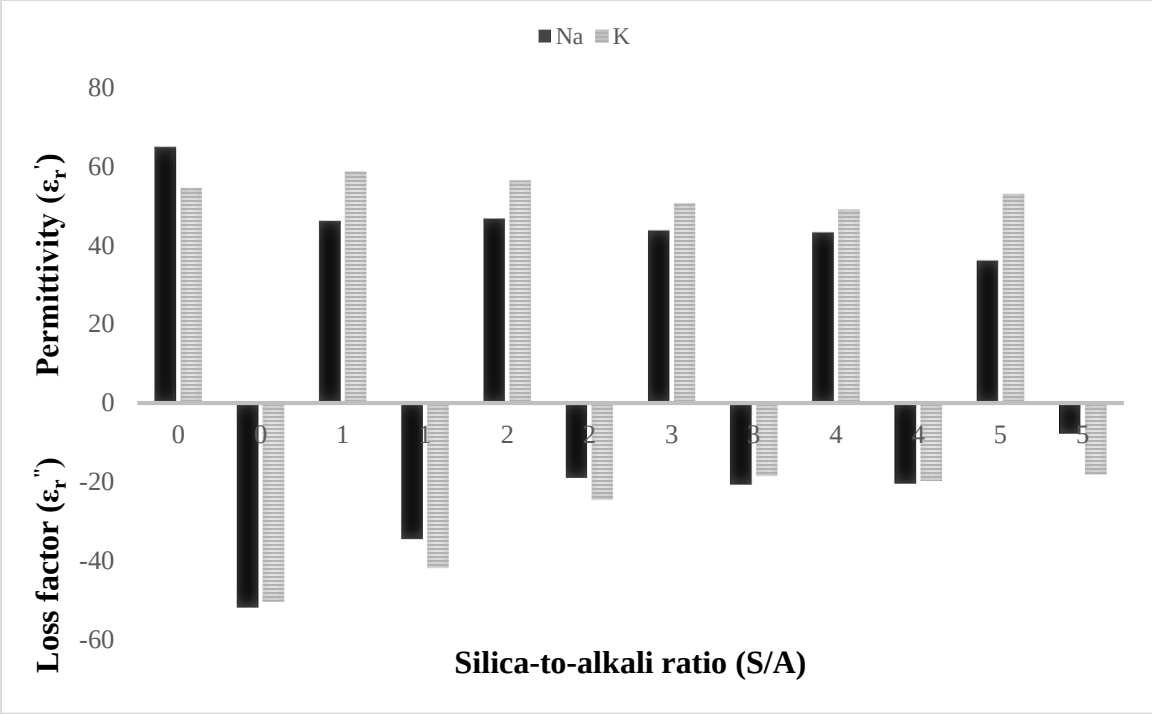

(a)

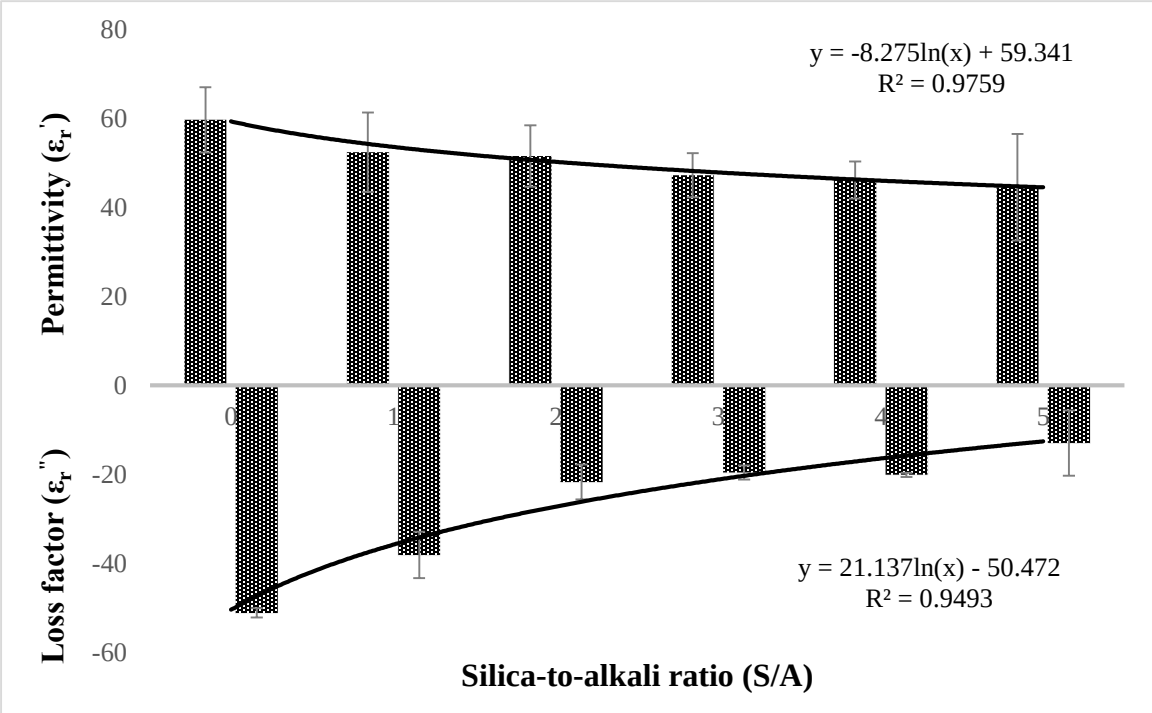

(b)

Figure 2. Dielectric constants of water glass at X-band, a) Na-, K-based samples, b) average.

5. CONCLUSIONS

Dielectric properties of twelve laboratory-produced water glasses, both Na- and K-based, were measured using open-ended waveguide technique at X-band (8.2-12.4 GHz). The measurement results showed loss factor to decrease exponentially as a function of increasing S/A ratio. This suggests an increase in the contribution of bound water and a decrease in the fluid ionic concentration in the gel within the samples. The results also suggest that water is more tightly bound to the Na-based gel samples resulting in lower dielectric properties than those measured for the K-based samples. This study provides critical inputs to a future dielectric mixing model of ASR-affected cement-based materials and to geopolymer materials.

REFERENCES

[1] R. Zoughi, *Microwave Non-Destructive Testing and Evaluation Principles*. Springer Science & Business Media, 2000.

[2] L. Chen, C. Ong, C. Neo, V. Varadan, and V. Varadan, *Microwave electronics: measurement and materials characterization*. 2004.

[3] D. Pozar, "Microwave engineering," 2009.

[4] S. Ramo, J. Whinnery, and T. Van Duzer, "Fields and waves in communication electronics," 2008.

[5] D. Hughes and R. Zoughi, "A Novel Method for Determination of Dielectric Properties of Materials Using a Combined Embedded Modulated Scattering and Near-Field Microwave Techniques—Part I: Forward Model," *IEEE Trans. Instrum. Meas.*, vol. 54, no. 6, pp. 2389–2397, Dec. 2005.

[6] D. Hughes and R. Zoughi, "A Novel Method for Determination of Dielectric Properties of Materials Using a Combined Embedded Modulated Scattering and Near-Field Microwave Techniques—Part II: Dielectric Property Recalculation," *IEEE Trans. Instrum. Meas.*, vol. 54, no. 6, pp. 2398–2401, Dec. 2005.

[7] S. Trabelsi, A. W. Kraszewski, and S. O. Nelson, "Simultaneous determination of density and water content of particulate materials by microwave sensors," *Electron. Lett.*, vol. 33, no. 10, pp. 874–876, 1997.

[8] S. N. Kharkovsky, M. F. Akay, U. C. Hasar, and C. D. Atis, "Measurement and monitoring of microwave reflection and transmission properties of cement-based specimens," *IEEE Trans. Instrum. Meas.*, vol. 51, no. 6, pp. 1210–1218, Dec. 2002.

[9] R. Zoughi, A. D. Benally, and K. J. Bois, "Near-field microwave non-invasive determination of NaCl in mortar," *IEE Proc. - Sci. Meas. Technol.*, vol. 148, no. 4, pp. 178–182, Jul. 2001.

[10] S. I. Ganchev, J. Bhattacharyya, S. Bakhtiari, N. Qaddoumi, D. Brandenburg, and R. Zoughi, "Microwave diagnosis of rubber compounds," *IEEE Trans. Microw. Theory Tech.*, vol. 42, no. 1, pp. 18–24, 1994.

[11] S. Gray, S. Ganchev, N. Qaddoumi, G. Beauregard, D. Radford, and R. Zoughi, "Porosity level estimation in polymer composites using microwaves," *Mater. Eval.*, vol. 53, no. 3, pp. 404–408, 1995.

[12] C. Vineis, P. K. Davies, T. Negas, and S. Bell, "Microwave dielectric properties of hexagonal perovskites," *Mater. Res. Bull.*, vol. 31, no. 5, pp. 431–437, May 1996.

[13] A. R. Djordjevic, V. D. Likar-Smiljanic, and T. K. Sarkar, "Wideband frequency-domain characterization of FR-4 and time-domain causality," *IEEE Trans. Electromagn. Compat.*, vol. 43, no. 4, pp. 662–667, Nov. 2001.

[14] Z. Fan, G. Luo, Z. Zhang, L. Zhou, and F. Wei, "Electromagnetic and microwave absorbing properties of multi-walled carbon nanotubes/polymer composites," *Mater. Sci. Eng. B*, vol. 132, no. 1–2, pp. 85–89, Jul. 2006.

[15] M. P. McNeal, S. J. Jang, and R. E. Newnham, "The effect of grain and particle size on the microwave properties of barium titanate (BaTiO3)," *J. Appl. Phys.*, vol. 83, no. 6, pp. 3288–3297, 1998.

[16] K. J. Bois, A. D. Benally, and R. Zoughi, "Microwave near-field reflection property analysis of concrete for material content determination," *IEEE Trans. Instrum. Meas.*, vol. 49, no. 1, pp. 49–55, 2000.

[17] K. J. Bois, A. Benally, P. S. Nowak, and R. Zoughi, "Microwave nondestructive determination of sand-to-cement ratio in mortar," *Res. Nondestruct. Eval.*, vol. 9, no. 4, pp. 227–238, 1997.

[18] K. Mubarak, K. J. Bois, and R. Zoughi, "A simple, robust, and on-site microwave technique for determining water-to-cement ratio (w/c) of fresh Portland cement-based materials," *IEEE Trans. Instrum. Meas.*, vol. 50, no. 5, pp. 1255–1263, 2001.

[19] K. J. Bois, A. D. Benally, P. S. Nowak, and R. Zoughi, "Cure-state monitoring and water-to-cement ratio determination of fresh Portland cement-based materials using near-field microwave techniques," *IEEE Trans. Instrum. Meas.*, vol. 47, no. 3, pp. 628–637, Jun. 1998.

[20] A. Hashemi, K. M. Donnell, R. Zoughi, and K. E. Kurtis, "Microwave nondestructive evaluation of hydration kinetics in mortars with and without sodium hydroxide inclusion," in *14th International Symposium on Nondestructive Characterization of Materials*, 2015.

[21] A. Hashemi, K. M. Donnell, R. Zoughi, O. C. Fawole, and M. Tabib-Azar, "THz materials characterization of mortar samples with and without alkali-silica reaction (ASR) gel," in *42th Annual Review of Progress in Quantitative Nondestructive Evaluation*, 2015.

[22] A. Hashemi, I. Mehdipour, K. M. Donnell, R. Zoughi, and K. H. Khayat, "Effect of alkali addition on microwave dielectric properties of mortars," *NDT E Int. - under Rev.*, 2015.

[23] A. Hashemi, M. Rashidi, K. M. Donnell, K. E. Kurtis, and R. Zoughi, "Curing conditions effects on the long-term dielectric properties of mortar samples containing ASR gel," in *IEEE Int. Instrum. Meas. Technol. Conf. Proc. (Submitted)*, 2016.

[24] A. Hashemi, M. Horst, K. E. Kurtis, K. M. Donnell, and R. Zoughi, "Comparison of Alkali–Silica Reaction Gel Behavior in Mortar at Microwave Frequencies," *IEEE Trans. Instrum. Meas.*, vol. 64, no. 7, pp. 1907–1915, Jul. 2015.

[25] A. Hashemi, S. Hatfield, K. M. Donnell, R. Zoughi, and K. E. Kurtis, "Microwave NDE method for health-monitoring of concrete structures containing alkali-silica reaction (ASR) gel," *AIP Conf. Proc.*, vol. 1581 33, pp. 787–792, 2014.

[26] K. M. Donnell, S. Hatfield, R. Zoughi, and K. E. Kurtis, "Wideband microwave characterization of alkali-silica reaction (ASR) gel in cement-based materials," *Mater. Lett.*, vol. 90, pp. 159–161, 2013.

[27] A. Hashemi, M. C. L. Knapp, K. M. Donnell, K. E. Kurtis, and R. Zoughi, "Microwave detection of carbonation in mortar using dielectric property characterization," *2014 IEEE Int. Instrum. Meas. Technol. Conf. Proc.*, pp. 216–220, May 2014.

[28] K. M. Donnell, R. Zoughi, and K. E. Kurtis, "Demonstration of microwave method for detection of alkali-silica reaction (ASR) gel in cement-based materials," *Cem. Concr. Res.*, vol. 44, pp. 1–7, 2013.

[29] A. Hashemi, K. M. Donnell, and R. Zoughi, "Effect of Humidity on Dielectric Properties of Mortars with Alkali-Silica Reaction (ASR) Gel," no. 3, pp. 6–10, 2015.

[30] A. Hashemi, M. Rashidi, K. E. Kurtis, K. M. Donnell, and R. Zoughi, "Microwave Dielectric Properties Measurements of Sodium and Potassium Water Glasses," *Mater. Lett.*, Nov. 2015.

[31] T. E. Stanton, "Expansion of concrete through reaction between cement and aggregate," *Proc. Am. Soc. Civ. Eng.*, vol. 66, no. 10, pp. 1781–1811, 1940.

[32] "ACI Concrete Terminology, ACI Standard CT-13, Jan." 2013.

[33] L. S. Dent Glasser and N. Kataoka, "The chemistry of 'alkali-aggregate' reaction," *Cem. Concr. Res.*, vol. 11, no. 1, pp. 1–9, Jan. 1981.

[34] F. Rajabipour, E. Giannini, C. Dunant, J. H. Ideker, and M. D. a. Thomas, "Alkali–silica reaction: Current understanding of the reaction mechanisms and the knowledge gaps," *Cem. Concr. Res.*, vol. 76, pp. 130–146, 2015.

[35] A. Pedneault, "Development of testing and analytical procedures for the evaluation of the residual potential of reaction, expansion and deterioration of concrete affected by ASR," Memoir, Laval University, Quebec City, Canada, 1996.

[36] A. Kraszewski, *Microwave aquametry: electromagnetic wave interaction with water-containing materials*. IEEE, 1996.

[37] A. Sihvola, *Electromagnetic mixing formulas and applications*. London, UK: IEE publishing, 1999.

[38] C. Dirksen and S. Dasberg, "Improved calibration of time domain reflectometry soil water content measurements," *Soil Science Society of America Journal*, vol. 57, no. 3. pp. 660–667, 1993.

[39] M. Hallikainen, F. Ulaby, M. Dobson, M. El-rayes, and L. Wu, "Microwave Dielectric Behavior of Wet Soil-Part 1: Empirical Models and Experimental Observations," *IEEE Trans. Geosci. Remote Sens.*, vol. GE-23, no. 1, pp. 25–34, Jan. 1985.

[40] V. Mironov and M. Dobson, "Generalized refractive mixing dielectric model for moist soils," *Geosci. Remote Sensing, IEEE Trans.*, vol. 42, no. 4, pp. 773–785, 2004.

[41] D. A. Robinson, S. B. Jones, J. M. Wraith, D. Or, and S. P. Friedman, "A review of advances in dielectric and electrical conductivity measurement in soils using time domain reflectometry," *Vadose Zo. J.*, vol. 2, no. 4, pp. 444–475, 2003.

[42] M. Vallone, A. Cataldo, and L. Tarricone, "Water content estimation in granular materials by time domain reflectometry: A key-note on agro-food applications," in *Conference Record - IEEE Instrumentation and Measurement Technology Conference*, 2007.

[43] M. T. Hallikainen, F. T. Ulaby, and M. Abdelrazik, "Dielectric properties of snow in the 3 to 37 GHz range," *IEEE Trans. Antennas Propag.*, vol. AP-34, no. 11, pp. 1329–1340, 1986.

[44] A. Paz, E. Thorin, and C. Topp, "Dielectric mixing models for water content determination in woody biomass," *Wood Sci. Technol.*, vol. 45, no. 2, pp. 249–259, Mar. 2010.

[45] A. H. Sihvola and J. A. Kong, "Effective Permittivity of Dielectric Mixtures.," *IEEE Trans. Geosci. Remote Sens.*, vol. 26, no. 4, pp. 420–429, 1988.

[46] W. R. Tinga, W. a G. Voss, and D. F. Blossey, "Generalized approach to multiphase dielectric mixture theory," *J. Appl. Phys.*, vol. 44, no. 9, pp. 3897–3902, 1973.

[47] C. A. R. Pearce, "The permittivity of two phase mixtures," *Br. J. Appl. Phys.*, vol. 6, no. 10, pp. 358–361, Oct. 1955.

[48] L. Klein and C. Swift, "An improved model for the dielectric constant of sea water at microwave frequencies," *Ocean. Eng. IEEE J.*, vol. 2, no. 1, pp. 104–111, 1977.

[49] A. Stogryn, "Equations for calculating the dielectric constant of saline water," *IEEE Transactions on Microwave Theory and Techniques*, vol. MTT-19, no. 8. pp. 733–736, 1971.

[50] J. Lane and J. Saxton, "Dielectric dispersion in pure polar liquids at very high radio-frequencies. I. Measurements on water, methyl and ethyl alcohols," *Proc. R. Soc. London A Math. Phys. Eng. Sci.*, vol. 213, no. 1114, 1952.

[51] F. T. Ulaby, R. K. Moore, and A. K. Fung, *Microwave remote sensing: Active and passive, vol. iii, volume scattering and emission theory, advanced systems and applications*. 1986.

[52] K. a. Snyder, X. Feng, B. D. Keen, and T. O. Mason, "Estimating the electrical conductivity of cement paste pore solutions from OH-, K+ and Na+ concentrations," *Cem. Concr. Res.*, vol. 33, no. 6, pp. 793–798, 2003.

[53] B. Christensen and T. Coverdale, "Impedance Spectroscopy of Hydrating Cement-Based Materials: Measurement, Interpretation, and Application," *J. ...*, 1994.

[54] K. J. Bois, L. F. Handjojo, A. D. Benally, K. Mubarak, and R. Zoughi, "Dielectric plug-loaded two-port transmission line measurement technique for dielectric property characterization of granular and liquid materials," *IEEE Trans. Instrum. Meas.*, vol. 48, no. 6, pp. 1141–1148, 1999.

[55] K. J. Leśnicki, J.-Y. Kim, K. E. Kurtis, and L. J. Jacobs, "Assessment of alkali–silica reaction damage through quantification of concrete nonlinearity," *Mater. Struct.*, vol. 46, no. 3, pp. 497–509, Dec. 2012.

[56] M. Kawamura and H. Fuwa, "Effects of lithium salts on ASR gel composition and expansion of mortars," *Cem. Concr. Res.*, vol. 33, no. 6, pp. 913–919, Jun. 2003.

[57] S. Multon, A. Sellier, and M. Cyr, "Chemo–mechanical modeling for prediction of alkali silica reaction (ASR) expansion," *Cem. Concr. Res.*, vol. 39, no. 6, pp. 490–500, Jun. 2009.

[58] F. Rajabipour, E. Giannini, C. Dunant, J. H. Ideker, and M. D. A. Thomas, "Alkali–silica reaction: Current understanding of the reaction mechanisms and the knowledge gaps," *Cem. Concr. Res.*, vol. 76, pp. 130–146, Oct. 2015.

[59] M. Kawamura and K. Iwahori, "ASR gel composition and expansive pressure in mortars under restraint," *Cem. Concr. Compos.*, vol. 26, no. 1, pp. 47–56, Jan. 2004.

[60] N. P. Mayercsik, R. Felice, M. T. Ley, and K. E. Kurtis, "A probabilistic technique for entrained air void analysis in hardened concrete," *Cem. Concr. Res.*, vol. 59, pp. 16–23, May 2014.

VI. EMPIRICAL MULTI-PHASE DIELECTRIC MIXING MODEL FOR CEMENT-BASED MATERIALS CONTAINING ALKALI-SILICA REACTION (ASR) GEL

ABSTRACT

Alkali-silica reaction (ASR) is recognized as one of the most common causes of concrete deterioration. The product of this reaction is known as ASR gel. Water, in the presence of reactive aggregates, used to make concrete, plays a major role in the formation, sustainment and promotion of this deleterious gel. Since microwave signals are sensitive to the presence of water in dielectric materials, microwave materials characterization techniques have the potential to detect ASR gel formation. Dielectric mixing models are physics-based models that relate the macroscopic (i.e., effective) dielectric constant of a material to the dielectric constant of its constituents and their respective volumetric contents. In this investigation, an empirical multiphase dielectric mixing model is developed in conjunction with measured dielectric constants of two sets of mortar samples with ASR-reactive and non-reactive aggregates at R-band (1.7 – 2.6 GHz). The model is capable of closely predicting the effective (temporal) dielectric constant of the samples. The modeling results are validated by a comparison with the measured temporal dielectric constant of the samples, showing good agreement. Through this investigation quantitative information on the influence of constituents of ASR-reactive mortar samples (including ASR gel) are obtained, and the pertinent results indicate significant potential for microwave materials characterization techniques for ASR detection and evaluation.

Index Terms: Microwave nondestructive testing, dielectric constant, alkali-silica reaction (ASR) gel, dielectric mixing model, cement-based materials, materials characterization.

1. INTRODUCTION

Alkali-silica reaction (ASR) is a deleterious chemical reaction which is known as one of the most common causes of deterioration in cement-based structures. It involves the reaction between alkali ions (sodium and potassium) in portland cement and certain siliceous rocks or minerals present in some aggregates [1]. This reaction produces a gel product, referred to as the ASR gel. Once the gel expands it causes progressive cracking of concrete in service, and eventually may lead to structural failure. There are three fundamental requirements for ASR formation, namely: reactive silica, sufficient alkali, and sufficient moisture [2]. Reactive silica is found in reactive minerals such as opaline, chert, strained quartz, and acidic volcanic glass that may be used as aggregates. Alkalis are present in portland cement commonly used to make concrete. However, other cementing materials (e.g., fly ash, slag and silica fume), chemical admixtures, wash water and external sources (e.g., sea water, deicing chemicals, etc.) may also provide additional amounts of alkalis for the reaction to take place. Moisture, the third essential requirement for ASR formation, is present in pore solution, and also it penetrates a structure through microcracks. Consequently, there is significant interest in the construction industry to predict, prevent, and mitigate ASR gel formation. To this end, various nondestructive testing (NDT) techniques have been developed for evaluating ASR. For instance, visual inspection and expansion measurements [3], both of which are inaccurate methods. Seismic-wave and ground penetrating radar (GPR) inspections are other techniques that have shown limited viability [4]–[6]. Linear and nonlinear acoustic-based methods [7]–[10] have also been widely used to detect ASR-related damage in concrete. In all, ASR gel is detected through the damage caused to the structure, as opposed to detecting the presence

of ASR gel directly. For instance, in acoustic-based approaches, ASR gel may be detected through microstructural changes such as microcrack formation.

Given the sensitivity of microwave signals to moisture content in dielectric materials (i.e., mortar, concrete, etc.), microwave materials characterization techniques have shown significant potential for ASR detection and evaluation. Microwave material characterization techniques have been successfully used to investigate various properties of cement-based materials including evaluation of water-to-cement (*w/c*), coarse aggregate-to-cement ratio (*ca/c*) and sand-to-cement (*s/c*) ratio [11]–[13], cure state monitoring [14], delamination between hardened cement paste and fiber-reinforced polymer (FRP) composites [15], carbonation [16], and chloride permeation [17]. Most recently, several different aspects of ASR gel formation have also been investigated with microwave materials characterization techniques [18]–[20].

In this paper, in support of and to evaluate the capability of microwave materials characterization for ASR gel detection, an empirical dielectric mixing model is developed based on the temporally measured dielectric constant of mortar samples with and without ASR gel at R-band (1.7 – 2.6 GHz). As such, the dielectric constant of the individual inclusions (pure water, ionic water, air, liquid ASR gel, and dry ASR gel) of the samples was acquired, as will be explained later. Through the developed dielectric mixing model and available ground truth data, the temporal volumetric content of the constituents was iteratively obtained for the two sample types. Subsequently, the results of the model, giving the effective dielectric constant of the two types of samples, are validated by comparing them with the temporal measured dielectric constants. The results of this investigation bring a thorough understanding to the complex process of ASR gel formation, and provide

quantitative information on the volume content of the samples' constituents including the ASR gel. A sensitivity analysis is also performed to examine the sensitivity of the mixing model to volumetric variations in the individual inclusions.

2. BACKGROUND

The interaction between electromagnetic energy and dielectric materials is macroscopically described by a parameter knows as the complex dielectric constant. When referenced to free-space, it is referred to as the relative dielectric constant (ε_r) and is denoted as $\varepsilon_r = \varepsilon'_r - j\varepsilon''_r$. The real part ($\varepsilon'_r$) is an indication of microwave energy storage (relative permittivity), and the imaginary part (ε''_r) indicates energy dissipation (relative loss factor). This complex parameter is intrinsic to a given material, and is independent of the measurement method. As it relates to the goals of this work, microwave materials characterization methods can be utilized to characterize the ASR gel formation, through complex dielectric constant measurements and modeling. ASR gel has a tendency to imbibe free water from its surroundings, where it partially transforms the available free water into bound water during the gel formation process. Since free water has significantly different dielectric constant than that of bound water [21], the gradual transformation of free to bound water (resulting from ASR gel formation) manifests itself as a change in the measured temporal dielectric constant of cement-based materials containing ASR gel. Therefore, microwave materials characterization techniques may be utilized to develop a new tool for ASR detection.

Dielectric mixing models are physics-based models that relate the macroscopic dielectric constant of a mixture to the dielectric constant, volumetric content, and geometry of its constituents [22]. In general, dielectric mixing models can be divided into multiple categories according to their development, applications, and inclusion geometry [23]. In development of such models, a mixture is considered to be a homogeneous medium and is comprised of a background or host medium with dielectric constant of ε_h, within which

inclusions (or phases) are randomly distributed. The medium can then be represented with an effective dielectric constant [22]. Dielectric mixing models can be developed empirically or semi-empirically, and for a single phase (inclusion) or multiphase material. Hence, there are a large number of dielectric mixing models that have been developed over the years, including: Maxwell-Garnett, power law, Polder van Santen, Wiener, and Pearce that are examples of some of the more well-known and classical dielectric mixing models [22]-[23]. In the end all such models, and in particular those developed based on using empirical factors obtained from actual measured data must be experimentally validated [25]. Such models have been used for radar remote sensing, material science and microwave materials characterization. For instance, multiple dielectric mixing models have been applied to soil [25]-[28], frozen soil [29]-[30], and granular materials [32]. Several classical mixing models have also been utilized to characterize snow [33], sea ice [22], and woody biomass [34]. In particular in [17], an electromagnetic model is developed to evaluate temporal water content distribution in cyclically soaked mortars. In this investigation, an empirical dielectric mixing model is developed for mortars with and without ASR gel whose dielectric constants temporally change during the ASR gel formation process.

3. MIX DESIGN AND CURING CONDITIONS

Two sets of mortar samples (3 similar samples in each set for averaging purpose) with the same mix design and different crushed aggregates (i.e., ASR-reactive and non-reactive) were cast. Samples made with ASR-reactive aggregates are susceptible to ASR formation, while the samples cast with non-reactive aggregate are not expected to form ASR gel. To accelerate ASR formation, sodium hydroxide (NaOH) was added to the mixing water of both sets of samples following ASTM 1293 [35]. Table I summarizes the mix design of the samples.

Table 1. Mix design

Mix Design	**Samples Type**	
	Reactive	***Nonreactive***
Cement Powder	Portland Type I/II	Portland Type I/II
Aggregate	Rhyolite	Limestone
w/c	0.47	0.47
ca/c	2.25	2.25
NaOH	0.9%	0.9%

Samples were cast in Plexiglas molds with a cross-section of 10.92 × 5.46 cm, corresponding to the standard R-band rectangular waveguide cross-section dimensions. The length of the samples was chosen to be ~2-3 cm (dielectric constant measurement is independent of sample length). All samples were stored in ambient conditions (22°C ± 3°C, 35% ± 5% relative humidity (RH)) for 24 hours after casting. Then, to provide sufficient moisture and promote ASR formation, they were placed in an environmental chamber with

a temperature of 38°C ± 2°C and 85% ± 5% RH, similar to the conditions in ASTM 1293 [35]. Every 2-3 days, the samples were removed from the chamber, and their reflection (S11) and transmission (S21) properties measured using an Agilent 8510C Vector Network Analyzer (VNA). Then, the temporal dielectric constants of the samples were calculated using their measured reflection and transmission properties, following the procedure outlined in [36]. After 28 days, the samples were removed from the chamber and placed in ambient conditions, with the measurements continuing for almost another two months. The temporal dielectric constant measurements of the samples and the pertinent details are reported in [19], and are not repeated here for brevity.

4. DIELECTRIC MIXING MODEL DEVELOPMENT

In mixing model development for a multiphase mixture (such as the mortar samples), a host (background) material is defined, and other constituents are considered as inclusions within the host. As such, different mixing models are distinguished from each other by the number of inclusions, shape of inclusions, and other factors that might be relevant to specific problems and applications [22]. To form the model, the number of inclusions as well as their dielectric constants are needed. In the proposed multiphase dielectric mixing model, mortar is considered as the host material, while absorbed (pure) water, ionic water, and air are the three inclusions for non-reactive samples. Liquid and dry ASR gel are two additional inclusions that are considered for the reactive samples. Figure 1 shows a simplified illustration of a reactive sample with the relevant inclusions.

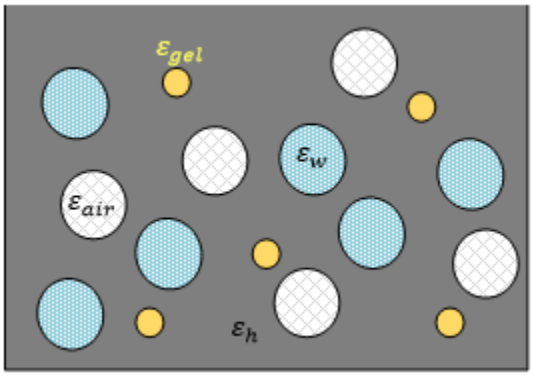

Figure 1. Simplified illustration of ASR-reactive sample with dielectric constant of host (ε_h), air (ε_{air}), water (ε_{water}), and ASR gel (ε_{gel}).

In order to find the base model for this investigation, several well-known dielectric mixing models including the Maxwell-Garnett, power law, and Pearce models were considered. Equation (1) shows the Maxwell-Garnett model that was initially used:

$$\varepsilon_{eff} = \varepsilon_h + 3\varepsilon_h \frac{\sum_{i=1}^{l} v_i \frac{\varepsilon_i - \varepsilon_h}{\varepsilon_i + 2\varepsilon_h}}{1 - \sum_{i=1}^{l} v_i \frac{\varepsilon_i - \varepsilon_h}{\varepsilon_i + 2\varepsilon_h}} \tag{1}$$

As can be seen in (1), the effective dielectric constant (ε_{eff}) is a function of ε_h (dielectric constant of the host), ε_i (dielectric constants of inclusions), and v_i (volumetric content of the inclusions). However, the Maxwell-Garnett (as well as the power law) model proved to be incapable of properly modeling the temporal effective dielectric constants of the samples, showing a weak correlation between modeling and measurement results. The reason for this may be attributed to the high contrast in the dielectric constants of the inclusions, as will be discussed later.

Alternatively, the Pearce model was applied, and proved to be the model that most closely predicted the effective temporal dielectric constant of the samples. In all of those modeling efforts, spherical and randomly oriented inclusions were assumed since all inclusion are much smaller than the operating wavelength at R-band. The basic Pearce model given in [25] is:

$$\frac{\varepsilon_{eff} - \varepsilon_h}{\varepsilon_i - \varepsilon_h} = \frac{(1-k)v_i}{1-kv_i} \tag{2}$$

As shown, the model includes an empirical factor, *k*, which plays a major role in its overall predictive performance. Unlike the empirical factor in the Wiener model [37], where *k* is a function of the inclusions' shapes, the *k* factor in the Pearce model depends on other empirical properties not necessarily related to the shape of the inclusions [38]. This empirical factor, *k*, is discussed in detail in the next section.

Due to the different temporal exposure conditions (environmental chamber vs. ambient), the material state of some of the inclusions changes as a function of time. For example, liquid ASR gel is present during the chamber conditions, while it becomes solid (dry) after being stored in the ambient condition for a long period of time. Hence, its dielectric constant must be evaluated (for both periods) and correspondingly incorporated into the mixing model. Moreover, the pore solution (specifically the water held in the pores) of the samples may have different chemical (ionic) properties compared to the water absorbed by the samples from the humid environment while in the environmental chamber. This difference in chemical properties of water also needs to be taken into account. Since there is limited information in the literature about the dielectric constant of liquid and dry ASR gel at microwave frequencies, those parameters were directly measured for incorporation into the model, while the dielectric constant of pure and ionic water (in the pore solution) were obtained from available and established models reported in the literature, as will be discussed later.

4.1. ABSORBED (PURE) WATER

A model for the complex dielectric constant of water was introduced by Debye [39]. This well-established model is used here to calculate the dielectric constant of water

absorbed from the chamber environment to the samples at a temperature, T, of 38 ºC, and frequency, f, of 2 GHz. According to the Debye model, the frequency and temperature dependence of the dielectric constant of pure water (ε_w) is given in (3).

$$\varepsilon_w = \varepsilon_{w\infty} + \frac{\varepsilon_{w0} - \varepsilon_{w\infty}}{1 + j2\pi f \tau_w} \tag{3}$$

where,

ε_{w0} = static dielectric constant of water, dimensionless,

ε_{w_∞} = high frequency limit of ε_w, dimensionless,

τ_w = relaxation time of water, (S)

f = frequency, (Hz).

From (3), the relative permittivity and loss factor of pure water are given as (4) and (5), respectively.

$$\varepsilon'_w = \varepsilon_{w\infty} + \frac{\varepsilon_{w0} - \varepsilon_{w\infty}}{1 + (2\pi f \tau_w)^2} \tag{4}$$

$$\varepsilon''_w = \frac{2\pi f \tau_w (\varepsilon_{w0} - \varepsilon_{w\infty})}{1 + (2\pi f \tau_w)^2} \tag{5}$$

It can be clearly seen from (4) and (5) that both permittivity and loss factor change as a function of frequency. However, the temperature (T) dependence is related to the static dielectric constant (ε_{w0}) and relaxation time (τ_w) of water according to the following expressions obtained by Kelein-Swift [48] and Stogryn [49], respectively.

$$\varepsilon_{w0}(T) = 88.045 - 0.4147T + 6.295\times10^{-4}T^2 + 1.075\times10^{-5}T^3 \quad (6)$$

$$2\pi\tau_w(T) = 1.1109\times10^{-10} - 3.824\times10^{-12}T + 6.938\times10^{-14}T^2 - 5.096\times10^{-16}T^3 \quad (7)$$

where T is in ºC. Furthermore, the magnitude of ε_{w_∞} was determined to be 4.9 by Lane and Saxton [50]. According to this model, the dielectric constant of the absorbed water can be determined for both (chamber and ambient) environments, and was determined to be ε_w = 73.4 - j5.2 for chamber conditions, and ε_w = 79.1 - j8.6 for ambient conditions.

4.2. IONIC WATER

The addition of NaOH to the mixing water of the samples changes its dielectric constant. As such, the dielectric constant of ionic water is also needed. To this end, the model for permittivity and loss factor of brine was used to mimic the ionic solution. Equations (8) and (9) express the permittivity (ε'_{iw}) and loss factor (ε''_{iw}) of brine, respectively [41].

$$\varepsilon'_{iw} = \varepsilon_{iw\infty} + \frac{\varepsilon_{iw0} - \varepsilon_{iw\infty}}{1+(2\pi f\tau_{iw})^2} \quad (8)$$

$$\varepsilon''_{iw} = \frac{2\pi f\tau_{iw}(\varepsilon_{iw0} - \varepsilon_{iw\infty})}{1+(2\pi f\tau_{iw})^2} + \frac{\sigma_{iw}}{2\pi\varepsilon_0 f} \quad (9)$$

where,

ε_0 = permittivity of free-space, 8.854 × 10 $^{-12}$, *F/m*,

σ_{iw} = ionic conductivity of ionic solution, *S/m.*

By comparing the two sets of equations for dielectric constants of pure and ionic water ((4), (5) versus (8), (9), it can be seen that although the permittivity of the two are formulated the same, they differ in loss factor by an additional term related to the ionic conductivity of the ionic solution (i.e., NaOH solution). As mentioned in [48], ionic conductivity is a function of solution temperature. Therefore, ionic conductivity must be determined for both chamber and ambient conditions. Based on the mix design used, the NaOH concentration was calculated to be 18.62 g/L. Then, according to the empirical expressions outlined in [48], [51], the ionic conductivity of the NaOH solution is calculated to be 15.52 (*S/m*) and 20.8 (*S/m*) for ambient and chamber conditions, respectively. These values are consistent with ionic conductivities reported in [52], [53]. Figure 2 shows the dielectric constant of NaOH solution for different frequencies and temperatures where at 2 GHz, those values are ε_{iw} = 44.2 - j189.8 and ε_{iw} = 47 - j143.6 for chamber and ambient conditions, respectively.

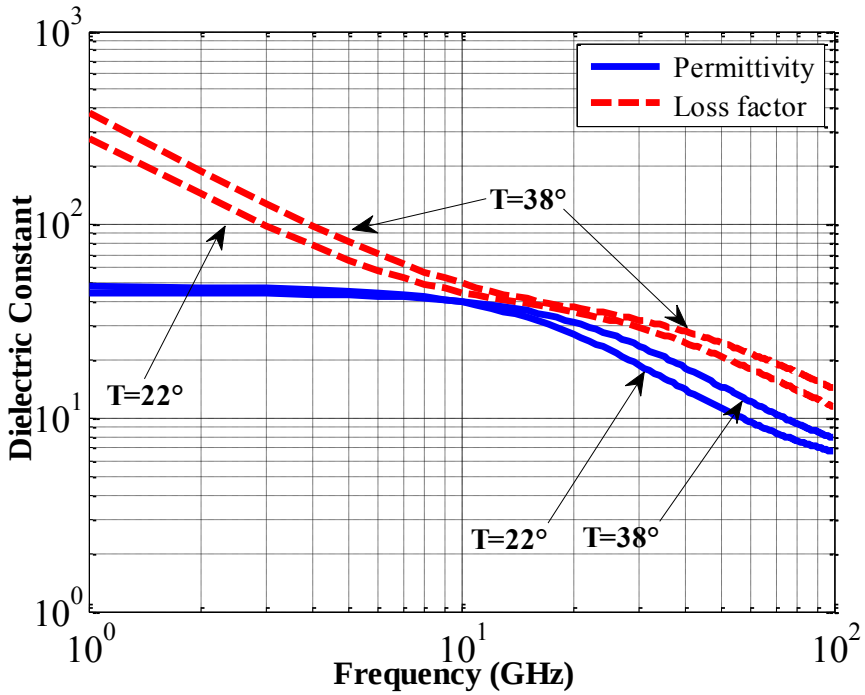

Figure 2. Dielectric constant of the NaOH solution.

4.3. AIR CONTENT

Another inclusion that needs to be incorporated into the mixing model is the air content (i.e., porosity) of the samples. Obviously, the (relative) dielectric constant of air is equal to unity, with no loss associated with it. Therefore, the contribution of air into the mixing model is directly determined by its volumetric content, as explained later in the next section.

4.4. ASR GEL (LIQUID)

Considering the temporal evolution of ASR gel formation in the samples, starting as a liquid and absorbing free water to finally becoming a solid product (in the absence of

moisture), its corresponding dielectric constants must be characterized accordingly. To obtain as accurate as possible estimation of the dielectric constant of the ASR gel during the chamber condition, twelve synthetic ASR gels were produced. The gels were prepared in the laboratory by the addition of amorphous fumed silicon (IV) oxide (300–350 m2/g surface area, Alfa Aesar) with concentrated solutions of sodium hydroxide (1.85M NaOH) or potassium hydroxide (1.82M KOH), prepared with deionized water and ACS-grade reagents. Six sodium-based (Na-based) and six potassium-based (K-based) gels were prepared at silica-to-alkali ratios (SiO2/Na2O or SiO2/K2O) (by mass) of zero, one, two, three, four, and five. The gels were prepared in sealed polypropylene containers, which were agitated for ten minutes after the addition of the silica, following the approach outlined by Zhang et al. [45]. The dielectric constant of all twelve ASR gel samples were measured using the open-ended waveguide technique, at X-band (8.2-12.4 GHz) suing the method outlined in [46]. Measurements were conducted at X-band due to the limited amount of synthesized gels (an X-band waveguide probe has smaller dimensions than an R-band probe). However, it can be shown that the influence of frequency on the dielectric constant of liquid ASR gel is not significant due to tiny volume fraction of the gel, as will be shown in the next section. Figure 3 shows the setup used to measure the dielectric constant of the liquid ASR gel. The detailed measurement methodology and results are reported in [47].

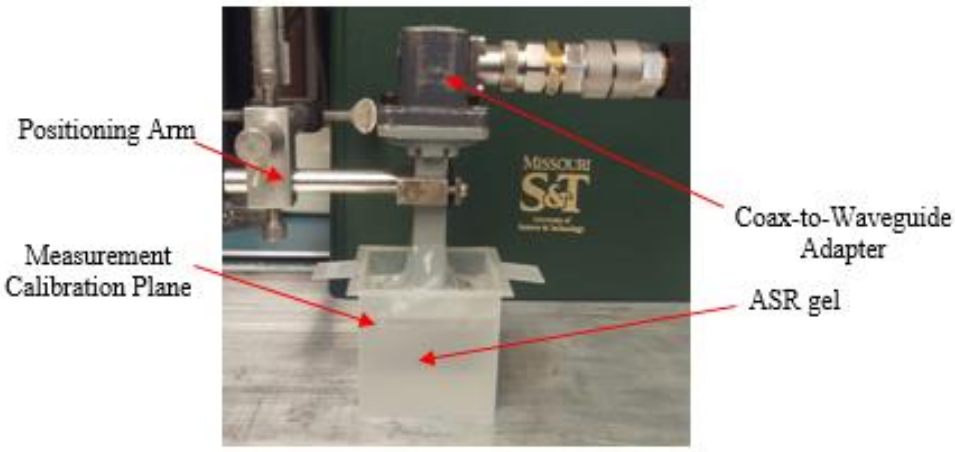

Figure 3. ASR gel (liquid) measurements setup.

Since the pore solution of cement-based materials often contains both Na^+ and K^+ ions, the average value of the 12 dielectric constant measurements is incorporated into the mixing model to mimic a more realistic case. The average dielectric constant of the liquid gel was determined to be $\varepsilon_{gel} = 50.27 - j27.29$.

4.5. ASR GEL (DRY)

To measure the dielectric constant of dry ASR gel, solid (powder) ASR was obtained from the field. The powder sample was compacted uniformly inside a rectangular X-band (8.2-12.4 GHz) waveguide sample holder, and was measured using the completely-filled waveguide technique [54], and its dielectric constant was measured to be $\varepsilon_{gel} = 4.45 - j0.1$. As was the case for liquid ASR, the measurements were conducted at X-band due to the limited amount of dry gel. Unlike the liquid ASR gel that is in the family of high permittivity and high loss materials, the dry powder gel is in the family of low permittivity and low loss materials. This is expected since the former contains a significant amount of

free water (which has higher dielectric constant compared to that of bound water), while the latter is expected to only contain bound water.

Table 2 summarizes all of the inclusions and their corresponding dielectric constants.

Table 2. Inclusions dielectric constants @ 2 GHz

Inclusions		**Dielectric Constant**	
		@ Chamber Conditions	***@ Ambient Conditions***
in R* & NR**	Absorbed water	73.4 - j5.2	79.1 - j8.6
in R & NR	Ionic water	44.2 - j189.8	47 - j143.6
in R & NR	Air	1 - j0	1 - j0
only in R	ASR-liquid	50.27 - j27.29	N/A
only in R	ASR-dry	N/A	4.45 - j0.1

*Reactive
**Non-Reactive

5. MIXING MODEL

Having determined the dielectric constant of the inclusions, the Pearce model can be applied for the non-reactive samples with 3 inclusions (ionic water, absorbed water, air), and for the reactive samples with 5 inclusions (ionic water, absorbed water, air, liquid ASR, dry ASR) as shown in (10) and (11), respectively:

$$\varepsilon_{eff\_Non-reactive} = \sum_{i=1}^{3} \frac{(\varepsilon_i - \varepsilon_h)(1-k_i)v_i}{1-k_i v_i} + \varepsilon_h \tag{10}$$

$$\varepsilon_{eff\_Reactive} = \sum_{i=1}^{5} \frac{(\varepsilon_i - \varepsilon_h)(1-k_i)v_i}{1-k_i v_i} + \varepsilon_h \tag{11}$$

where,

ε_{eff} : effective dielectric constant of the mixture,

ε_h : dielectric constant of host (background material),

$\varepsilon_i(freq,T)$: dielectric constant of inclusions as a function of frequency and temperature,

v_i : volume fraction of inclusions,

i : number of inclusions,

k_i : empirical factor.

Since the samples were exposed to different conditions (chamber versus ambient), different empirical factors (k) were determined. These k values may represent other influential chemical reactions (such as hydration effects) that might happen at the same time with ASR and not accounted for in the mixing model. Equations (12) – (15) show the

empirical factors incorporated into the model for each period for reactive and non-reactive samples.

$$k_{i,Humid\_NR} = \sum_{i=1}^{3} \frac{\varepsilon_i - \varepsilon_h}{1.12\varepsilon_i + \varepsilon_h} \tag{12}$$

$$k_{i,Humid\_R} = \sum_{i=1}^{5} \frac{\varepsilon_i - \varepsilon_h}{1.12\varepsilon_i + \varepsilon_h} \tag{13}$$

$$k_{i,Dry\_NR} = \sum_{i=1}^{3} \frac{\varepsilon_i - \varepsilon_h}{1.12\varepsilon_i + 12\varepsilon_h} \tag{14}$$

$$k_{i,Dry\_R} = \sum_{i=1}^{5} \frac{\varepsilon_i - \varepsilon_h}{12(\varepsilon_i + \varepsilon_h)} \tag{15}$$

The *k* values were determined through an iterative process. The iterative process involved changing both volume fractions of the inclusions and empirical factors iteratively in order to achieve a good match between the measured and modeled effective dielectric constant.

5.1. DETERMINATION OF VOLUME FRACTIONS

During measurement time period, the mass of the samples was also measured in order to determine the amount of water absorbed by the samples from the chamber environment. This information is related (through the density of water) to the volume fraction of the absorbed water. The percentage change in mass (with respect to the mass at the first day of each period) is shown in Fig. 4. As can be seen, the mass of non-reactive

samples increased more as compared to the reactive samples during chamber conditions. This may be attributed to higher air content in the non-reactive samples compared to the reactive samples (assuming pores are partially filled by ASR gel in reactive samples), which facilitates absorption of more water by the former. From the results of Fig. 4, the average (over the three samples of each type) volume fraction of absorbed water can be inferred accordingly, as shown in Fig. 5a (non-reactive) and 5b (reactive).

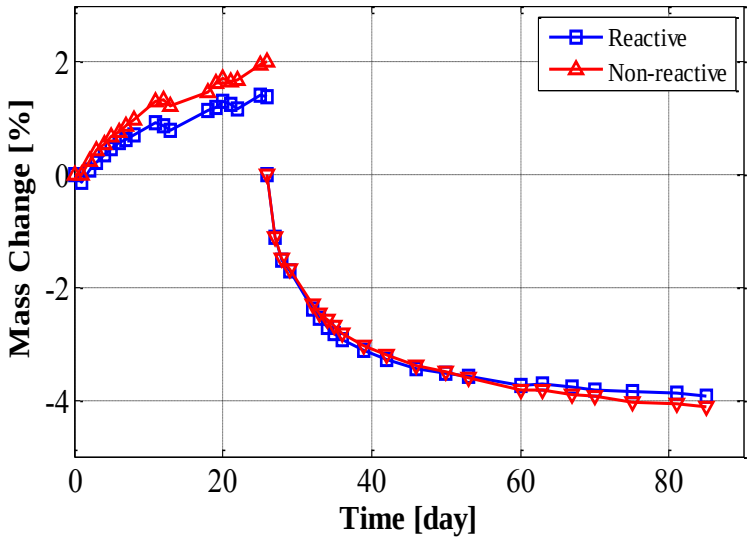

Figure 4. Average mass change of the samples.

With respect to the volume fraction of ASR gel present in the reactive samples, since most classical NDT approaches in ASR evaluation are based on expansion measurements, any quantitative data on the amount of produced ASR is deficient in those approaches [55]–[58]. One of the reasons for this is that the small volumetric quantity of produced ASR gel makes it difficult to obtain quantitative data. However it has been

reported that the amount of ASR gel produced is within ~0.5 % - ~2% as a function of alkali content [59]. As such, this range was used as starting points, to determine ASR gel volume, in the mixing model. Subsequently, those volume fractions were optimized to achieve the best match between the modeled and measured dielectric constant. The resulting optimized gel temporal volume fraction for the reactive samples during the chamber and drying periods is shown in Fig. 5b.

The other important volume fraction is that of ionic water. Since NaOH was used in the mix water of both sets of samples, the initial ionic water volume fraction is identical for both sample types. However, the rate of change (of the ionic water), (determined empirically through the iterative process), is different for the two sample types. This difference (i.e., higher absorption of ionic water in reactive samples) may be related to the higher tendency of reactive sample to use the amount of available ionic water for ASR production. The temporal volume fraction of ionic water is shown in Fig. 5a (non-reactive) and 5b (reactive).

Out of the five inclusions, the only volume fraction that could be measured directly was the air content (porosity) of the samples. Following the approach outline in [60], the air content of the samples was measured and an average value of 5.3% was determined. This value was incorporated into the model initially and subsequently iteratively optimized in accordance with the changes of the other inclusions in order to achieve a good match between the measured and modeled effective dielectric constant.

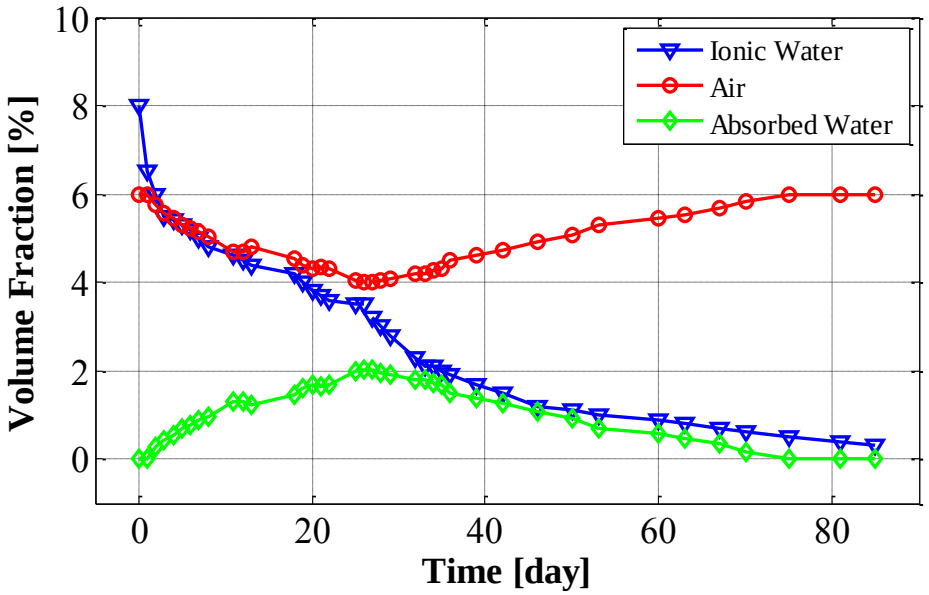

(a)

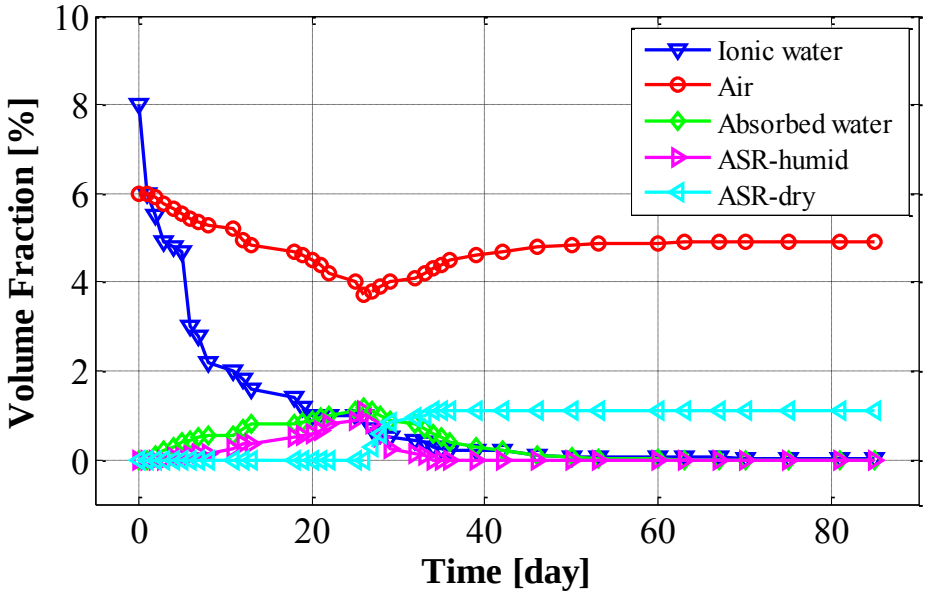

(b)

Figure 5. Volume fractions of inclusions in: a) non-reactive samples, b) reactive samples.

Related to the porosity of the samples is the relationship between the volume fractions of air and absorbed water. For the non-reactive samples, as can be seen in Fig. 5a, during both chamber and ambient conditions, the changes in these two quantities are symmetric. In other words, a reduction in air content of the samples corresponds to an identical increase volume fraction of absorbed water, and vice versa. This symmetric change represents how the (empty, air-filled) pores are filled with absorbed water from the humid environment. On the other hand, during the time samples were kept in ambient conditions, the additional water within the pores evaporates. As a result, the volume fraction of air increases accordingly (representing the water lost through evaporation).

Comparing the changes in temporal volume fraction of ionic water in the non-reactive samples vs. the reactive samples, it can be clearly seen that the amount of available ionic water is reduced faster in the reactive samples. This may be an indication of a higher tendency of the reactive samples to absorb available water, due to presence of ASR gel. Comparing the amount of absorbed water within the two types of samples, it can be seen that reactive samples gained less water from the humid environment compared to the non-reactive samples. This trend is consistent with measured sample mass shown in Fig. 4, and is an indication of higher air content in non-reactive samples compared to reactive samples. As was the case for the non-reactive samples, during the ambient conditions for the reactive samples, the changes in air and absorbed water volume fractions are also mutually compensating, indicating replacement of one by the other. Moreover, for the reactive samples, the air content does not reach the same values as it does for the non-reactive samples. The reason for this may be attributed to the assumption that some of the pores are

(totally or partially) filled with ASR gel in the reactive samples, while in the non-reactive there is no ASR gel.

With respect to the ASR gel volume fraction, obviously, there is only liquid ASR gel during chamber conditions, and as the samples transition to ambient storage, the humid gel becomes dry. Once all liquid ASR gel becomes dry, its volume remains constant since no additional ASR production is expected during drying period. These changes are shown in Fig. 5b.

6. MODELING RESULTS AND SENSITIVITY ANALYSIS

Finally, the modeled and measured of the complex dielectric constants for both sample types are shown in Figs. 6a-b. As can be seen the ASR-reactive and non-reactive samples are clearly distinguishable through microwave dielectric measurements. Additionally, the presented mixing model is capable to closely predict the effective dielectric constants of the sample. As mentioned earlier, since the main purpose of this paper was to quantify the volume fraction of the inclusion in ASR-reactive mortars, the comprehensive (qualitative) discussion of the temporal behavior of the measured dielectric constants of the two sample types (across three different frequency bands) is not repeated here for brevity, and the reader is encouraged to refer to [19] for further details.

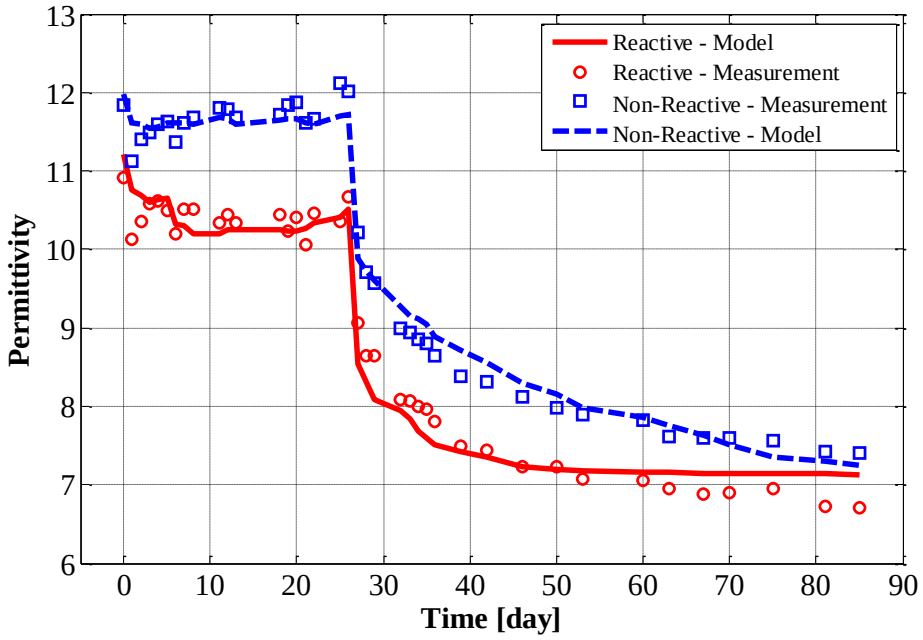

(a)

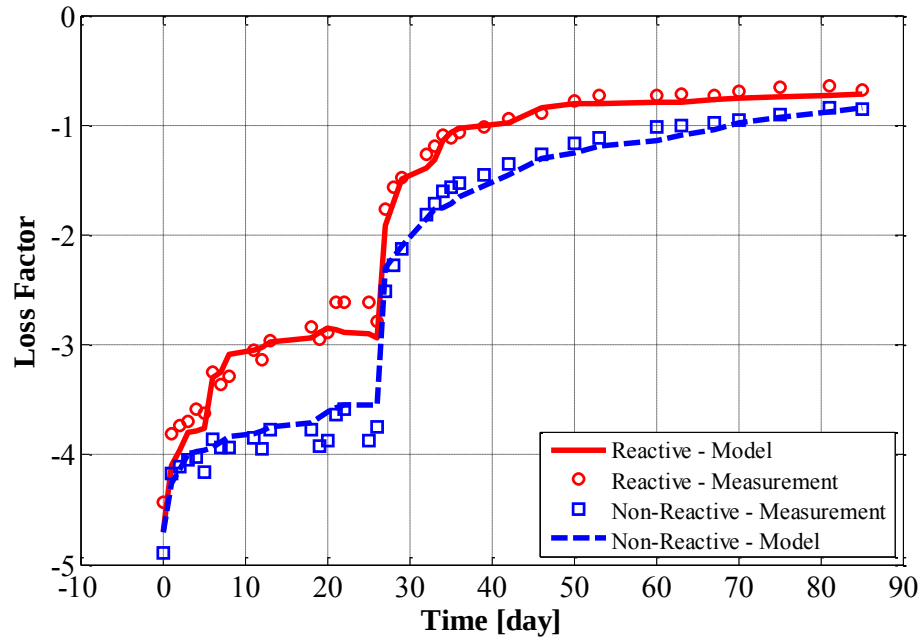

(b)

Figure 6. Measured and modeled dielectric constants: a) permittivity of ASR-reactive and non-reactive samples, b) loss factor of ASR-reactive and non-reactive samples.

Once an empirical dielectric mixing model is developed, an analysis of its sensitivity to different constituent properties is beneficial in the overall understating of the results. Sensitivity analysis of a model not only provides insight to the correlation between the model's input parameters and its output, but also highlights the critical parameters that may need further attention in future research efforts [54]. A simple approach to parameter sensitivity analysis is the one-at-a-time (OAT) approach. This technique varies one parameter while keeping other parameters fixed, and the model output is calculated based on the changes [55]. In order to quantify the sensitivity of the model to each parameter, a sensitivity index (SI) is defined as (16).

$$SI = \frac{\varepsilon_{eff,max} - \varepsilon_{eff,min}}{\varepsilon_{eff,max}} \tag{16}$$

With respect to the developed mixing model, the volume fractions of the inclusions were considered for the sensitivity analysis and changed (one-at-a-time) from -20% to +20% of their nominal values (given in Fig. 5). This analysis provides an important insight into quantifying the contribution of each inclusion's volume fraction in the overall model performance and hence the temporal variation of the dielectric constant of both mortar sample types.

Figure 7 shows the SI calculated for permittivity and loss factor of both reactive and non-reactive samples at three different stages of the measurement time period, namely: chamber, early ambient, and late ambient. The results show that changes in the amount of ionic water is responsible for the highest variations (and subsequently the highest sensitivity index) in the effective dielectric constant of the non-reactive samples.

Furthermore, those changes are more pronounced in the loss factor rather than permittivity. This can be attributed to the increased availability of ionic water in the non-reactive samples (compared to the reactive samples) during the three stages.

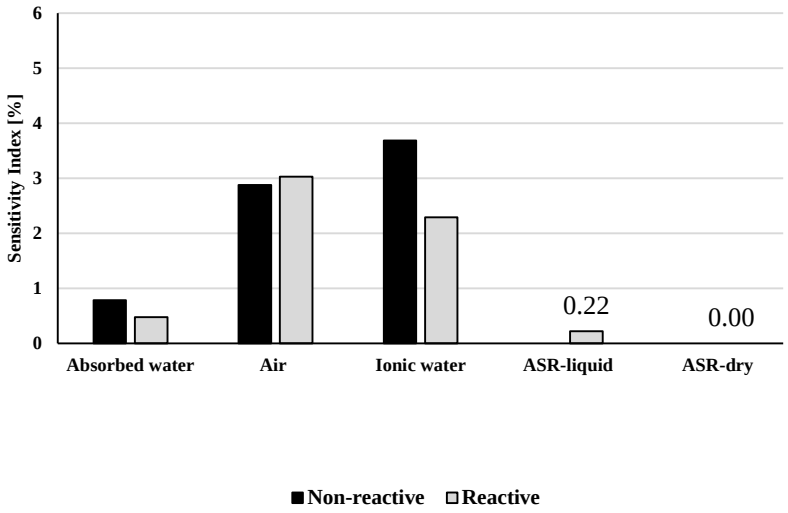

(a)

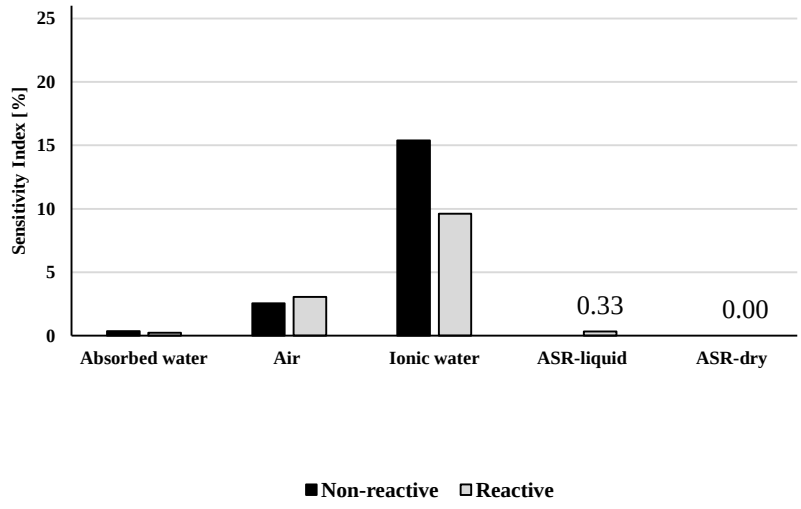

(b)

Figure 7. Sensitivity analysis of the model for: a,b) permittivity and loss factor of chamber stage, c,d) permittivity and loss factor of early ambient, and e,f) permittivity and loss factor of late ambient.

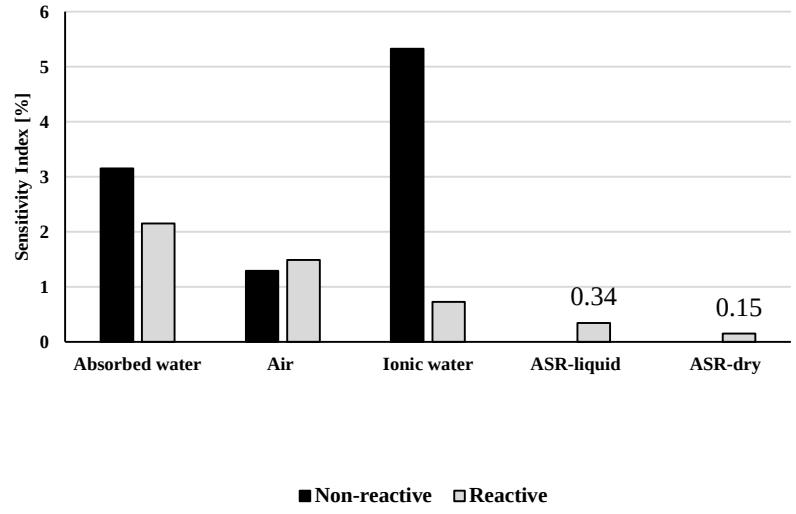

(c)

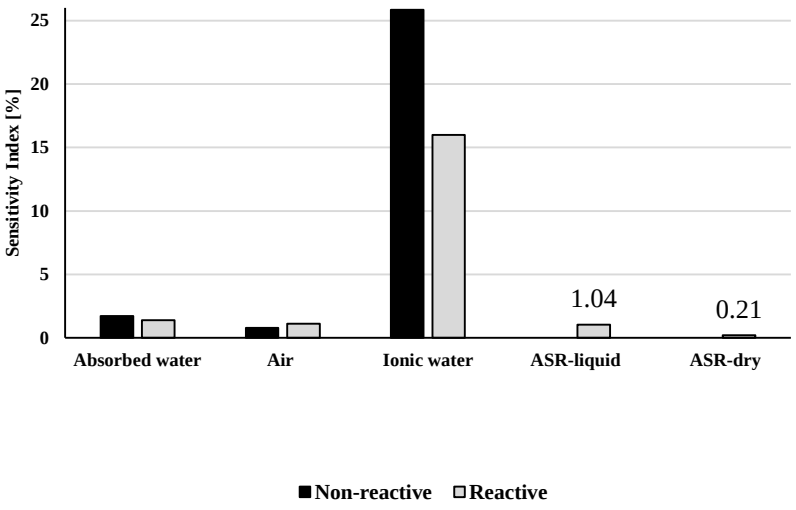

(d)

Figure 7. Sensitivity analysis of the model for: a,b) permittivity and loss factor of chamber stage, c,d) permittivity and loss factor of early ambient, and e,f) permittivity and loss factor of late ambient (cont.).

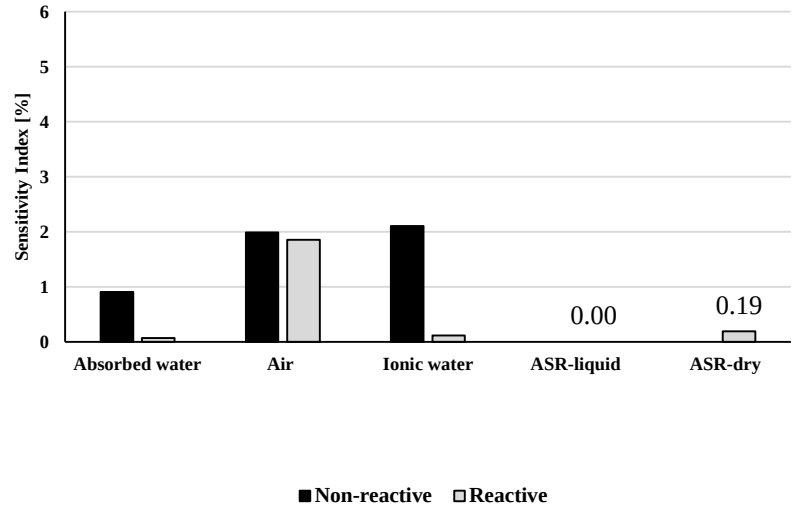

(e)

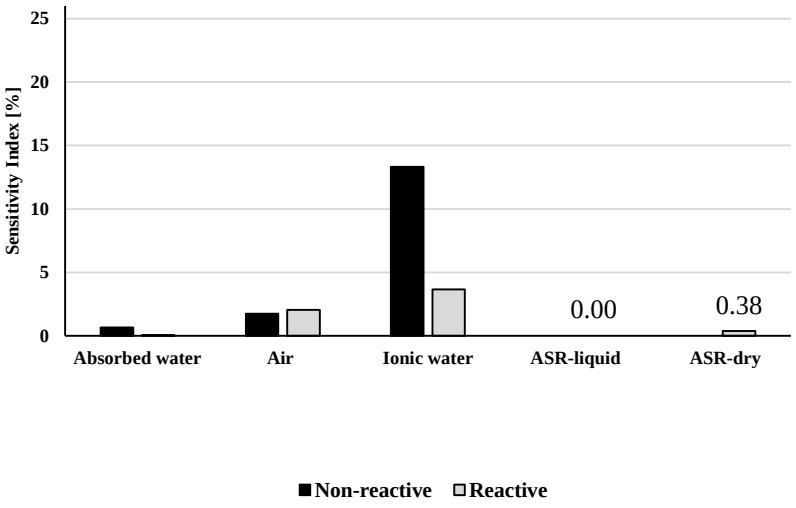

(f)

Figure 7. Sensitivity analysis of the model for: a,b) permittivity and loss factor of chamber stage, c,d) permittivity and loss factor of early ambient, and e,f) permittivity and loss factor of late ambient (cont.).

Regarding the reactive samples, during the chamber (Fig. 7a-b) the SI of the mixing model to the ASR gel volume (either liquid or dry gel) is significantly less than the SI of ionic water. However, this trend changes during the early ambient and late ambient stages. For instance, at late ambient period (Fig. 7e-f), SI of ASR-dry is the highest compared to the corresponding SI of the earlier periods. In other words, as the samples age beyond the first 28 days of curing, the SI of ASR-dry increases. This observation highlights the practicality of the presented approach, indicating higher sensitivity of the model to the presence of ASR gel as the samples lose water, which is the more realistic case for an existing structures to be inspected for ASR detection. As a result, microwave materials characterization techniques take advantage of the sensitivity of the microwave region to the interaction of water with ASR gel in order to detect the presence of ASR gel either directly (once samples are mature) or indirectly (during hydration period).

7. CONCLUDING REMARKS

Through this investigation, a comprehensive multiphase dielectric mixing model was developed for mortar samples with ASR-reactive and non-reactive aggregates. The model was based on the temporal changes of the dielectric constant and volumetric content of the inclusions. The dielectric constant of the inclusions was either modeled (as a function of frequency, temperature, and ionic conductivity) or measured directly. To validate the model, the modeled temporal dielectric constant was compared to the measured temporal dielectric constant of the samples at 2 GHz, and a good agreement was observed.

A sensitivity analysis was performed for three different time periods to determine the factors that most influence the model outcome. Through this analysis, it was shown that as the samples go beyond the chamber and early ambient condition, the sensitivity to the presence of ASR gel increases, which highlights the potential of this approach for ASR detection in existing structures.

It must be emphasized that, due to the complicated process of ASR gel formation and other chemical properties associated with cement-based materials (i.e., hydration, etc.) which may vary from one mix design to another, any proposed dielectric mixing model needs be modified accordingly. Finally, the results of this investigation provide a new insight into ASR evolution from a microwave materials characterization standpoint, and the model can be further utilized as part of the development of a microwave nondestructive technique for evaluating ASR gel formation in existing cement-based infrastructure.

REFERENCES

[1] "ACI Concrete Terminology, ACI Standard CT-13, Jan." 2013.

[2] L. S. Dent Glasser and N. Kataoka, "The chemistry of 'alkali-aggregate' reaction," Cem. Concr. Res., vol. 11, no. 1, pp. 1–9, Jan. 1981.

[3] G. Fu, Inspection and monitoring techniques for bridges and civil structures. Elsevier, 2005.

[4] O. Omikrine Metalssi, B. Godart, and F. Toutlemonde, "Effectiveness of Nondestructive Methods for the Evaluation of Structures Affected by Internal Swelling Reactions: A Review of Electric, Seismic and Acoustic Methods Based on Laboratory and Site Experiences," Exp. Tech., vol. 39, no. 2, pp. 65–76, Mar. 2015.

[5] O. Büyüköztürk and M. A. Taşdemir, Nondestructive Testing of Materials and Structures, vol. 6. Dordrecht: Springer Netherlands, 2013.

[6] F. Moradi-Marani and P. Rivard, "Nondestructive assessment of alkali-silica reaction in concrete: A review," Nondestruct. Test. Mater. …, 2013.

[7] Y. Farnam, M. R. Geiker, D. Bentz, and J. Weiss, "Acoustic emission waveform characterization of crack origin and mode in fractured and ASR damaged concrete," Cem. Concr. Compos., vol. 60, pp. 135–145, Jul. 2015.

[8] K. J. Leśnicki, J.-Y. Kim, K. E. Kurtis, and L. J. Jacobs, "Characterization of ASR damage in concrete using nonlinear impact resonance acoustic spectroscopy technique," NDT E Int., vol. 44, no. 8, pp. 721–727, Dec. 2011.

[9] J. Chen, A. R. Jayapalan, J.-Y. Kim, K. E. Kurtis, and L. J. Jacobs, "Rapid evaluation of alkali–silica reactivity of aggregates using a nonlinear resonance spectroscopy technique," Cem. Concr. Res., vol. 40, no. 6, pp. 914–923, Jun. 2010.

[10] X. J. Chen, J.-Y. Kim, K. E. Kurtis, J. Qu, C. W. Shen, and L. J. Jacobs, "Characterization of progressive microcracking in Portland cement mortar using nonlinear ultrasonics," NDT E Int., vol. 41, no. 2, pp. 112–118, Mar. 2008.

[11] K. J. Bois, A. Benally, P. S. Nowak, and R. Zoughi, "Microwave nondestructive determination of sand-to-cement ratio in mortar," Res. Nondestruct. Eval., vol. 9, no. 4, pp. 227–238, 1997.

[12] K. J. Bois, A. D. Benally, and R. Zoughi, "Microwave near-field reflection property analysis of concrete for material content determination," IEEE Trans. Instrum. Meas., vol. 49, no. 1, pp. 49–55, 2000.

[13] K. Mubarak, K. J. Bois, and R. Zoughi, “A simple, robust, and on-site microwave technique for determining water-to-cement ratio (w/c) of fresh Portland cement-based materials,” IEEE Trans. Instrum. Meas., vol. 50, no. 5, pp. 1255–1263, 2001.

[14] K. J. Bois, A. D. Benally, P. S. Nowak, and R. Zoughi, “Cure-state monitoring and water-to-cement ratio determination of fresh Portland cement-based materials using near-field microwave techniques,” IEEE Trans. Instrum. Meas., vol. 47, no. 3, pp. 628–637, Jun. 1998.

[15] S. Kharkovsky, A. C. Ryley, V. Stephen, and R. Zoughi, “Dual-Polarized Microwave Near-Field Reflectometer for Non-Invasive Inspection of Carbon Fiber Reinforced Polymer (CFRP) Strengthened Structures,” in IEEE Instrumentation and Measurement Technology Conference Proceedings, 2006.

[16] A. Hashemi, M. C. L. Knapp, K. M. Donnell, K. E. Kurtis, and R. Zoughi, “Microwave detection of carbonation in mortar using dielectric property characterization,” 2014 IEEE Int. Instrum. Meas. Technol. Conf. Proc., pp. 216–220, May 2014.

[17] S. Peer, K. E. Kurtis, and R. Zoughi, “Evaluation of microwave reflection properties of cyclically soaked mortar based on a semiempirical electromagnetic model,” IEEE Trans. Instrum. Meas., vol. 54, no. 5, pp. 2049–2060, 2005.

[18] A. Hashemi, S. Hatfield, K. M. Donnell, R. Zoughi, and K. E. Kurtis, “Microwave NDE method for health-monitoring of concrete structures containing alkali-silica reaction (ASR) gel,” in AIP Conference Proceedings, 2014, vol. 1581 33, pp. 787–792.

[19] A. Hashemi, M. Horst, K. E. Kurtis, K. M. Donnell, and R. Zoughi, “Comparison of Alkali–Silica Reaction Gel Behavior in Mortar at Microwave Frequencies,” IEEE Trans. Instrum. Meas., vol. 64, no. 7, pp. 1907–1915, Jul. 2015.

[20] A. Hashemi, K. M. Donnell, R. Zoughi, and K. E. Kurtis, “Effect of humidity on dielectric properties of mortars with alkali-silica reaction (ASR) gel,” in 2015 IEEE International Instrumentation and Measurement Technology Conference (I2MTC) Proceedings, 2015, pp. 1502–1506.

[21] A. Kraszewski, Microwave aquametry: electromagnetic wave interaction with water-containing materials. IEEE, 1996.

[22] A. Sihvola, Electromagnetic mixing formulas and applications. London, UK: IEE publishing, 1999.

[23] W. R. Tinga, W. a G. Voss, and D. F. Blossey, “Generalized approach to multiphase dielectric mixture theory,” J. Appl. Phys., vol. 44, no. 9, pp. 3897–3902, 1973.

[24] A. H. Shivola, “Self-consistency aspects of dielectric mixing theories,” IEEE Trans. Geosci. Remote Sens., vol. 27, no. 4, pp. 403–415, 1989.

[25] A. H. Shivola, “Self-consistency aspects of dielectric mixing theories,” IEEE Trans. Geosci. Remote Sens., vol. 27, no. 4, pp. 403–415, Jul. 1989.

[26] C. Dirksen and S. Dasberg, “Improved calibration of time domain reflectometry soil water content measurements,” Soil Science Society of America Journal, vol. 57, no. 3. pp. 660–667, 1993.

[27] M. Hallikainen, F. Ulaby, M. Dobson, M. El-rayes, and L. Wu, “Microwave Dielectric Behavior of Wet Soil-Part 1: Empirical Models and Experimental Observations,” IEEE Trans. Geosci. Remote Sens., vol. GE-23, no. 1, pp. 25–34, Jan. 1985.

[28] V. Mironov and M. Dobson, “Generalized refractive mixing dielectric model for moist soils,” Geosci. Remote Sensing, IEEE Trans., vol. 42, no. 4, pp. 773–785, 2004.

[29] D. A. Robinson, S. B. Jones, J. M. Wraith, D. Or, and S. P. Friedman, “A review of advances in dielectric and electrical conductivity measurement in soils using time domain reflectometry,” Vadose Zo. J., vol. 2, no. 4, pp. 444–475, 2003.

[30] R. van Dam, R. L. van Dam, B. Borchers, and J. M. H. Hendrickx, “Methods for prediction of soil dielectric properties: A review,” Detect. Remediat. Technol. Mines Minelike Targets X, March 28, 2005 - April 1, 2005, vol. 5794, no. 1, pp. 188–197, 2005.

[31] H. He and M. Dyck, “Application of Multiphase Dielectric Mixing Models for Understanding the Effective Dielectric Permittivity of Frozen Soils,” Vadose Zo. J., vol. 12, no. 1, 2013.

[32] M. Vallone, A. Cataldo, and L. Tarricone, “Water content estimation in granular materials by time domain reflectometry: A key-note on agro-food applications,” in Conference Record - IEEE Instrumentation and Measurement Technology Conference, 2007.

[33] M. T. Hallikainen, F. T. Ulaby, and M. Abdelrazik, “Dielectric properties of snow in the 3 to 37 GHz range,” IEEE Trans. Antennas Propag., vol. AP-34, no. 11, pp. 1329–1340, 1986.

[34] A. Paz, E. Thorin, and C. Topp, “Dielectric mixing models for water content determination in woody biomass,” Wood Sci. Technol., vol. 45, no. 2, pp. 249–259, Mar. 2010.

[35] ASTM C 1293-08b, “Determination of length change of concrete due to alkali–silica reaction (concrete prismtest),” ASTM Int., 2008.

[36] K. J. Bois, L. F. Handjojo, A. D. Benally, K. Mubarak, and R. Zoughi, “Dielectric plug-loaded two-port transmission line measurement technique for dielectric property characterization of granular and liquid materials,” IEEE Trans. Instrum. Meas., vol. 48, no. 6, pp. 1141–1148, 1999.

[37] O. Wiener, “Zur theorie der refraktionskonstanten,” Berichre iiber die Verhandlungen der K. sdchsischen Gesellschafi der Wissenschafien zu Leipzig, vol. Math.-phys, no. 62, pp. 256–277, 1910.

[38] C. A. R. Pearce, “The permittivity of two phase mixtures,” Br. J. Appl. Phys., vol. 6, no. 10, pp. 358–361, Oct. 1955.

[39] P. Debye, Polar molecules. Chemical Catalog Company, Incorporated, 1929.

[40] L. Klein and C. Swift, “An improved model for the dielectric constant of sea water at microwave frequencies,” Ocean. Eng. IEEE J., vol. 2, no. 1, pp. 104–111, 1977.

[41] A. Stogryn, “Equations for calculating the dielectric constant of saline water,” IEEE Transactions on Microwave Theory and Techniques, vol. MTT-19, no. 8. pp. 733–736, 1971.

[42] F. T. Ulaby, R. K. Moore, and A. K. Fung, Microwave remote sensing: Active and passive, vol. iii, volume scattering and emission theory, advanced systems and applications. 1986.

[43] K. a. Snyder, X. Feng, B. D. Keen, and T. O. Mason, “Estimating the electrical conductivity of cement paste pore solutions from OH-, K+ and Na+ concentrations,” Cem. Concr. Res., vol. 33, no. 6, pp. 793–798, 2003.

[44] B. J. Christensen, T. Coverdale, R. a. Olson, S. J. Ford, E. J. Garboczi, H. M. Jennings, and T. O. Mason, “Impedance Spectroscopy of Hydrating Cement-Based Materials: Measurement, Interpretation, and Application,” J. Am. Ceram. Soc., vol. 77, no. 11, pp. 2789–2804, 1994.

[45] J. Zhang, J. L. Provis, D. Feng, and J. S. J. van Deventer, “Geopolymers for immobilization of Cr(6+), Cd(2+), and Pb(2+).,” J. Hazard. Mater., vol. 157, no. 2–3, pp. 587–98, Sep. 2008.

[46] M. T. Ghasr, D. Simms, and R. Zoughi, “Multimodal Solution for a Waveguide Radiating Into Multilayered Structures—Dielectric Property and Thickness Evaluation,” IEEE Trans. Instrum. Meas., vol. 58, no. 5, pp. 1505–1513, May 2009.

[47] A. Hashemi, M. Rashidi, K. E. Kurtis, D. K.M, and R. Zoughi, "Microwave Dielectric Properties Measurements of Water Glass," Mater. Lett. (in Press., 2015.

[48] K. J. Leśnicki, J.-Y. Kim, K. E. Kurtis, and L. J. Jacobs, "Assessment of alkali–silica reaction damage through quantification of concrete nonlinearity," Mater. Struct., vol. 46, no. 3, pp. 497–509, Dec. 2012.

[49] M. Kawamura and H. Fuwa, "Effects of lithium salts on ASR gel composition and expansion of mortars," Cem. Concr. Res., vol. 33, no. 6, pp. 913–919, Jun. 2003.

[50] S. Multon, A. Sellier, and M. Cyr, "Chemo–mechanical modeling for prediction of alkali silica reaction (ASR) expansion," Cem. Concr. Res., vol. 39, no. 6, pp. 490–500, Jun. 2009.

[51] F. Rajabipour, E. Giannini, C. Dunant, J. H. Ideker, and M. D. A. Thomas, "Alkali–silica reaction: Current understanding of the reaction mechanisms and the knowledge gaps," Cem. Concr. Res., vol. 76, pp. 130–146, Oct. 2015.

[52] M. Kawamura and K. Iwahori, "ASR gel composition and expansive pressure in mortars under restraint," Cem. Concr. Compos., vol. 26, no. 1, pp. 47–56, Jan. 2004.

[53] N. P. Mayercsik, R. Felice, M. T. Ley, and K. E. Kurtis, "A probabilistic technique for entrained air void analysis in hardened concrete," Cem. Concr. Res., vol. 59, pp. 16–23, May 2014.

[54] D. M. Hamby, "A review of techniques for parameter sensitivity analysis of environmental models.," Environ. Monit. Assess., vol. 32, no. 2, pp. 135–54, Sep. 1994.

[55] D. Hamby, "A comparison of sensitivity analysis techniques," Health Phys., pp. 1–20, 1995.

SECTION

2. CONCLUSION AND FUTURE WORK

The overarching objective of this research was to bring new understanding to some fundamental aspects of the alkali-silica reaction (ASR) and ASR gel production in mortar, through microwave materials characterization techniques. The goal was to take advantage of the sensitivity of microwave signals to mortar constituent dielectric properties in particular moisture content, in its free and bound states, and to the ensuing alkali-silica chemical reaction to detect temporal ASR gel formation and evolution. In section "Paper I" a comprehensive study was presented in which the microwave dielectric properties measurement results were analyzed regarding the behavior of ASR formation across three distinct frequency bands. Sections "Paper II", "paper III", and "paper IV" investigated other critical parameters (such as humidity, alkali addition, and curing conditions) during ASR gel formation. Section "Paper V" reported the synthetic ASR gel dielectric properties measurements which served as a critical input to the mixing model development. Finally, section "paper VI" presented the dielectric mixing model development and its results. Several abstracts and conference papers (leading to the final outcome of the research presented in this dissertation) were also published, and were cited in the pertinent papers listed in this dissertation.

To achieve the objectives of this investigation, two primary tasks were followed. First, the temporal dielectric properties of chemically-different mortar samples were measured (i.e., measurement phase). Second, a dielectric mixing model was developed based on the measurement outcomes (i.e., modeling phase). Microwave signals are

sensitive to the moisture content in dielectric materials (e.g., mortar, concrete). Therefore, temporal microwave dielectric property measurements (as they relate to the physical and chemical properties of materials) were employed to evaluate ASR gel formation in mortars. Since this study was the first effort of its type as it relates to ASR evaluation with microwaves, multiple mortar samples (with different aggregate type and mix design) were cast and their dielectric properties examined at three distinct frequency bands: R-band (1.7 - 2.6 GHz), S-band (2.6 - 3.95 GHz), and X-band (8.2 - 12.4 GHz). Through these investigations, a distinct difference between dielectric properties of mortar samples with and without the presence of ASR gel was observed. Additionally, it was shown that lower frequencies (i.e., R-band) may be more sensitive to presence of bound water, as opposed to S-band with higher sensitivity to the presence of free water in mortars containing ASR gel. Moreover, effects of other critical factors (such as humidity, alkali addition, and long-term curing) on dielectric properties of mortar samples containing ASR gel were investigated. For instance, a correlation between the measured dielectric loss factor, bulk resistivity, and compressive strength of the mortars with different alkali contents was observed. Also, twelve chemically different synthetic ASR gel were prepared, and their dielectric properties characterized. This significant amount of data provided a comprehensive database for further analysis of ASR temporal dielectric properties, and served as a critical inputs to the modeling phase.

For the modeling phase, an empirical dielectric mixing model was developed for mortar samples with and without the presence of ASR gel. The model was founded based on the temporal changes of both dielectric properties and volumetric content of mortar inclusions (i.e., mortar paste, water, air, ASR gel). The dielectric properties of the

inclusions were either modeled (as a function of frequency, temperature, ionic conductivity) or measured directly. To validate the model, the results were compared to the measured dielectric properties of mortar samples, and a good agreement was observed between the model and the corresponding measurement results.

It must be emphasized that due to the complicated process of ASR formation, and other chemical properties associated with cement curing which may vary from one mix design to the other, any proposed empirical dielectric mixing model needs be modified accordingly. As a result, devising a versatile mixing model capable of performing well for all varieties of mixtures while challenging, has a lot of promise.

The ultimate outcome of this research significantly adds to the understating of the behavior of microwave signals interacting with cementitious materials and structures as they undergo physical and chemical changes. Therefore, this methodology, once become more mature, will bring new insight to ASR reaction which is increasingly damaging to concrete infrastructure, allowing for advancements in design, mitigation, and has the potential to be utilized as an effective inspection tool for infrastructure health-monitoring of existing structures.

REFERENCES

[1] R. Zoughi, *Microwave Non-Destructive Testing and Evaluation Principles*. Springer Science & Business Media, 2000.

[2] L. Chen, C. Ong, C. Neo, V. Varadan, and V. Varadan, *Microwave electronics: measurement and materials characterization*. 2004.

[3] D. Pozar, "Microwave engineering," 2009.

[4] S. Ramo, J. Whinnery, and T. Van Duzer, "Fields and waves in communication electronics," 2008.

[5] D. Hughes and R. Zoughi, "A Novel Method for Determination of Dielectric Properties of Materials Using a Combined Embedded Modulated Scattering and Near-Field Microwave Techniques—Part I: Forward Model," *IEEE Trans. Instrum. Meas.*, vol. 54, no. 6, pp. 2389–2397, Dec. 2005.

[6] D. Hughes and R. Zoughi, "A Novel Method for Determination of Dielectric Properties of Materials Using a Combined Embedded Modulated Scattering and Near-Field Microwave Techniques—Part II: Dielectric Property Recalculation," *IEEE Trans. Instrum. Meas.*, vol. 54, no. 6, pp. 2398–2401, Dec. 2005.

[7] S. Trabelsi, A. W. Kraszewski, and S. O. Nelson, "Simultaneous determination of density and water content of particulate materials by microwave sensors," *Electron. Lett.*, vol. 33, no. 10, pp. 874–876, 1997.

[8] S. N. Kharkovsky, M. F. Akay, U. C. Hasar, and C. D. Atis, "Measurement and monitoring of microwave reflection and transmission properties of cement-based specimens," *IEEE Trans. Instrum. Meas.*, vol. 51, no. 6, pp. 1210–1218, Dec. 2002.

[9] R. Zoughi, A. D. Benally, and K. J. Bois, "Near-field microwave non-invasive determination of NaCl in mortar," *IEE Proc. - Sci. Meas. Technol.*, vol. 148, no. 4, pp. 178–182, Jul. 2001.

[10] S. I. Ganchev, J. Bhattacharyya, S. Bakhtiari, N. Qaddoumi, D. Brandenburg, and R. Zoughi, "Microwave diagnosis of rubber compounds," *IEEE Trans. Microw. Theory Tech.*, vol. 42, no. 1, pp. 18–24, 1994.

[11] S. Gray, S. Ganchev, N. Qaddoumi, G. Beauregard, D. Radford, and R. Zoughi, "Porosity level estimation in polymer composites using microwaves," *Mater. Eval.*, vol. 53, no. 3, pp. 404–408, 1995.

[12] C. Vineis, P. K. Davies, T. Negas, and S. Bell, "Microwave dielectric properties of hexagonal perovskites," *Mater. Res. Bull.*, vol. 31, no. 5, pp. 431–437, May 1996.

[13] A. R. Djordjevic, V. D. Likar-Smiljanic, and T. K. Sarkar, "Wideband frequency-domain characterization of FR-4 and time-domain causality," *IEEE Trans. Electromagn. Compat.*, vol. 43, no. 4, pp. 662–667, Nov. 2001.

[14] Z. Fan, G. Luo, Z. Zhang, L. Zhou, and F. Wei, "Electromagnetic and microwave absorbing properties of multi-walled carbon nanotubes/polymer composites," *Mater. Sci. Eng. B*, vol. 132, no. 1–2, pp. 85–89, Jul. 2006.

[15] M. P. McNeal, S. J. Jang, and R. E. Newnham, "The effect of grain and particle size on the microwave properties of barium titanate (BaTiO3)," *J. Appl. Phys.*, vol. 83, no. 6, pp. 3288–3297, 1998.

[16] K. J. Bois, A. D. Benally, and R. Zoughi, "Microwave near-field reflection property analysis of concrete for material content determination," *IEEE Trans. Instrum. Meas.*, vol. 49, no. 1, pp. 49–55, 2000.

[17] K. J. Bois, A. Benally, P. S. Nowak, and R. Zoughi, "Microwave nondestructive determination of sand-to-cement ratio in mortar," *Res. Nondestruct. Eval.*, vol. 9, no. 4, pp. 227–238, 1997.

[18] K. Mubarak, K. J. Bois, and R. Zoughi, "A simple, robust, and on-site microwave technique for determining water-to-cement ratio (w/c) of fresh Portland cement-based materials," *IEEE Trans. Instrum. Meas.*, vol. 50, no. 5, pp. 1255–1263, 2001.

[19] K. J. Bois, A. D. Benally, P. S. Nowak, and R. Zoughi, "Cure-state monitoring and water-to-cement ratio determination of fresh Portland cement-based materials using near-field microwave techniques," *IEEE Trans. Instrum. Meas.*, vol. 47, no. 3, pp. 628–637, Jun. 1998.

[20] A. Hashemi, K. M. Donnell, R. Zoughi, and K. E. Kurtis, "Microwave nondestructive evaluation of hydration kinetics in mortars with and without sodium hydroxide inclusion," in *14th International Symposium on Nondestructive Characterization of Materials*, 2015.

[21] A. Hashemi, K. M. Donnell, R. Zoughi, O. C. Fawole, and M. Tabib-Azar, "THz materials characterization of mortar samples with and without alkali-silica reaction (ASR) gel," in *42th Annual Review of Progress in Quantitative Nondestructive Evaluation*, 2015.

[22] A. Hashemi, I. Mehdipour, K. M. Donnell, R. Zoughi, and K. H. Khayat, "Effect of alkali addition on microwave dielectric properties of mortars," *NDT E Int. - under Rev.*, 2015.

[23] A. Hashemi, M. Rashidi, K. M. Donnell, K. E. Kurtis, and R. Zoughi, "Curing conditions effects on the long-term dielectric properties of mortar samples containing ASR gel," in *IEEE Int. Instrum. Meas. Technol. Conf. Proc. (Submitted)*, 2016.

[24] A. Hashemi, M. Horst, K. E. Kurtis, K. M. Donnell, and R. Zoughi, "Comparison of Alkali–Silica Reaction Gel Behavior in Mortar at Microwave Frequencies," *IEEE Trans. Instrum. Meas.*, vol. 64, no. 7, pp. 1907–1915, Jul. 2015.

[25] A. Hashemi, S. Hatfield, K. M. Donnell, R. Zoughi, and K. E. Kurtis, "Microwave NDE method for health-monitoring of concrete structures containing alkali-silica reaction (ASR) gel," *AIP Conf. Proc.*, vol. 1581 33, pp. 787–792, 2014.

[26] K. M. Donnell, S. Hatfield, R. Zoughi, and K. E. Kurtis, "Wideband microwave characterization of alkali-silica reaction (ASR) gel in cement-based materials," *Mater. Lett.*, vol. 90, pp. 159–161, 2013.

[27] A. Hashemi, M. C. L. Knapp, K. M. Donnell, K. E. Kurtis, and R. Zoughi, "Microwave detection of carbonation in mortar using dielectric property characterization," *2014 IEEE Int. Instrum. Meas. Technol. Conf. Proc.*, pp. 216–220, May 2014.

[28] K. M. Donnell, R. Zoughi, and K. E. Kurtis, "Demonstration of microwave method for detection of alkali-silica reaction (ASR) gel in cement-based materials," *Cem. Concr. Res.*, vol. 44, pp. 1–7, 2013.

[29] A. Hashemi, K. M. Donnell, and R. Zoughi, "Effect of Humidity on Dielectric Properties of Mortars with Alkali-Silica Reaction (ASR) Gel," no. 3, pp. 6–10, 2015.

[30] A. Hashemi, M. Rashidi, K. E. Kurtis, K. M. Donnell, and R. Zoughi, "Microwave Dielectric Properties Measurements of Sodium and Potassium Water Glasses," *Mater. Lett.*, Nov. 2015.

[31] T. E. Stanton, "Expansion of concrete through reaction between cement and aggregate," *Proc. Am. Soc. Civ. Eng.*, vol. 66, no. 10, pp. 1781–1811, 1940.

[32] "ACI Concrete Terminology, ACI Standard CT-13, Jan." 2013.

[33] L. S. Dent Glasser and N. Kataoka, "The chemistry of 'alkali-aggregate' reaction," *Cem. Concr. Res.*, vol. 11, no. 1, pp. 1–9, Jan. 1981.

[34] F. Rajabipour, E. Giannini, C. Dunant, J. H. Ideker, and M. D. a. Thomas, "Alkali–silica reaction: Current understanding of the reaction mechanisms and the knowledge gaps," *Cem. Concr. Res.*, vol. 76, pp. 130–146, 2015.

[35] A. Pedneault, "Development of testing and analytical procedures for the evaluation of the residual potential of reaction, expansion and deterioration of concrete affected by ASR," Memoir, Laval University, Quebec City, Canada, 1996.

[36] A. Kraszewski, *Microwave aquametry: electromagnetic wave interaction with water-containing materials*. IEEE, 1996.

[37] A. Sihvola, *Electromagnetic mixing formulas and applications*. London, UK: IEE publishing, 1999.

[38] C. Dirksen and S. Dasberg, "Improved calibration of time domain reflectometry soil water content measurements," *Soil Science Society of America Journal*, vol. 57, no. 3. pp. 660–667, 1993.

[39] M. Hallikainen, F. Ulaby, M. Dobson, M. El-rayes, and L. Wu, "Microwave Dielectric Behavior of Wet Soil-Part 1: Empirical Models and Experimental Observations," *IEEE Trans. Geosci. Remote Sens.*, vol. GE-23, no. 1, pp. 25–34, Jan. 1985.

[40] V. Mironov and M. Dobson, "Generalized refractive mixing dielectric model for moist soils," *Geosci. Remote Sensing, IEEE Trans.*, vol. 42, no. 4, pp. 773–785, 2004.

[41] D. A. Robinson, S. B. Jones, J. M. Wraith, D. Or, and S. P. Friedman, "A review of advances in dielectric and electrical conductivity measurement in soils using time domain reflectometry," *Vadose Zo. J.*, vol. 2, no. 4, pp. 444–475, 2003.

[42] M. Vallone, A. Cataldo, and L. Tarricone, "Water content estimation in granular materials by time domain reflectometry: A key-note on agro-food applications," in *Conference Record - IEEE Instrumentation and Measurement Technology Conference*, 2007.

[43] M. T. Hallikainen, F. T. Ulaby, and M. Abdelrazik, "Dielectric properties of snow in the 3 to 37 GHz range," *IEEE Trans. Antennas Propag.*, vol. AP-34, no. 11, pp. 1329–1340, 1986.

[44] A. Paz, E. Thorin, and C. Topp, "Dielectric mixing models for water content determination in woody biomass," *Wood Sci. Technol.*, vol. 45, no. 2, pp. 249–259, Mar. 2010.

[45] A. H. Sihvola and J. A. Kong, "Effective Permittivity of Dielectric Mixtures.," *IEEE Trans. Geosci. Remote Sens.*, vol. 26, no. 4, pp. 420–429, 1988.

[46] W. R. Tinga, W. a G. Voss, and D. F. Blossey, "Generalized approach to multiphase dielectric mixture theory," *J. Appl. Phys.*, vol. 44, no. 9, pp. 3897–3902, 1973.

[47] C. A. R. Pearce, "The permittivity of two phase mixtures," *Br. J. Appl. Phys.*, vol. 6, no. 10, pp. 358–361, Oct. 1955.

[48] L. Klein and C. Swift, "An improved model for the dielectric constant of sea water at microwave frequencies," *Ocean. Eng. IEEE J.*, vol. 2, no. 1, pp. 104–111, 1977.

[49] A. Stogryn, "Equations for calculating the dielectric constant of saline water," *IEEE Transactions on Microwave Theory and Techniques*, vol. MTT-19, no. 8. pp. 733–736, 1971.

[50] J. Lane and J. Saxton, "Dielectric dispersion in pure polar liquids at very high radio-frequencies. I. Measurements on water, methyl and ethyl alcohols," *Proc. R. Soc. London A Math. Phys. Eng. Sci.*, vol. 213, no. 1114, 1952.

[51] F. T. Ulaby, R. K. Moore, and A. K. Fung, *Microwave remote sensing: Active and passive, vol. iii, volume scattering and emission theory, advanced systems and applications*. 1986.

[52] K. a. Snyder, X. Feng, B. D. Keen, and T. O. Mason, "Estimating the electrical conductivity of cement paste pore solutions from OH-, K+ and Na+ concentrations," *Cem. Concr. Res.*, vol. 33, no. 6, pp. 793–798, 2003.

[53] B. Christensen and T. Coverdale, "Impedance Spectroscopy of Hydrating Cement-Based Materials: Measurement, Interpretation, and Application," *J. ...*, 1994.

[54] K. J. Bois, L. F. Handjojo, A. D. Benally, K. Mubarak, and R. Zoughi, "Dielectric plug-loaded two-port transmission line measurement technique for dielectric property characterization of granular and liquid materials," *IEEE Trans. Instrum. Meas.*, vol. 48, no. 6, pp. 1141–1148, 1999.

[55] K. J. Leśnicki, J.-Y. Kim, K. E. Kurtis, and L. J. Jacobs, "Assessment of alkali–silica reaction damage through quantification of concrete nonlinearity," *Mater. Struct.*, vol. 46, no. 3, pp. 497–509, Dec. 2012.

[56] M. Kawamura and H. Fuwa, "Effects of lithium salts on ASR gel composition and expansion of mortars," *Cem. Concr. Res.*, vol. 33, no. 6, pp. 913–919, Jun. 2003.

[57] S. Multon, A. Sellier, and M. Cyr, "Chemo–mechanical modeling for prediction of alkali silica reaction (ASR) expansion," *Cem. Concr. Res.*, vol. 39, no. 6, pp. 490–500, Jun. 2009.

[58] F. Rajabipour, E. Giannini, C. Dunant, J. H. Ideker, and M. D. A. Thomas, "Alkali–silica reaction: Current understanding of the reaction mechanisms and the knowledge gaps," *Cem. Concr. Res.*, vol. 76, pp. 130–146, Oct. 2015.

[59] M. Kawamura and K. Iwahori, "ASR gel composition and expansive pressure in mortars under restraint," *Cem. Concr. Compos.*, vol. 26, no. 1, pp. 47–56, Jan. 2004.

[60] N. P. Mayercsik, R. Felice, M. T. Ley, and K. E. Kurtis, "A probabilistic technique for entrained air void analysis in hardened concrete," *Cem. Concr. Res.*, vol. 59, pp. 16–23, May 2014.

VITA

Ashkan Hashemi was born in Tehran, Iran, in 1985. He received the B.Sc. degree in Electrical Engineering from IAU, Iran, in 2007, and the M.Sc. degree in Electronics Design from Mid Sweden University (Mittuniversitietet), Sundsvall, Sweden in 2012. Afterwards, he joined the Applied Microwave Nondestructive Testing Laboratory (*amntl*) as a graduate research assistant. In May, 2016, he received his Ph.D. in Electrical Engineering from Missouri University of Science and Technology (Missouri S&T). His research interests include microwave and millimeter-wave nondestructive testing techniques, material characterization, digital electronics design, RF design, and electromagnetics. Ashkan is a member of multiple IEEE societies including Instrumentation and Measurement, Electromagnetic Compatibility, Antennas and Propagation. He is an active member of Eta Kappa Nu IEEE honor society, as well as American Society for Nondestructive Testing (ASNT). He has been awarded multiple travel grants from different professional societies, and was honored with the Ph.D. Dissertation Completion Fellowship at Missouri S&T in June 2015.